

Copyright
by
Aaron John Brown
2017

**The Dissertation Committee for Aaron John Brown Certifies that this is the
approved version of the following dissertation:**

**Chemokine CXCL7 Monomer, Homodimer, and Heterodimer:
Structural Insights, CXCR2 Receptor Function, and
Glycosaminoglycan Interactions**

Committee:

Krishna Rajarathnam, PhD, Supervisor

James Lee, PhD, Chair

Junji Iwahara, PhD

Roberto Garofalo, MD

Margaret Cheung, PhD

Dean, Graduate School

**Chemokine CXCL7 Monomer, Homodimer, and Heterodimer:
Structural Insights, CXCR2 Receptor Function, and
Glycosaminoglycan Interactions**

by

Aaron John Brown, B.S.

Dissertation

Presented to the Faculty of the Graduate School of
The University of Texas Medical Branch
in Partial Fulfillment
of the Requirements
for the Degree of

Doctor of Philosophy

**The University of Texas Medical Branch
March, 2017**

Dedication

With love and gratitude to my parents, Carl and Laura Brown

Acknowledgements

I would like to start by thanking my mentor, Dr. Krishna Rajarathnam, for taking me in and for all the support he has given me. By his example, I have learned the kind of hard work it takes to succeed in science and have witnessed and learned from his passion and love for what he does. He has been an amazing mentor and I am incredibly grateful for the time I have gotten to spend learning from him. I would also like to thank my fellow lab members Prem, Mohan, and Kirti. They have been an invaluable resource and companions to me from the beginning. Thank you for welcoming me in and putting up with my constant questions. I could not have gotten to this point without you.

I would also like to thank the members of my dissertation committee: Dr. James Lee, Dr. Junji Iwahara, Dr. Roberto Garofalo, and Dr. Margaret Cheung. Thank you for your time, support, and feedback throughout my time in Galveston. And a special thanks to Dr. Lee and Dr. Iwahara who always opened their doors to me when I had a question and never turned me away.

I would also like to give a very special thanks to the love of my life, Kathy Wilson. You have been a wonderful support and so patient throughout the long years here. Living apart this whole time has not been easy, but you have constantly pushed me to do what needed to be done, and yet still made sure that I found time to enjoy life. These passed years would not have been the same without you.

I would also like to thank the wonderful people I met here in Galveston for their support and friendship. Thanks to Justin and Timi for welcoming me into their lives and

for all the fun we shared together. Dan, I'm so glad I got to know you. Lunch wouldn't be the same without you. Thanks to Tyler and Ashley, who have been wonderful friends and have made Galveston feel more like home. And of course my buddy Juan, you have been a great friend and, as you say, 'partner in crime' throughout my time here. I'm so glad we had the chance to be roommates.

Also, I would like to give a special thanks to Cory, David, Jared, and Micah. Just knowing you guys are there to always support me has been a huge blessing. Thank you.

I would like to extend a very special thanks to my family. I could not have done this without you. Thank you mom and dad for your unwavering support and love and thanks to Jeremy and Dani for just making life better, you guys are the reason I am who I am today and I am so grateful to have you in my life. Love you guys.

Finally, I'd like to thank God, through whom all things are possible and in whom I find constant love and support.

**Chemokine CXCL7 Monomer, Homodimer, and Heterodimer:
Structural Insights, CXCR2 Receptor Function, and
Glycosaminoglycan Interactions**

Publication No. _____

Aaron J. Brown, PhD

The University of Texas Medical Branch, 2017

Supervisor: Krishna Rajarathnam

Platelet-derived chemokine CXCL7 (NAP-2) plays a critical role in mediating the crosstalk between platelets and neutrophils for initiating repair during vascular injury. CXCL7 function is coupled to CXCR2 receptor activation and interactions with sulfated glycosaminoglycans (GAG) that regulate receptor activity. CXCL7 exists as monomers and dimers and there is also evidence that it could form heterodimers. Currently, nothing is known regarding the structural features of the monomer, dimer, and heterodimer, and the molecular basis by which these various forms mediate receptor and GAG interactions. We have addressed this missing knowledge as a part of this doctoral thesis. Structural characterization of each of the different CXCL7 forms was challenging because multiple species (say monomer and dimer) always coexist, and structural studies demand that only a single species is present for unambiguous characterization. Using a combination of solution conditions and concentrations, NMR spectroscopy, modeling, protein engineering, and cellular assays, the structural features of the monomer, homodimer, and heterodimer, their receptor activity, and GAG interactions have been successfully

characterized. Our findings indicated that the receptor activity and binding interactions were similar for all the variants, with the CXCR2 N-domain binding a hydrophobic groove along the CXCL7 N-loop. However, the GAG binding properties of the monomer, homodimer, and heterodimer vary, and most interestingly, dimer is favored in the GAG bound form. This was an unexpected finding as the dimer is the minor species in solution. Further, several of the residues involved in GAG binding are also involved in receptor interactions, indicating that the GAG-bound monomer, homodimer, and heterodimer cannot activate the receptor. We conclude that both homodimers and heterodimers play an important role in mediating CXCL7 function via their interactions with GAG and propose that the GAG-bound dimers regulate the steepness and duration of concentration gradients, which in turn regulates the levels of free monomer available for CXCR2 activation and neutrophil recruitment. Further, this work provides proof-of-concept that the disulfide trapping strategy can serve as a valuable tool for characterizing the structural and functional features of a chemokine heterodimer for a variety of chemokine pairs.

TABLE OF CONTENTS

List of Tables	xi
List of Figures	xii
List of Abbreviations	xvi
Chapter 1	1
Introduction.....	1
Structure and Characteristics of Chemokines	3
Chemokine Oligomerization.....	5
Role of GAG Binding	8
Chemokine Heterodimers	10
Chemokine-Receptor Interactions	11
Neutrophil Activating Chemokines	14
Characterizing CXCL7 Interactions	17
Chapter 2.....	18
Structural Basis of Native CXCL7 Monomer Binding to the CXCR2 Receptor N- domain and Glycosaminoglycan Heparin.....	18
Abstract.....	18
Introduction.....	19
Results.....	21
CXCL7 Monomer Chemical Shifts	21
Structural Model of the Native Monomer.....	23
CXCL7: CXCR2 N-domain Interactions	26
CXCL7 Monomer-Heparin dp8 Interactions	30
Discussion.....	35
Materials and Methods.....	38
Reagents and Protein Expression.....	38
Chemical Shift Assignments of the CXCL7 Monomer	38
NMR Titrations.....	39
Model of the Monomer Structure	39

Molecular Docking Using HADDOCK.....	40
Chapter 3.....	41
CXCL7 Homodimer: Structural Insights, CXCR2 Receptor Function, and Glycosaminoglycan Interactions.....	41
Abstract.....	41
Introduction.....	42
Results.....	43
CXCL7 Dimer Chemical Shift Assignments.....	44
CXCL7 Dimer-GAG Interactions.....	47
CXCL7 Dimer Binding to the CXCR2 N-domain.....	51
Discussion.....	53
Materials and Methods.....	58
Reagents and Protein Expression.....	58
Chemical Shift Assignments of the CXCL7 Monomer	58
NMR Titrations.....	58
Molecular Docking Using HADDOCK.....	59
Chapter 4.....	60
Chemokine CXCL7 Heterodimers: Structural Insights, CXCR2 Receptor Function, and Glycosaminoglycan Interactions.....	60
Abstract.....	60
Introduction.....	61
Results.....	63
NMR Characterization of CXCL7 Heterodimers	63
Molecular Dynamics of Chemokine Heterodimers	68
Design and Characterization of a Trapped Heterodimer	71
Heterodimer-GAG Interactions	75
Heterodimer Receptor Binding Activity.....	80
Discussion.....	81
Materials and Methods.....	84
Molecular Dynamics Simulations of heterodimers	84
Expression and Purification of Chemokines.....	84

NMR Characterization of Heterodimer	85
Characterization of Heparin GAG and Heterodimer	85
Heterodimer-GAG Docking	86
Receptor Activity of the Heterodimer	86
Chapter 5	88
Conclusions and Future Directions	88
Appendix A Tables and Figures	95
References	100
Vita	116

List of Tables

Table 1.1:	Dimerization/dissociation constants of neutrophil activating chemokines	16
Table 2.1:	Distribution of CXCL7 monomers, dimers, and tetramers as a function of solution conditions.....	20
Table A1:	Assignments for CXCL7 monomer	95

List of Figures

Figure 1.1: Chemokine-Receptor Interaction NetworkEr
ror! Bookmark not defined.	
Figure 1.2: Structure of a Chemokine Monomer	5
Figure 1.3: Structures of chemokine dimers and tetramers	8
Figure 1.4: Chemical structure of GAG	10
Figure 1.5: Overview of Site-I and Site-II interactions	14
Figure 1.6: Sequence alignment of neutrophil activating chemokines	16
Figure 2.1: Sequence alignment of neutrophil activating chemokines	20
Figure 2.2: NMR Characteristics of the CXCL7 Monomer	24
Figure 2.3: Structural Features of the CXCL7 monomer	27
Figure 2.4: CXCL7 monomer binding to CXCR2 N-domain	29
Figure 2.5: Model of the CXCL7-CXCR2 N-domain complex	30
Figure 2.6: CXCL7 monomer binding to heparin dp8	33
Figure 2.7: Models of the CXCL7-GAG heparin complexes	34
Figure 2.8: Overlap between GAG and CXCR2 binding domains	37

Figure 3.1:	CXCL7 dimer is the high-affinity GAG ligand	45
Figure 3.2:	^1H-^{15}N HSQC spectrum of a trapped CXCL7 dimer	47
Figure 3.3:	CXCL7 dimer binding to heparin dp26	49
Figure 3.4:	WT vs Trapped Dimer GAG Binding	50
Figure 3.5:	CXCL7 dimer-GAG binding models	51
Figure 3.6:	Sequence alignment of neutrophil activating chemokines	56
Figure 3.7:	Overlap between GAG and CXCR2 binding domains	57
Figure 4.1:	NMR characterization of chemokine heterodimers	66
Figure 4.2:	Characterization of the native CXCL7-CXCL1 heterodimer	67
Figure 4.3:	Structural features of the CXCL7 heterodimers	70
Figure 4.4:	Characterization of the CXCL7-CXCL1 Trapped Heterodimer	73
Figure 4.5:	NMR structural features of the trapped heterodimer	74
Figure 4.6:	Histogram plots of chemical shift changes on Heparin binding to trapped heterodimer	78
Figure 4.7:	NMR characteristics of trapped heterodimer-heparin interactions	79
Figure 4.8:	A model of heparin-bound CXCL7-CXCL1 heterodimer complex	80

Figure 4.9: CXCR2 activity of the heterodimer	81
Figure 5.1: Relative populations of monomer, homodimers, and heterodimers	92
Figure 5.2: Schematic of CXCL7-mediated neutrophil recruitment	93
Figure 5.3: Gradient formation in the vasculature	94
Figure A1: HSQC spectra of the pH titration from pH 4.0 to 7.0	97
Figure A2: HSQC spectrum of the C7 peak splitting	97
Figure A3: Structural features of the CXCL7-CXCL8 heterodimer	98

List of Abbreviations

AIR	Ambiguous interaction restraints
CSP	Chemical shift perturbation
CXCL	CXC ligand
CXCL7/NAP-2	Neutrophil-activating peptide 2
CXCR2	CXC chemokine receptor 2
CXCR2Nd	CXCR2 N-terminal domain
dp8	Heparin octasaccharide
dp26	Heparin 26-mer
GAG	Glycosaminoglycan
GPCR	G-protein coupled receptor
HSQC	Heteronuclear single quantum coherence
NAC	Neutrophil activating chemokine
NMR	Nuclear magnetic resonance
NOE	Nuclear Overhauser effect

Chapter 1

Introduction

An essential component of many biological processes is the directed trafficking of various cell types to the target tissue. This phenomenon is controlled by several families of signaling proteins that include growth factors, cytokines, and chemokines. Of these signaling proteins, the chemoattractant cytokines, or chemokines, play a fundamental role in host immunity either by active recruitment of leukocytes to an area of infection or injury or during regular immune surveillance¹⁻⁵. The general mechanism of trafficking involves release of chemokines, which diffuse through the surrounding tissue to the site of the target cell, often in the blood. Chemokines function by activating seven transmembrane G-protein couple receptors (GPCRs), which initiate signaling through G-protein and β -arrestin mediated pathways. These signals ultimately result in cellular motility leading to the directed movement of cells down the established chemokine gradient. Chemokines also bind to extracellular glycosaminoglycans (GAGs) that play a role in regulating the recruitment process.

Chemokines are relatively small proteins of approximately 70 to 90 amino acids in length and have a molecular weight of ~ 8 to 10 kDa. In addition to leukocyte recruitment, chemokines have been shown to play a role in proliferation, extracellular matrix remodeling, development, tissue repair, and angiogenesis⁶⁻¹². Humans express around 50 chemokines, which are classified based on the position of the first two conserved cysteines near the N-terminus as CXC, CC, CX₃C, and XC. The chemokine system exhibits incredible complexity, which in turn provides exquisite sensitivity and control. This is achieved, in part, through a complex network of receptor-chemokine interactions. Many chemokines bind multiple receptors, while others are specific to just

		Receptors																	
		CC							CXC										
		CCR1	CCR2	CCR3	CCR4	CCR5	CCR6	CCR7	CCR8	CCR9	CCR10	CXCR1	CXCR2	CXCR3	CXCR4	CXCR5	CXCR6	CX3CR1	XCR1
Chemokines	CC	CCL1	•					•											
		CCL2		•	•														
		CCL3	•		•		•												
		CCL4	X	X		•													
		CCL5	•		•	•								•					
		CCL7	•	•	•	X								X					
		CCL8	•	•	•	•													
		CCL11		•	•	•								X					
		CCL13	•	•	•	•								•					
		CCL14	•			•													
		CCL15	•		•														
		CCL16	•	•		•													
		CCL17				•													
		CCL18	X		X														
		CCL19						•						•					
		CCL20					•							•					
		CCL21						•											
		CCL22			•														
		CCL23	•																
		CCL24		X	•														
		CCL25								•									
		CCL26		X	•														
		CCL27									•								
		CCL28			•							•							
	CXC	CXCL1											•						
		CXCL2											•						
		CXCL3											•						
		CXCL4																	
		CXCL5											•						
		CXCL6										•	•						
		CXCL7											•						
		CXCL8										•	•						
CXCL9				X										•					
CXCL10				X										•					
CXCL11				X										•					
CXCL12													•		•				
CXCL13													•			•			
CXCL14																			
CXCL16																•			
CXCL17																			
CX3CL1																	•		
XCL1																		•	
XCL2																			

Figure 1.1: **Chemokine-Receptor Interaction Network.** A table of the known interactions of chemokines with their cognate receptors. Green circles represent an agonist, while red 'x' represents an antagonist. Table is adapted from Stone MJ, *et al.*, *Int J Mol Sci*, 2017.

one. Likewise, many receptors bind multiple chemokine ligands while others are very selective (Figure 1.1)^{5,13,14}. Further, these chemokine networks are regulated by both chemokine dimerization and GAG interactions that play a fundamental role in the spatial/temporal regulation of chemokine signaling. Because these multiple interactions contribute to tight regulation, dysfunction at any point along these signaling pathways will lead to collateral tissue damage and disease^{13,15}. In fact, chemokines have been implicated in a variety of inflammatory and autoimmune diseases such as rheumatoid arthritis, atherosclerosis, asthma, transplant rejection, and multiple sclerosis, as well as in diseases such as HIV, bacterial pneumonia, meningitis, and cancer¹⁶⁻²⁷. For this reason, understanding the molecular mechanisms that regulate chemokine dimerization, chemokine-receptor and chemokine-GAG interactions at each step of recruitment is essential for developing improved therapeutics for a variety of disease states.

STRUCTURE AND CHARACTERISTICS OF CHEMOKINES

One of the remarkable features of chemokines is that despite a diverse range of target receptors and functions, all chemokines have a high degree of structural homology at the monomer level. The first chemokine structure was solved in 1990 for CXCL8 (also known as interleukin-8, IL-8) using NMR spectroscopy²⁸. Since then, many different structures have been solved and all share a common “chemokine” tertiary fold. This fold is characterized by an unstructured N-terminus, followed by an N-loop, which together are responsible for binding the receptor^{29,30}. This is followed by a 3₁₀ helix that leads into three anti-parallel β -strands forming a β -sheet and a C-terminal α -helix that runs across the β -sheet (Figure 1.2)^{31,32}. This common fold also includes several conserved features, which are crucial for function. N-terminal conserved cysteines form disulfides: the first cysteine with the third cysteine on the 30s loop and the second cysteine with the fourth cysteine on the third β -strand. Removal of these disulfides results in significant structural changes and loss of function^{33,34}. For example, reduction of the first disulfide in CCL18

(MIP-4) results in reduced recruitment of T-cells³⁵. Another study showed the disulfides for CXCL8 impart structural stability that is critical for both protein fold and function³⁶. Chemokines that differ from this canonical pair of disulfides include the XC chemokines, which have only one disulfide and a group of CC-type chemokines, such as CCL15 (HCC-2) and CCL23 (MPIF-1) that have an additional disulfide³⁷⁻³⁹. There is also a group of CX chemokines from zebrafish that, like the XC chemokines, have only one canonical disulfide, yet form a total of three disulfides⁴⁰.

Another conserved structural feature is the hydrophobic core, which is required for proper chemokine folding. Mutations of residues in this core result in misfolding and loss of function. There are also conserved residues, such as proline, which are also important for protein folding⁴¹. These conserved features serve as a scaffold that present specific residues to the corresponding receptor and provide an explanation for how structural homology could result in such varied signaling pathways and binding partners¹⁵.

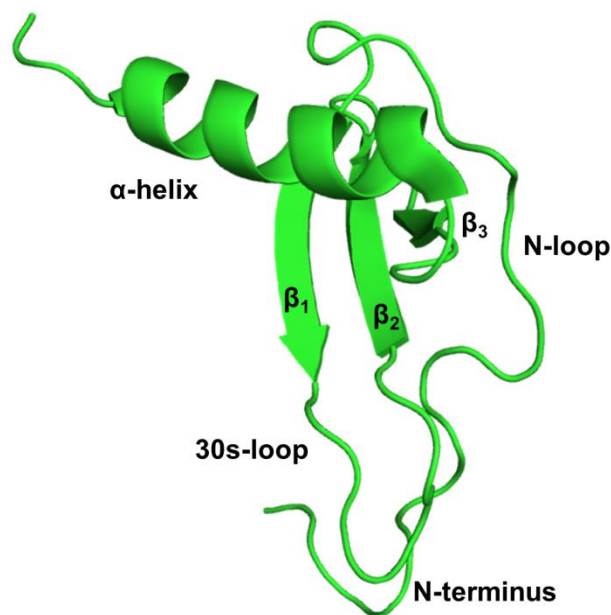


Figure 1.2: **Structure of a Chemokine Monomer.** Ribbon diagram of a typical chemokine monomer structure. The important structural elements are labeled for reference. Structure is chain A of the MGSA dimer (PDB ID: 1MGS)

CHEMOKINE OLIGOMERIZATION

Another pivotal chemokine feature is that some chemokines exist not only as monomers, dimers, but also as tetramers, oligomers, and higher order polymers. The first chemokine structure, for CXCL8, was dimeric under both NMR and X-ray conditions^{28,42,43}. Several other structures followed and were either tetrameric or dimeric. For example, the first CC-type chemokine structure was solved for CCL4 (MIP-1 β) using NMR spectroscopy and was also dimeric⁴⁴. In the structures that followed, the dimerization potential for many chemokines varied, indicating a diverse range of oligomerization properties. For instance, many of the early CC-type chemokine structures, such as that of CCL5 (RANTES), were solved at very low pH due to aggregation effects. Low pH, in turn, had a large effect on the monomer-dimer equilibrium, favoring the monomer over dimer⁴⁵⁻⁴⁷. Other chemokines such as CCL1 (I-

309), CCL15, and CCL23 do not form dimers in solution even at higher pH and high mM concentrations used in NMR studies^{38,48,49}.

Another interesting difference between chemokine oligomers was observed when comparing CC and CXC type dimers. CC dimers form an elongated structure with a new, mini β -strand along the N-terminus, anti-parallel to the corresponding monomer's N-terminus, forming a mini β -sheet (Figure 1.3A). CXC dimers form a globular structure through interactions along the first β -strand, forming an extended, six stranded β -sheet stabilized by the C-terminal helix extending over the second monomer (Figure 1.3B). The CXC type dimer interface interactions largely consist of hydrophobic packing between the first β -strand and α -helix to the corresponding monomer's β -sheet. These hydrophobic residues are more common in CXC-type chemokines than in CC chemokines⁵⁰. Another important interaction that stabilizes the CXC-type dimer is the network of six H-bonds between the β_1 -strands of each monomer. Further, some of the CXC dimers are also stabilized by electrostatic interactions between residues on the α -helix and the corresponding β -sheet or across the first two β -strands. These electrostatic interactions vary to a greater extent between different chemokines compared to packing interactions.

Structures for many chemokines fall within one of these two types of dimer structures. These include CXCL1^{51,52}, CXCL2^{53,54}, CXCL5⁵⁵, CXCL7^{56,57}, CXCL12⁵⁸, CCL2^{59,60}, CCL4⁴⁴, CCL5^{45,46}, CCL11⁴⁷, and CCL26⁶¹, where the CXC chemokines form CXC dimers and CC chemokines form CC dimers. Of course, there are exceptions to this rule. Some CC chemokines form CXC-type dimers⁶²⁻⁶⁴, while some CXC chemokines form CC-type dimers⁶⁵. Chemokines that form globular tetramers exhibit both CXC and CC dimer interfaces^{57,66,67}. Further, lymphotactin, the only member of the XC family, shows both a typical chemokine fold and a completely different fold as a function of pH and solution conditions³⁹.

On top of this complex system of different dimerization interfaces is the fact that many chemokines form tetramers and some can form higher order oligomers and polymers. CXCL4 and CXCL7, for instance, are examples of tetramers^{66,68}. They both form a globular tetramer as a dimer of CXC dimers (Figure 1.3C). Chemokines such as CCL3, CCL4, and CCL5 form high order polymers^{67,69,70}. These polymers consist of elongated tetramer units that form a linear, extended chain like structure (Fig 1.3D). These interactions are also mediated by a combination of hydrophobic and electrostatic interactions, as seen for dimers.

Observance of dimeric/oligomeric structures originally led to the belief that the dimer was the active form in vivo and that receptor binding was at least in part along the dimer interface^{29,44}. However, development of obligate monomers, as well as studies at low concentrations, showed this was not the case and that monomer was active in vivo⁷¹⁻⁷⁵. In addition, studies of the monomer-dimer equilibrium revealed monomer is likely present at physiological concentrations and is the high affinity ligand for the receptor⁷⁵. However, more recent evidence for the importance of dimerization has swung the pendulum back towards an interest in understanding the role of dimers in regulating chemokine function⁷⁶⁻⁷⁸. Furthermore, the varied oligomerization properties of chemokines, which remarkably arise from a group of proteins that have the same tertiary fold, point to the inherent structural plasticity of the dimer interface.

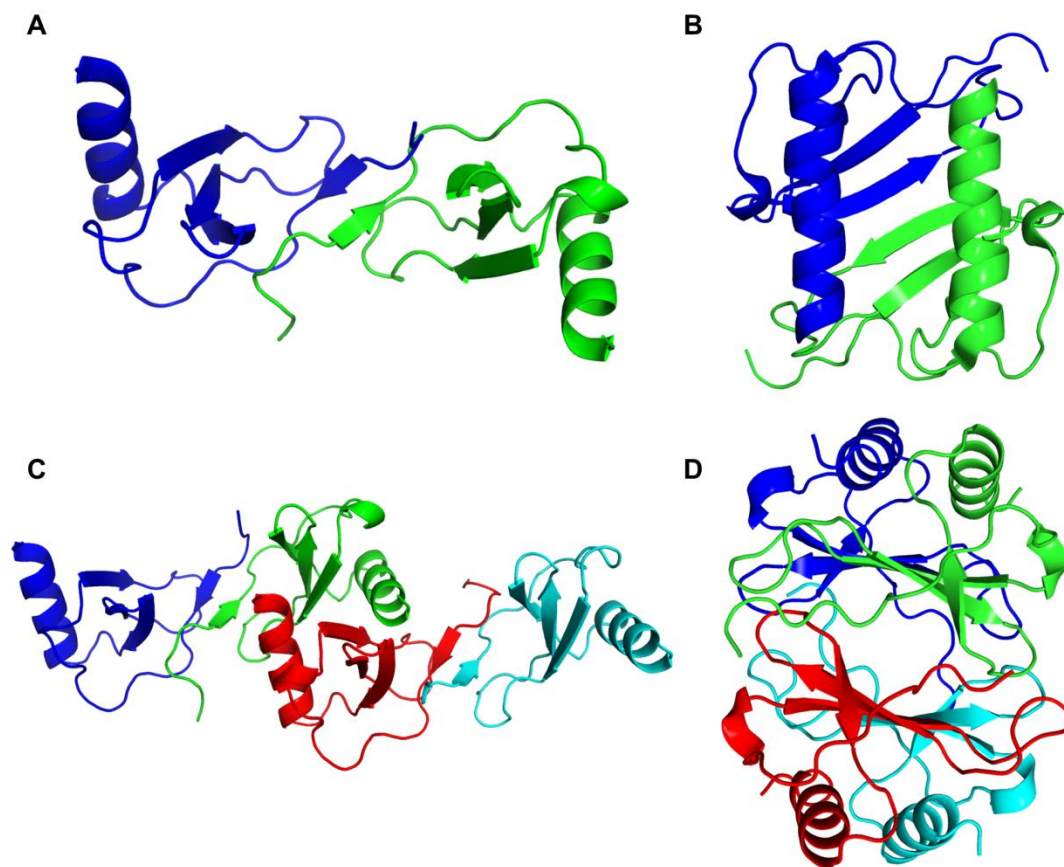


Figure 1.3: **Structures of chemokine dimers and tetramers.** (A) Structure of a CC-type dimer from CCL5 (PDB ID: 2L9H). (B) Structure of a CXC-type dimer from CXCL8 (PDB ID: 1IL8). (C) Elongated tetramer as a dimer of CC-dimers from CCL5 (PDB ID: 2L9H). Long polymers may form through the same interaction surface. (D) Globular tetramer as a dimer of CXC-dimers from CXCL7 (PDB ID: 1NAP). For each structure, each monomer subunit is represented by a different color.

ROLE OF GAG BINDING

One of the key aspects linking chemokine dimerization to function is their interactions with glycosaminoglycans (GAG). GAGs are highly sulfated polysaccharides that are commonly attached to membrane proteins and are called proteoglycans⁷⁹. They are found on many different cell surfaces, in intracellular granules of certain cell types, in the basement membranes of various tissues, as well as in the extracellular matrix^{80,81}.

GAGs also bind to a variety of proteins involved in cell growth and development, cell attachment, migration, viral invasion, organogenesis, angiogenesis, cancer, blood coagulation, inflammation, and responses to injury⁸²⁻⁹¹. The most common GAGs in relation to chemokine biology are heparan sulfate (HS) and chondroitin sulfate (CS). However, studying HS or CS in vitro is extremely challenging due to the inherent heterogeneity of GAG polysaccharides. Unlike proteins or DNA, synthesis of GAGs is not template driven, and therefore, in vitro production of uniformly sulfated GAGs is extremely challenging. For this reason, heparin is commonly used for in vitro studies as it is more or less uniformly sulfated and is commercially available at a variety of lengths. HS and heparin are also composed of the same disaccharide units, with differences mainly in their sulfation patterns, providing a rationale for using heparin as a mimic for highly sulfated regions of the HS (Figure 1.4).

All GAGs are composed of repeating units of an uronic acid and an amino sugar. In the case of HS, the basic structural unit is a β 1-4 linked D-glucuronic acid and an α 1-4 linked N-acetyl-D-glucosamine⁸⁹. The basic unit of CS is composed of a β 1-4 linked D-glucuronic acid and a β 1-3 linked N-acetyl-D-galactosamine⁹². These GAGs have varying degrees of sulfation and are often found with regions of high sulfation followed by regions of little or no sulfation. In the case of HS, sulfate groups are located at the C2 position of the glucuronic acid and at either the C6 or C3 position of the glucosamine (Figure 1.4). The structural implications of these sulfation patterns are of increasing interest. For instance, structures of largely unsulfated HS at various lengths were determined using a multidisciplinary approach and were found to have increased flexibility when compared to the heparin structure⁸⁸. These varied structures, chain lengths, and sulfation patterns may well be responsible for the differential regulation of recruitment in various tissues. For instance, our lab has shown recruitment in the lung differs from the peritoneum in a mouse model and is also dependent on the monomer-dimer equilibrium^{72,93}. Another example is CXCL7, which recruits neutrophils to the

thrombus. CXCL7 is released in relatively high concentrations from activated platelets, and the established gradient promotes leukocyte polarization and motility⁹⁴. The role of GAG in this recruitment differs from recruitment across the endothelium, and further highlights the contextual importance of GAG-binding. Therefore, knowledge of the molecular mechanisms that mediate GAG interactions is essential to understand the link between GAG binding, chemokine dimerization/oligomerization, and gradient formation for a host of biological systems.

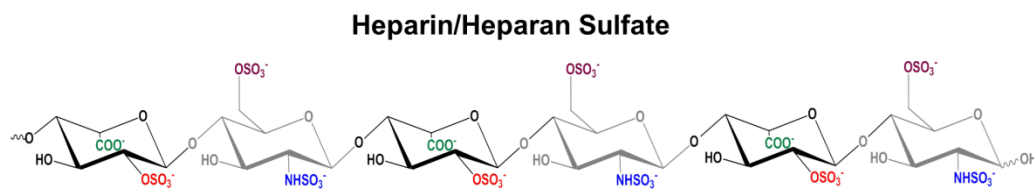


Figure 1.4: **Chemical structure of GAG.** The chemical structure for heparin is shown. The potential sulfation sites are highlighted in red, blue, and purple. Heparan sulfate has the same composition as heparin, except for differences in epimerization of the carboxylate group (green) and sulfation patterns.

CHEMOKINE HETERODIMERS

As addressed above, chemokine oligomerization and GAG interactions play an important role in regulating chemokine function. However, recent evidence indicates an additional interaction may add a further layer to the complexity: formation of chemokine heterodimers. Considering the high structural homology between chemokines, that many chemokines form similar types of dimers, and that many chemokines are co-expressed *in vivo*, it follows that chemokines are capable of forming heterodimers. However, very little is known regarding heterodimer formation i.e., which chemokines form

heterodimers, how heterodimer formation relates to homodimer, and how heterodimer regulates chemokine function in vivo?

Several studies to date have provided evidence for chemokine ‘synergy,’ wherein the presence of multiple chemokines results in enhance or altered activity⁹⁵⁻¹⁰¹. Synergy is thought to play a role at the onset of inflammation, or when multiple chemokines are present at high concentrations. However, heterodimer formation is not the only possible explanation for chemokine synergy. Altered receptor signaling and competitive GAG interactions, in addition to heterodimer formation, have all been proposed to play a role in the synergistic effect¹⁰²⁻¹⁰⁵. Nevertheless, several studies have provided evidence that chemokines do form heterodimers. For example, heterodimer formation was shown for CXCL4 and CXCL8 using NMR¹⁰⁶, for several CC-type chemokines using mass spectrometry¹⁰⁷, for a number of CC and CXC chemokines using molecular dynamics¹⁰⁸, and for platelet-derived chemokines using mass spectrometry¹⁰⁹. Further, the functional potential of chemokine heterodimers was demonstrated for CXCL4 and CCL5 using a peptide inhibitor to disrupt heterodimer formation, resulting in reduced plaque formation in an atherosclerosis mouse model¹¹⁰. These studies provide strong evidence for the importance of chemokine heterodimers, but fail to provide the structural features and molecular mechanisms that dictate heterodimer formation. Further, these studies don’t provide insights into how heterodimers interact with their cognate receptors or GAGs. Characterizing these interactions is crucial towards understanding how heterodimers contribute to regulating chemokine function.

CHEMOKINE-RECEPTOR INTERACTIONS

For chemokines, the primary mode of signal transduction is via binding and activating seven transmembrane G-protein coupled receptors (GPCRs). This binding causes structural changes in the GPCR that lead to the activation of G-protein mediated

signaling pathways. These signaling pathways involve the release and activation of associated G α i and G β γ subunits. The G α i subunit is converted to its GTP-bound, active state and dissociation results in upregulation of intracellular messengers such as cAMP, Ca²⁺, diacylglycerol and inositol-1,4,5-triphosphates. G β γ subunits activate PI3K which phosphorylates PI₂ to PI₃. These signals activate several further pathways that lead to motility, growth, and gene expression^{111,112}. In addition, GPCRs also signal through β -arrestin pathways that promote receptor internalization or activate downstream signals such as MAPK¹¹³.

From the perspective of the chemokine, the important interaction is the initial binding of the chemokine to the extracellular portion of the receptor. However, determining the structural characteristics of the chemokine-receptor complex is challenging. While chemokine structures have been extensively characterized, the receptors are much more difficult due to the inherent challenges that come with studying membrane proteins. The first GPCR structure was solved for rhodopsin¹¹⁴. Other structures followed, which provided structural insights into receptor structure and activation, especially for the rhodopsin family of receptors¹¹⁵. Recently, the structure of free CXCR1, as well as other chemokine receptors bound to an antagonist or small molecule inhibitor has been reported^{116,117}. However, there is still no structure for CXCR2 or for a chemokine bound receptor. Sequence analysis of chemokine receptors indicates that most receptors have similar structural motifs consisting of seven transmembrane domains, three extracellular loops, three cytoplasmic loops, an unstructured N-terminal domain, and a C-terminal segment that binds to the associated G-protein. Comparison to the known structures suggests that the extracellular loops and N-terminal domain are likely close together in space and held together by disulfide bonds¹¹⁸. This is important because a variety of studies have shown that the N-terminus and N-loop of chemokines bind to the N-terminus and one or more extracellular loops of the target receptor^{33,34,41,119-145}.

These studies have resulted in a two-site binding model to describe chemokine-receptor interactions. Site-I consists of interactions between the N-loop of the chemokine and the N-terminal domain of the receptor. Site-II consists of the N-terminal domain of the chemokine interacting with one or more extracellular loops and transmembrane regions of the receptor (Figure 1.5). The binding affinity for a chemokine to its target receptor is thus a composite of Site-I and Site-II binding and coupled interactions. This has been shown through several mutagenesis studies and chimeric chemokines that have also shown Site-I (chemokine N-loop) is responsible for binding affinity and selectivity, while Site-II (chemokine N-terminus) is essential for binding affinity and activation¹³. For instance, swapping N-loop residues in CXCL1 and CXCL8 resulted in a swap of receptor specificity¹⁴⁶. Further, addition of a single methionine to the CCL5 N-terminus resulted in loss of activity, and deletion of the first two N-terminal residues in CXCL12 resulted in no change to the binding affinity, but resulted in loss of activity^{58,147}. These studies have laid the groundwork for understanding chemokine-receptor interactions. However, there is still a lack of insight into the structural basis and molecular mechanisms that dictate these interactions for a variety of chemokine-receptor pairs, and understanding these interactions is critical for developing therapeutics for chemokine-mediated diseases.

In lieu of the two-site model and the difficulty in determining receptor structures, a divide and conquer approach is an appropriate alternative for studying Site-I interactions. In this method, a peptide from the extracellular N-terminus of the receptor is used to examine the interactions with its cognate chemokine. As an early example, the structure of CXCL8 complexed to the CXCR1 receptor N-terminal domain was determined and provided insights into the structural features that mediate binding and selectivity¹⁴¹. A similar approach has been used for various chemokine-receptor pairs using NMR and other biophysical techniques^{30,139,148-154}. These studies provided valuable structural information on chemokine-receptor interactions and also provide proof of

concept for using the same approach to study other chemokine pairs, such as CXCL7 with the N-terminal domain of CXCR2.

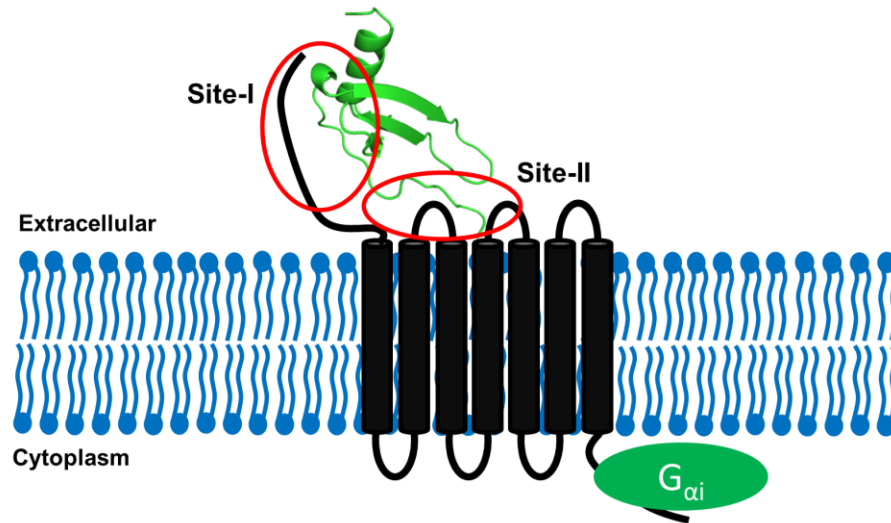


Figure 1.5: **Overview of Site-I and Site-II interactions.** A schematic of a GPCR embedded in the cellular membrane. The chemokine binds first to Site-I, and then to the extracellular loops at Site-II that activates the receptor. The signal is propagated through the receptor resulting in release of the bound G-proteins (green circle).

NEUTROPHIL ACTIVATING CHEMOKINES

In addition to the location of conserved cysteine residues, chemokines are often grouped based on their functional roles and receptor interactions¹⁵⁵. One such group of CXC-type chemokines are characterized by their N-terminal 'ELR' motif as well as their role as agonists for the CXCR1 and CXCR2 receptor. The members of this subfamily include CXCL1, CXCL2, CXCL3, CXCL5, CXCL6, CXCL7, and CXCL8 (Figure 1.6). Aside from CXCL3 and CXCL6, structures of the others are known. Though all form CXC-type dimer, there are some interesting differences. Most of these chemokines form dimer with a low μM K_d . However, CXCL7 forms a much weaker dimer with a $K_d > 100$

μM . Despite this weak dimer, CXCL7 is the only one of this group to form a tetramer. In addition, the solution conditions have different effects on dimer formation for different chemokines. For CXCL8, dimerization is favored at lower pH compared to higher pH^{75,156}. CXCL7, on the other hand, weakly dimerizes at low pH but forms a relatively stronger dimer at higher pH (Table 1.1)⁷³. These properties likely contribute to differential regulation for each chemokine.

Among their many functions, these ‘ELR’ chemokines are responsible for recruiting neutrophils to the site of tissue injury and infection¹⁵⁷. The mechanism of recruitment involves production of these chemokines from various cell types including epithelial cells and resident macrophages in response to signaling molecules such as TNF- α and IFN- γ . These chemokines travel across the endothelium into the blood stream, where they bind to GAGs on the endothelial surface. GAG bound chemokine regulates the availability of the free chemokine for activating CXCR1 (in the case of CXCL8) and CXCR2 receptors on circulating neutrophils. Receptor activation results in cellular migration to the site of infection via chemokine gradients^{158,159}. Once at the site of infection, neutrophils can fulfill their role in killing microbes and perpetuating the inflammatory response¹⁶⁰. Neutrophils accomplish this by releasing proteases, antimicrobial peptides, and reactive oxygen species that serve to kill and clear any microbes¹⁶¹, phagocytosis of foreign microbes for further clearance and killing^{160,162}, and finally they release their chromatin along with a host of other proteins as neutrophil extracellular traps that play a further role in killing microbes^{163,164}.

While the general mechanism of neutrophil recruitment is shared among these chemokines, many have specialized roles in a variety of systems. These roles highlight how the individual structural characteristics of a chemokine further contribute to the specificity of chemokine-mediated recruitment. As an example, CXCL5 plays a role in recruitment in the lung and adipose tissue, and has also been connected to cancer metastasis and obesity¹⁶⁵⁻¹⁶⁸. In comparison, CXCL7 plays a role in recruiting neutrophils

into the thrombus during clot formation, as demonstrated by a CXCL7 knockout mouse model⁹⁴. As discussed above, these varied roles can be attributed to altered structural characteristics, GAG binding properties, and/or receptor binding characteristics.

```

              1      10      20      30      40      50      60
CXCL7  -----AELRCMIKTTSG-IHPKNIQSLEVIQKGTHCNQVEVIATLKDGRKICLDPDAPRIKKIVQKKLAGDESAD
CXCL1  ----ASVATELRCQCLQTLQG-IHPKNIQSVNVKSPGPHCAQTEVIATLKNGRKACLNPASPIVKKIIIEKMLNSDKSN-
CXCL2  ----APLATELRCQCLQTLQG-IHLKNIQSVKVKSPGPHCAQTEVIATLKNGQKACLNPASPMVKKIIIEKMLKNGKSN-
CXCL3  ----ASVVTELRCQCLQTLQG-IHLKNIQSVNVKSPGPHCAQTEVIATLKNGKKACLNPASPMVQKIIIEKILNKGSTN-
CXCL5  AGPAAAVLRELRCVCLQTTQG-VHPKMISNLQVFAIGPQCSKVEVVASLKNGKEICLDPEAPFLKKVIQKILDGGNKEN
CXCL6  -GPVSAVLTELRCCLRVTLR-VNPKTIGKLQVFAPGQCSKVEVVASLKNGKQVCLDPEAPFLKKVIQKILDSGNKKN
CXCL8  -----SAKELRCQIKTYSKPFHPKFIKELRVIESGPHCANTEIIVKLSDGRELCLDPKENWVQRVVEKFLKRAENS-

```

Figure 1.6: **Sequence alignment of neutrophil activating chemokines.** Conserved residues are highlighted in red, and the ‘ELR’ motif responsible for activating the CXCR1 and CXCR2 receptors are in green.

Protein	Dissociation Constant (μ M)	Solution Conditions	Reference
CXCL1	4	50mM Na-Phos, 100 mM NaCl, pH 7.0, 20°C	Rajaratnam, et al. J. Biol. Chem. 1996
	43	50 mM Na-Phos, 100mM NaCl, pH 5.0, 20°C	Same as above
CXCL5	0.5	50 mM Phos, pH 6.0	Sepuru, et al., PLOS One, 2014
CXCL7	53	50mM Na-Phos, 100mM NaCl, pH 7.0, 20°C	Rajaratnam, et al. J. Biol. Chem. 1996
	102	50mM Na-Phos, 100mM NaCl, pH 5.0, 20°C	Same as above
	300 (monomer:dimer)	250 mM NaCl, pH 7.0, 30°C	Yang, et al., J. Biol. Chem. 1994
	900 (dimer:tetramer)	Same as above	Same as above
CXCL8	21	Phosphate-buffer, pH 7.4, 8°C	Paolini, J. F., et al., J. Immunol. 1994
	14	20mM NaPO ₄ , 150mM NaCl, pH 7.4, 25°C	Burrows, S. D. et al., Biochemistry, 1994
	18	same as above, except at 37°C	Same as above
	<0.1	50 mM phos, pH 5.7, 20°C	Lowman, et al. Protein Sci. 1997
	12	50 mM Phos, pH 7.0	Rajagopalan, et al., Biophys. J. 2007

Table 1.1: **Dimerization/dissociation constants of neutrophil activating chemokines.** A compilation of known binding constants at various buffer conditions.

CHARACTERIZING CXCL7 INTERACTIONS

In this dissertation, the structural basis and molecular mechanisms that regulate CXCL7 monomer-dimer formation, GAG binding, receptor interactions, and heterodimer formation were investigated. These interactions are critical to the controlled recruitment of neutrophils into the thrombus. During recruitment, CXCL7 is released in high concentration from activated platelets. In addition, platelet granules contain a variety of other chemokines, including neutrophil activating chemokines. CXCL7 also has the unique property of forming a weak dimer, yet also forming a tetramer. These characteristics make CXCL7 an ideal system for gaining fundamental insights into the native chemokine monomer-GAG interactions, characterizing the structural basis of heterodimer formation, and elucidating the role of GAG binding in heterodimer mediated regulation.

In order to characterize these interactions, we use an NMR based approach, along with protein engineering, biochemical, and modeling techniques. NMR is extremely useful for observing interactions of monomer, homodimer, and heterodimer in equilibrium, and is the only technique that can simultaneously give insights into the molecular level interactions involved in binding. Protein engineering was used to develop a disulfide linked trapped homodimer and heterodimer for structural and functional studies. Together, these experiments have provided valuable insights into the molecular mechanisms that regulate chemokine-receptor, chemokine-chemokine, and chemokine-GAG interactions for CXCL7 and related neutrophil activating chemokines.

Chapter 2

Structural Basis of Native CXCL7 Monomer Binding to the CXCR2

Receptor N-domain and Glycosaminoglycan Heparin

ABSTRACT

CXCL7/NAP-2, a chemokine highly expressed in platelets, orchestrates neutrophil recruitment during thrombosis and related pathophysiological processes by interacting with CXCR2 receptor and sulfated glycosaminoglycans (GAG). CXCL7 exists as monomers and dimers, and dimerization ($\sim 150\mu\text{M}$) and CXCR2 binding ($\sim 10\text{nM}$) constants indicate CXCL7 is a potent agonist as a monomer. Currently, nothing is known regarding the structural basis by which receptor and GAG interactions mediate CXCL7 function. Using solution NMR spectroscopy, we characterized the binding of CXCL7 monomer to the CXCR2 N-terminal domain (CXCR2Nd) that constitutes a critical docking site and to GAG heparin. We found that CXCR2Nd binds a hydrophobic groove and that ionic interactions also play a role in mediating binding. Heparin binds a set of contiguous basic residues indicating a prominent role for ionic interactions. Modeling studies reveal that the binding interface is dynamic and that GAG adopts different binding geometries. Most importantly, several residues involved in GAG binding are also involved in receptor interactions, suggesting GAG-bound monomer cannot activate the receptor. Further, this is the first study that describes the structural basis of receptor and GAG interactions of a native monomer of the neutrophil-activating chemokine family.

INTRODUCTION

Chemokines, a large family of signaling proteins, mediate diverse biological functions including inflammation, development, and tissue repair^{4,5,8}. Chemokines mediate their function by activating seven transmembrane G-protein coupled receptors (GPCRs) and binding sulfated glycosaminoglycans (GAGs) that regulate receptor function^{78,169,170}. Another key feature of chemokines is their ability to reversibly exist as monomers and dimers, and sometimes as higher order oligomers. Humans express ~ 50 different chemokines, which are classified on the basis of conserved cysteines near the N-terminus as CXC, CC, CX₃C, and XC. Chemokine CXCL7 (also known as NAP-2), released by activated platelets, plays a prominent role in recruiting neutrophils to the injury site during thrombosis^{94,171,172}. CXCL7 belongs to a subset of CXC neutrophil-activating chemokines (NACs) that are characterized by an N-terminal 'ELR' motif and function as potent agonists for the CXCR2 receptor¹⁵⁷. Other members of the ELR-chemokines include CXCL1, CXCL2, CXCL3, CXCL5, CXCL6, and CXCL8 (Figure 2.1).

Monomer-dimer equilibrium constants have been determined for CXCL1, CXCL5, CXCL7, and CXCL8. Among them, CXCL7 stands out, as it forms a much weaker dimer^{55,73,156,173}. Whereas the dimerization constant for CXCL7 is ~ 100 to 200 μ M, the values for other chemokines vary around ~1 to 10 μ M. Our early dilution experiments confirmed that the dimer levels increase with increasing concentration up to a point after which tetramer levels populate, and dimer levels do not go beyond ~50% at any given condition (Table 2.1). The structure of CXCL7 determined by crystallography corresponded to the tetrameric state⁵⁷, which is not surprising, as crystallography by its very nature results in the higher oligomeric state. The solution structure of a CXCL7 monomer determined in the presence of 2-chloroethanol that is known to disrupt

intermolecular dimer and tetramer interactions has been reported, but its coordinates are not available in the public domain⁵⁶.

```

          5    10    15    20    25    30    35    40    45    50    55    60    65    70
CXCL7 -----AELRCMCIKTTSG-IHPKNIQSLEVIGKGTNCNQVEVIATLKDGRICLDPDAPRIKKIVQKKLAGDESAD
CXCL1 ----ASVATELRCQCLQTLQG-IHPKNIQSVNVKSPGPHCAQTEVIATLKNGKACLNPASPIVKKIIEKMLNSDKSN-
CXCL2 ----APLATELRCQCLQTLQG-IHLKNIQSVKVKSPGPHCAQTEVIATLKNGQKACLNPASPMVKKIIEKMLKNGKSN-
CXCL3 ----ASVTELRCQCLQTLQG-IHLKNIQSVNVKSPGPHCAQTEVIATLKNGKACLNPASPMVQKIIEKILNKGSTN-
CXCL5 AGPAAAVLRELRCVCLQTTQG-VHPKMISNLQVFAIGPQCSKVEVVASLKNGEICLDPEAPFLKKVIQKILDGGNKEN
CXCL6 -GPVSAVLTELRCTCLRVTLR-VNPKTIGKLQVFAPGQCSKVEVVASLKNGKQVCLDPEAPFLKKVIQKILDSGNKKN
CXCL8 -----SAKELRCQCIKYSKFPFHPKFIKELRVIESGPHCANTEIIVKLSDGELCLDPKENWVQRVVEKFLKRAENS-

```

Figure 2.1: **Sequence alignment of neutrophil activating chemokines.** Conserved ‘ELR’ motif is shown in green. Basic residues that mediate GAG and receptor interactions and hydrophobic residues that mediate receptor interactions for CXCL7 identified in this study are shown in blue and red, respectively. The corresponding residues in other chemokines are likewise highlighted. Residues K9 and R54 shown to be involved in binding only in CXCL7 are italicized and underlined.

Concentration (μ M)	pH	Temp (C)	Buffer	Distribution
77	4.2	35°	50 mM NaPi	~95% M, ~5% D
77	4.4	35°	50 mM NaPi	~85% M, ~15% D
77	5.0	35°	50 mM NaPi	~80% M, ~20% D
77	6.0	35°	50 mM NaPi	~70% M, ~30% D
77	7.0	35°	50 mM NaPi	~65% M, ~35% D
77	7.5	35°	50 mM NaPi	~60% M, ~40% D
77	7.5	25°	50 mM NaPi	~65% M, ~35% D
77	7.5	35°	50 mM NaPi , 100 mM NaCl	~65% M, ~35% D
300	4.0	35°	50 mM NaPi	~95% M, ~5% D
300	4.0	25°	50 mM NaPi	~95% M, ~5% D
300	6.0	35°	50 mM NaPi	~50% M, ~50% D
450	6.0	35°	50 mM NaPi	~55% D, ~45% M
600	6.0	35°	50 mM NaPi	M/D/T*
840	6.0	35°	50 mM NaPi	~100% T

Table 2.1: **Distribution of CXCL7 monomers, dimers, and tetramers as a function of solution conditions.** M, D, T stand for monomer, dimer, and tetramer, respectively. Pi = phosphate. ‘*’ indicates monomer, dimer, and tetramer levels could not be determined reliably.

Receptor binding and activity measurements have shown that CXCL7 binds CXCR2 with nanomolar (nM) affinity, indicating the monomer is a potent agonist¹⁷⁴. Presently, nothing is known regarding the structural basis or molecular mechanisms by which the CXCL7 monomer interacts with the receptor. Knowledge of the GAG interactions is also essential as GAG interactions regulate receptor function. Using solution nuclear magnetic resonance (NMR) spectroscopy, we characterized the binding of the native CXCL7 monomer to the CXCR2 N-terminal domain (N-domain) that functions as a critical ligand binding site and heparin that serves as a representative and well-studied, sulfated GAG. Towards this end, we first assigned the chemical shifts of the native monomer that are essential for characterizing receptor and GAG interactions and also developed a chemical shift-based structural model of the CXCL7 monomer. We observed that receptor binding is largely mediated by hydrophobic interactions, that electrostatic and H-bonding interactions also play a role, and that the CXCR2 N-domain binds a groove comprising the N-loop and adjacent β -strand residues. On the other hand, heparin binding is predominantly mediated by electrostatic interactions. We observed that heparin adopts different binding geometries and that the binding interface is highly plastic. Most interestingly, our data indicate that GAG-bound CXCL7 monomer cannot bind the receptor. Further, this is the first study characterizing the GAG and receptor interactions of a native neutrophil activating chemokine monomer.

RESULTS

CXCL7 Monomer Chemical Shifts

Chemical shifts are exquisitely sensitive to local changes in the electronic environment, and as such, serve as useful probes for mapping the binding interface of macromolecular interactions. The binding interface is inferred from binding-induced chemical shifts obtained from heteronuclear single quantum coherence (HSQC) titrations of an unlabeled ligand to a ¹⁵N-labeled protein. Therefore, knowledge of the native

CXCL7 monomer chemical shifts is essential to describe the molecular basis of receptor and GAG interactions. We first characterized how monomer/dimer/tetramer levels vary as a function of buffer, temperature, and pH from relative peak intensities in the 2D HSQC spectra. A summary of the distribution is shown in Table 1.1. Our data indicate that pH had the highest impact, with the monomer dominating at lower pH and tetramer dominating at higher pH. The dimer was always observed in the presence of monomer or tetramer and was not prevalent at any pH. Other variables such as temperature, ionic strength, and buffer condition had much less effect. On the basis of these experiments, a 300 μ M sample at pH 4.0 was selected for monomer assignments. Under these experimental conditions, the protein exists as 95% monomer with the remaining 5% as dimer. The HSQC spectrum under these conditions is shown in Figure 2.2A. A table of the chemical shifts is also provided (Table A1). Because receptor and GAG interactions were carried out at $\text{pH} \geq 6$, which better reflects physiological conditions, chemical shifts at these pH were needed. HSQC spectra were recorded as a function of pH from 4.0 to 7.5 that allowed assigning monomer chemical shifts at the higher pH despite elevated dimer levels. The backbone assignments at pH 6.0 were also confirmed using triple resonance experiments. Interestingly, HSQC spectra collected as a function of pH also identified several intramolecular interactions. The M6 amide proton is significantly downfield shifted at higher pH (Figure 2.2B), and the corresponding residue in various human and murine chemokines is also downfield shifted^{28,51-55,175}. On the basis of previous mutagenesis studies in CXCL8 and CXCL1, the chemical shift profile of M6 can be attributed to an intramolecular H-bond between the E35 side chain carboxylate and M6 amide proton¹⁷⁶. The K17 amide proton is likewise downfield shifted at higher pH (Figure 2.2C), which can be attributed to H-bonding to the imidazole group of H15⁴². The corresponding residue in other NACs has also been shown to be downfield shifted. Mutagenesis studies in related NACs have also shown that these interactions are critical for receptor function^{132,177}. Further, significant chemical shift changes were observed for

C7, and most interestingly, two distinct peaks at pH 5.0 and a distinct shoulder could also be observed at higher pH (Figure A2). Structures have shown that the disulfides are dynamic and that the disulfides, in addition to structure, also play crucial roles in receptor function¹⁷⁸.

Structural Model of the Native Monomer

A structure of the ethanol-induced monomer of CXCL7 has been previously reported, but its coordinates are not available in the protein data bank⁵⁶. Generally, nuclear Overhauser effect (NOE)-driven structures require a sufficient number of long-range NOEs to describe different structural elements, their relative orientation, and the global fold. We could not obtain sufficient unambiguous long range NOEs to generate a structure. In particular, NOEs between the β -strands and the helix could not be unambiguously assigned. As our objective was to characterize the binding of the monomer, and not determine the monomer structure *per se*, we generated a chemical shift-based structure.

It is now well established that ^1H , ^{15}N , $\text{C}\alpha$, and $\text{C}\beta$ chemical shifts can give an accurate structural model provided related structures are available. We first used our chemical shifts to predict the secondary structure and backbone torsion angles using TALOS-N^{179,180}. Secondary structure prediction indicated three β -strands, an α -helix, as well as a structured N-loop commonly observed in chemokines. Predicted torsion angles were also well within favorable limits for a folded protein. We then generated a *de novo* monomer structure using CS-ROSETTA. The resulting structure was a well-folded protein with all the major chemokine structural motifs (Figure 2.3A). The torsion angles and intramolecular H-bonds were analyzed, and the torsion angles for 67 residues fall within favorable limits with the remaining three falling within acceptable limits.

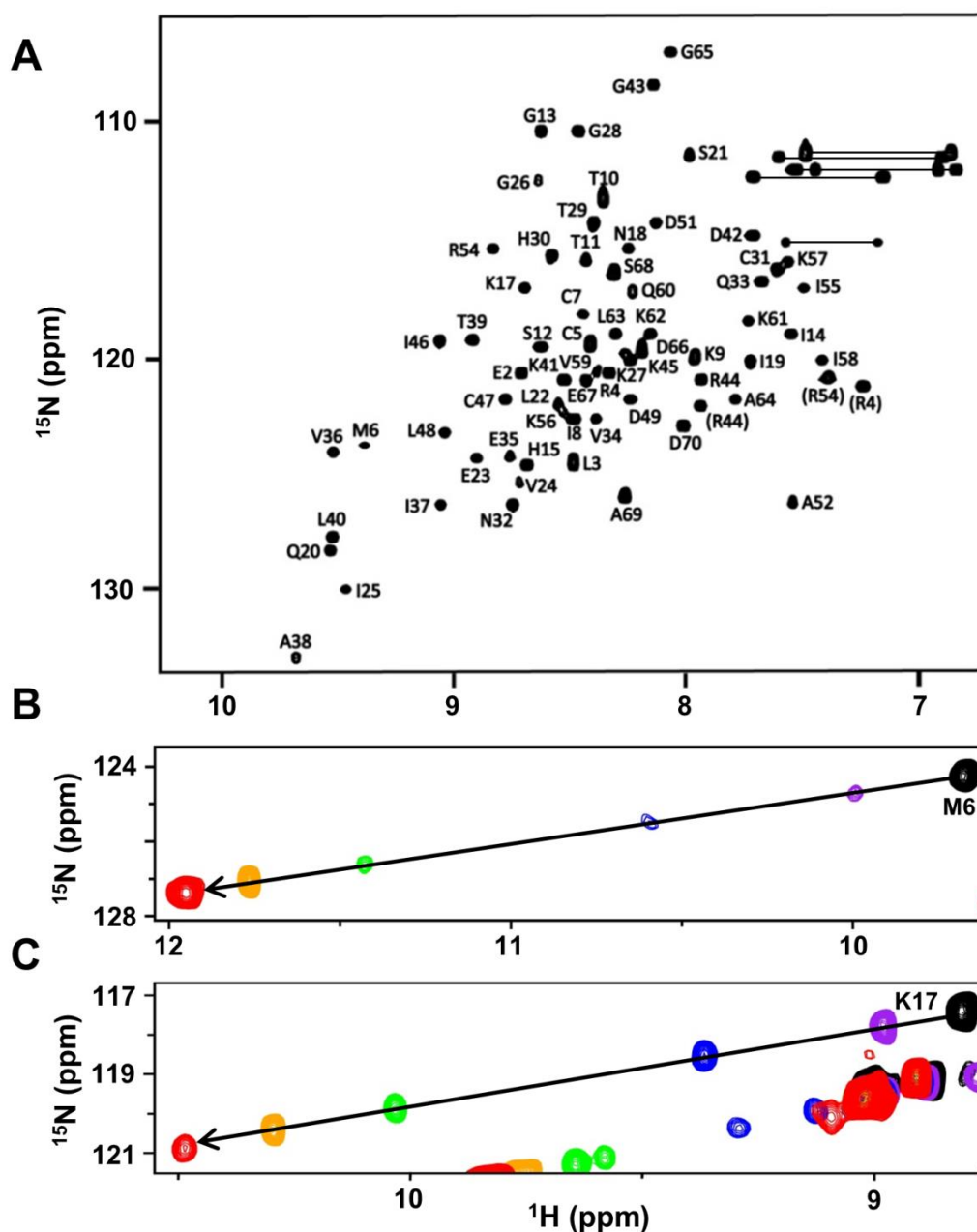


Figure 2.2: **NMR Characteristics of the CXCL7 Monomer.** (A) The HSQC spectrum shows excellent chemical shift dispersion indicating a well-folded single species at pH 4.0. The folded arginine side chain peaks are indicated in closed brackets. (B,C) Large chemical shift changes observed as a function of pH are shown for M6 and K17. Transition is from pH 4.2 (black), 4.4 (purple), 5.0 (blue), 5.5 (green) 6.0 (orange), and 7.0 (red).

We next compared the new monomer structure to the previously described monomer units of the tetramer crystal structure (PDB ID 1NAP)⁵⁷. Superimposition of the monomer units from the tetramer reveals a backbone root-mean-square deviation (RMSD) of 0.32Å for structured β -strands and α -helix (Q20-G26, V34-L40, and R44-A64). The new monomer structure showed a backbone RMSD of 0.82Å compared to the monomer units of the tetramer over the same regions, and differences in these regions are mainly due to extended β -strands and a slight change in the orientation of the helix. The largest differences between the new monomer and the tetramer structure were observed for the N-terminus and 30s-loop residues, which can be attributed to their conformational flexibility^{56,181,182} (Figure 2.3A). In general, the more dynamic a region is, the greater the difference in its backbone RMSD. We further examined the N-loop and helical regions as these are potentially involved in GAG and receptor interactions. Overall, the N-loop and helix closely resemble those of the crystal structure, with an average backbone RMSD of 0.64 Å. The CS-based structure has a helix that spans from residues 54-64, similar to that observed in the tetramer. It is interesting that residues 65 to 70 are also unstructured in the tetramer, as C-terminal residues adopt a more defined helical structure in other NAC dimers. For instance, in CXCL8, the last six residues (66 to 72) are unstructured in the monomer whereas the helix extends up to residue 70 in the dimer structures^{28,175}. Similarly, only the last two or three residues are unstructured in the CXCL1 and CXCL5 dimer structures^{51,52,55}. A shorter helix in CXCL7 could in part explain weak dimerization, as the corresponding residues in other NAC structures are involved in favorable interactions across the dimer interface.

To better understand the dynamic properties of the native monomer, we also carried out backbone ^1H - ^{15}N -heteronuclear relaxation measurements. Heteronuclear NOEs are sensitive to motions in the picosecond-nanosecond timescale. Structured residues tend to have high NOE values (~ 0.8), and less structured or dynamic residues have lower NOE values. Our data indicated that the N-terminal residues preceding the

CXC motif, C-terminal residues 66 to 70, and parts of the N-loop are dynamic, while the rest of the protein appears highly ordered (Figure 2.3B). Comparison of our data to the previously reported relaxation data of CXCL7 in the presence of chloroethanol shows striking differences for the 30s loop residues. Heteronuclear NOE measurements in the presence of 2-chloroethanol indicate a highly dynamic 30s loop, especially residues Q33, V34, and E35, showing very low NOE values observed for the very terminal residues, whereas our values are similar to those of structured residues^{56,181,182}. These observations suggest that chloroethanol influences dynamic properties, and so these data may not fully reflect the dynamics of the native protein.

CXCL7: CXCR2 N-domain Interactions

Currently nothing is known regarding the structural basis of how CXCL7 binds the CXCR2 receptor. Previous studies have indicated a two-site binding model for chemokine-receptor activation^{13,142,183}. Site-I, which functions as a critical docking site, involves interactions between the chemokine N-loop region and receptor N-terminal domain. Site-II functions as the activating site and involves interactions between the chemokine N-terminal domain and receptor extracellular/transmembrane residues. As characterizing the structural basis of binding to the whole receptor is experimentally challenging, albeit possible¹⁸⁴, we used a divide and conquer approach to characterize the Site-I binding of CXCL7 to a CXCR2 N-terminal domain peptide. Such an approach has been extensively used to characterize Site-I interactions for a number of chemokines using different biophysical techniques including solution NMR spectroscopy^{30,139,148-154}.

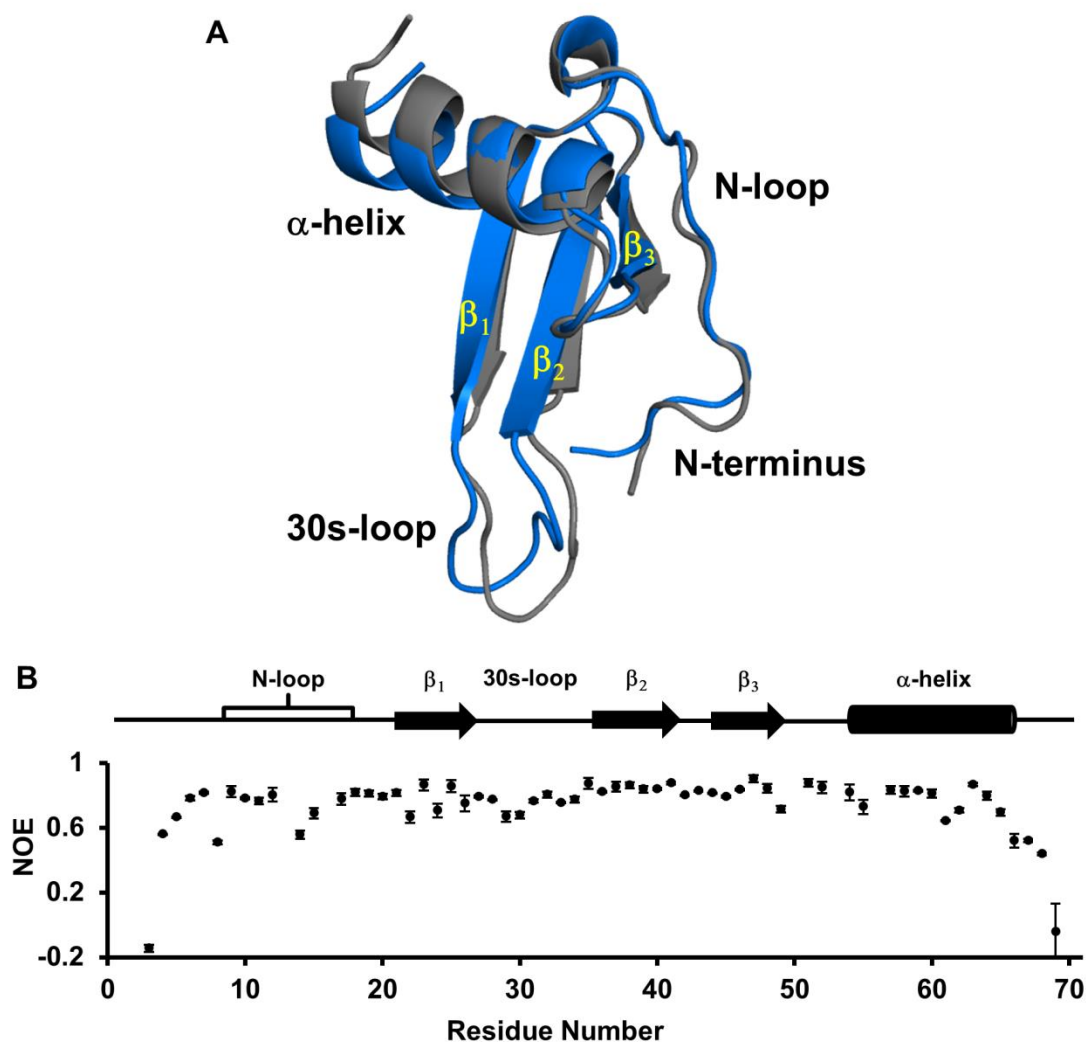


Figure 2.3: **Structural Features of the CXCL7 monomer.** (A) Ribbon diagram of the CS-based CXCL7 monomer (blue) overlaid on a monomer of the tetramer (gray). Major structural regions are labeled. (B) Heteronuclear NOE data of the native CXCL7 monomer is shown. Secondary structural elements are given for reference.

The native chemokine monomer binding to the CXCR2 N-terminal domain (CXCR2Nd) was characterized at pH 6.0 using 2D-HSQC NMR titration experiments. Significant chemical shift perturbations (CSP) were observed for hydrophobic residues M6, G13, I14, I46 and A52, polar residues C7, T10, T11, N18, Q20 and C47, and charged residues K17, E23, D49, R54, and the R44 side chain (Figure 2.4). Most of these residues constitute a continuous surface primarily along the N-loop and adjacent β -strand.

The perturbation of cysteines is likely due to indirect interactions, as these residues are buried and so cannot be involved in direct interactions. Residues Q20 and E23 are located on the opposite face from the other residues, suggesting their perturbations are also due to indirect interactions.

To gain further insight into the binding, a model for the CXCR2Nd-CXCL7 monomer complex was generated using HADDOCK-based calculations that utilize CSP data as ambiguous interaction restraints along with shape complementarity and energetics to drive the docking process. Modeling revealed a single binding mode with the N-domain nestled along a groove between the N-loop and the β_3 -strand. Binding in our model is principally mediated by packing interactions between CXCL7 residues I8, T11, I14, and I46 and CXCR2 residues L28, L29, A31, and C34 (Figure 2.5). Comparison of the chemokine sequences reveal that these residues are highly conserved (Figure 2.1), further indicating they are critical to receptor binding. These observations also suggest that the CSP of M6, T10, and A52 are due to indirect interactions. In addition, several transient interactions for charged and polar residues are observed in many, but not all, of the models. These include an aromatic π -stacking interaction between CXCL7 H15 and CXCR2 F27 and an H-bonding interaction between CXCL7 K17 side chain NH_3^+ and CXCR2 S22 side chain hydroxyl groups. CXCL7 R54 is also involved in binding, forming either an H-bond between its guanidine side chain and CXCR2 P28 backbone carbonyl or a cation- π interaction with CXCR2 F27 (Figure 2.5). The remaining residues were not involved in direct binding interactions, indicating their CSPs are likely due to binding-induced structural changes. Interestingly, H-bonding interactions were observed between the CXCL7 K9 side chain NH_3^+ and the CXCR2 D30 carboxylate, though K9 showed no chemical shift perturbation. It is likely that the absence of chemical shift changes is due to cancellation between contributions from direct and indirect interactions of similar magnitudes but opposite sign. Lack of CSP of lysine residues involved in GAG binding has been previously observed in other chemokines¹⁸⁵⁻¹⁸⁸. The docking model and

CSP data collectively indicate that hydrophobic packing, guided by H-bonding and ionic interactions, mediates Site-I binding.

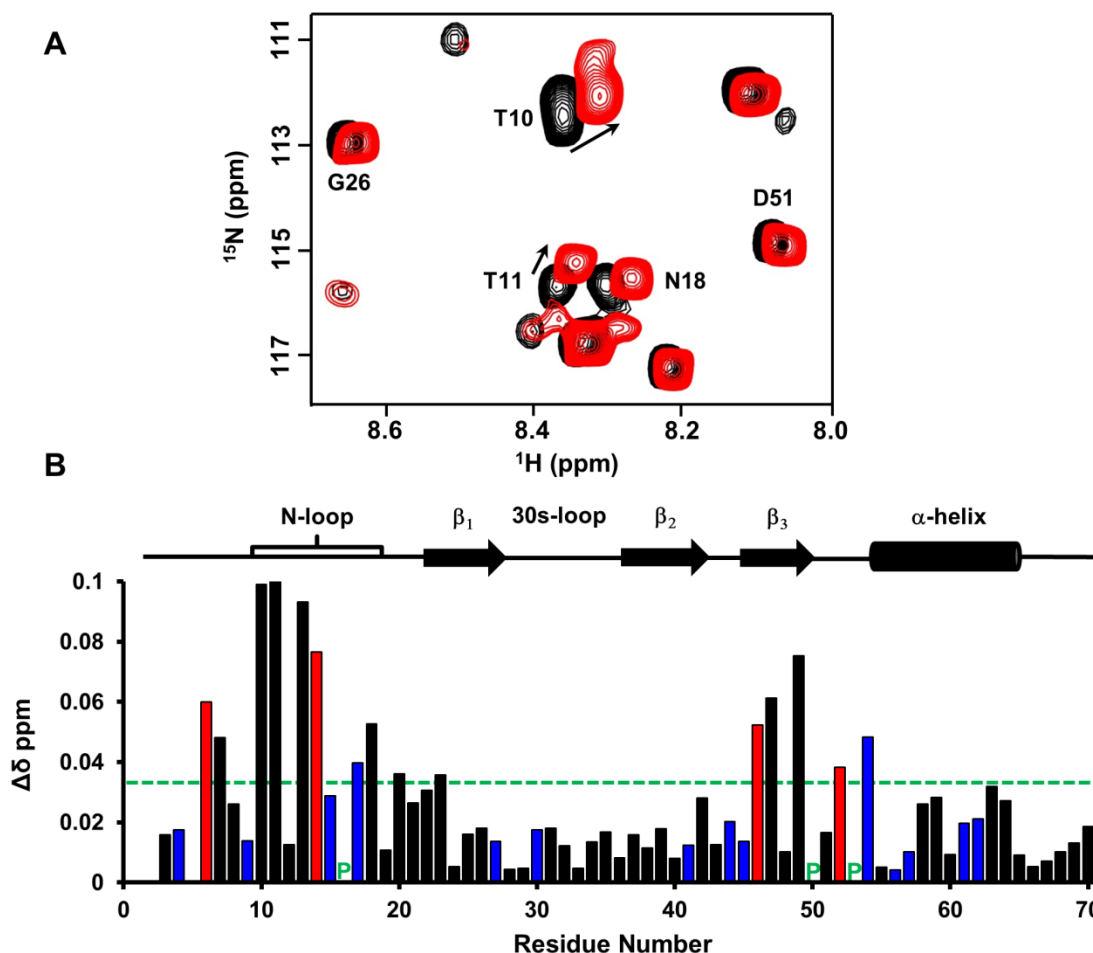


Figure 2.4: **CXCL7 monomer binding to CXCR2 N-domain.** (A) Portion of the 2D HSQC spectrum showing the overlay of CXCL7 in the free (back) and in the presence of CXCR2 N-domain at 1:3.5 molar ratio (red). Residues showing significant perturbations are labeled and arrows indicate the direction of the peak movement. (B) Histogram plot of binding-induced chemical shift changes in the CXCL7 monomer as a function of amino acid sequence. Basic residues are shown in blue. Hydrophobic residues with significant CSP are shown in red. Prolines are indicated by a green 'P'. Residues that show CSP above the threshold (dashed line) are considered involved in binding. Secondary structural elements are given for reference.

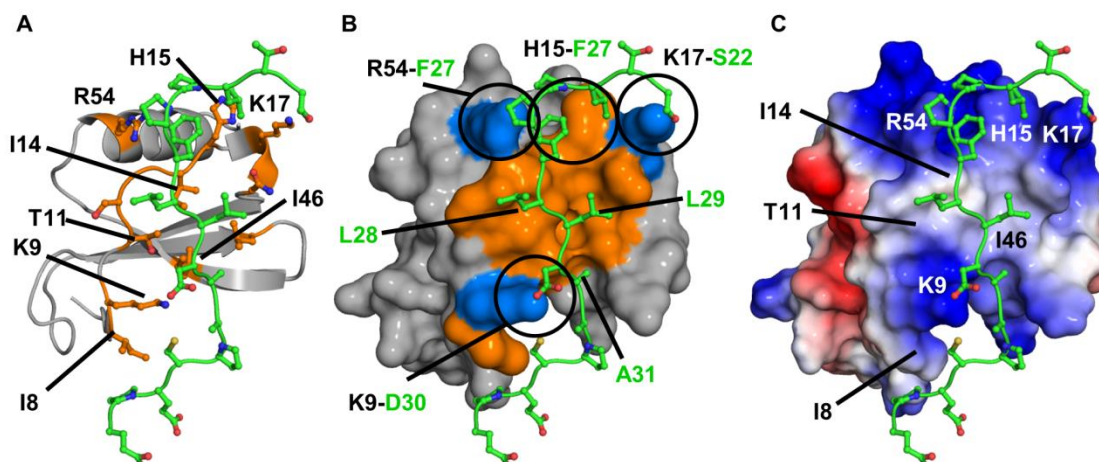


Figure 2.5: **Model of the CXCL7-CXCR2 N-domain complex.** (A) The ribbon diagram highlights the important binding residues on CXCL7 (orange). The receptor peptide is shown in green. (B) A surface filling model of the complex in the same orientation as shown in Panel A, highlighting residues involved in packing (orange) and ionic (blue) interactions. Several intermolecular interactions are circled and CXCL7 and receptor residues are labeled in black and green, respectively. (C) A schematic of the electrostatic surface in the same orientation as shown in Panels A and B highlighting the hydrophobic pocket and the flanking basic residues. Important CXCL7 residues are labeled for reference.

CXCL7 Monomer-Heparin dp8 Interactions

CSP analysis of heparin dp8 titrated into CXCL7 showed significant perturbation for residues in the N-loop, β_3 -strand, and the α -helix (Figure 2.6). As basic residues are known to mediate GAG binding, we focused on residues K9, H15, and K17 from the N-loop, R44 from the β_3 -strand, and R54, K56, and K57 from the helix. Peaks corresponding to residues H15 and K17 are broadened out in the free protein but appear during the GAG titration, indicating they are dynamic in the free form and become structured upon binding. We could measure the CSP for K17 as the peak appears early in the titration but not for H15 as it appears late in the titration. CSPs of hydrophobic and acidic residues, which are located either proximal to basic residues or on the C-terminal helix (residues L63-E67) are likely due to indirect interactions. Chemical shift

perturbations reveal that helical residues L63-E67 are unstructured in the free form, and the observation that the shifts move upfield in the bound form suggests that GAG binding stabilizes and promotes formation of the helix. Further, as the peaks corresponding to monomer and homodimer could be tracked simultaneously, we note that the equilibrium does not shift upon GAG binding and that monomer continues to dominate, indicating the monomer and dimer have similar affinities to heparin dp8.

To gain insight into the binding geometry, models of the dp8-bound monomer structures were generated using HADDOCK. All significantly perturbed residues, including hydrophobic and negatively charged residues, were used as restraints in generating the models. However, all of the models showed interactions with only basic residues indicating that the CSP of non-basic residues must be due to indirect interactions. Docking models resulted in several families, and interestingly, no one family could satisfy all of the residues that were perturbed in NMR CSP measurements. Models indicate that all binding geometries share a common core consisting of H15 and K17 of the N-loop and R54 of the α -helix. Whereas residues corresponding to H15 and K17 are highly conserved, R54 is unique and only present in CXCL7 (Figure 2.1). The GAG chain adopts three different orientations about this core due to selective binding to the peripheral residues K9, R44, or K57, defined as models A, B, and C, respectively (Figure 2.7). Structures failed to show interactions for K56, which is oriented away from the N-loop and towards the dimer interface, indicating its CSP perturbations are due to indirect interactions. The same is true of the C-terminal residues L63 to E67, further supporting our hypothesis that their CSPs are due to structural changes. These data collectively indicate that the binding interface is plastic, and that multiple binding geometries mediate monomer-GAG interactions. Additional docking experiments, where one of the peripheral residues K9, R44, or K57 were excluded, resulted in the two remaining geometries with no additional new geometries (Figure 2.7).

The only previous monomer-GAG characterization is for CXCL8 using an engineered monomer¹⁸⁵. Interestingly, the binding interactions for the CXCL8 monomer were more stringent, with a single binding geometry similar to that observed in model A. The more stringent geometry is mediated by a much larger core domain involving six residues in contrast to only three in CXCL7. Additional core residues in CXCL8 include the C-terminal helical residues R60, K64, K67, and R68 (corresponding to K57, K61, A64, and G65 in CXCL7). The smaller core in CXCL7 appears to grant more degrees of freedom, allowing the GAG to adopt a range of geometries about the core. Another key difference is K11 in CXCL8, the residue corresponding to K9 in CXCL7, which shows no interactions, and instead, K15 (equivalent to G13 in CXCL7), a residue unique to CXCL8, mediates binding. These data collectively indicate that both conserved and specific residues play differential roles in mediating GAG interactions and binding geometry in a chemokine-specific manner.

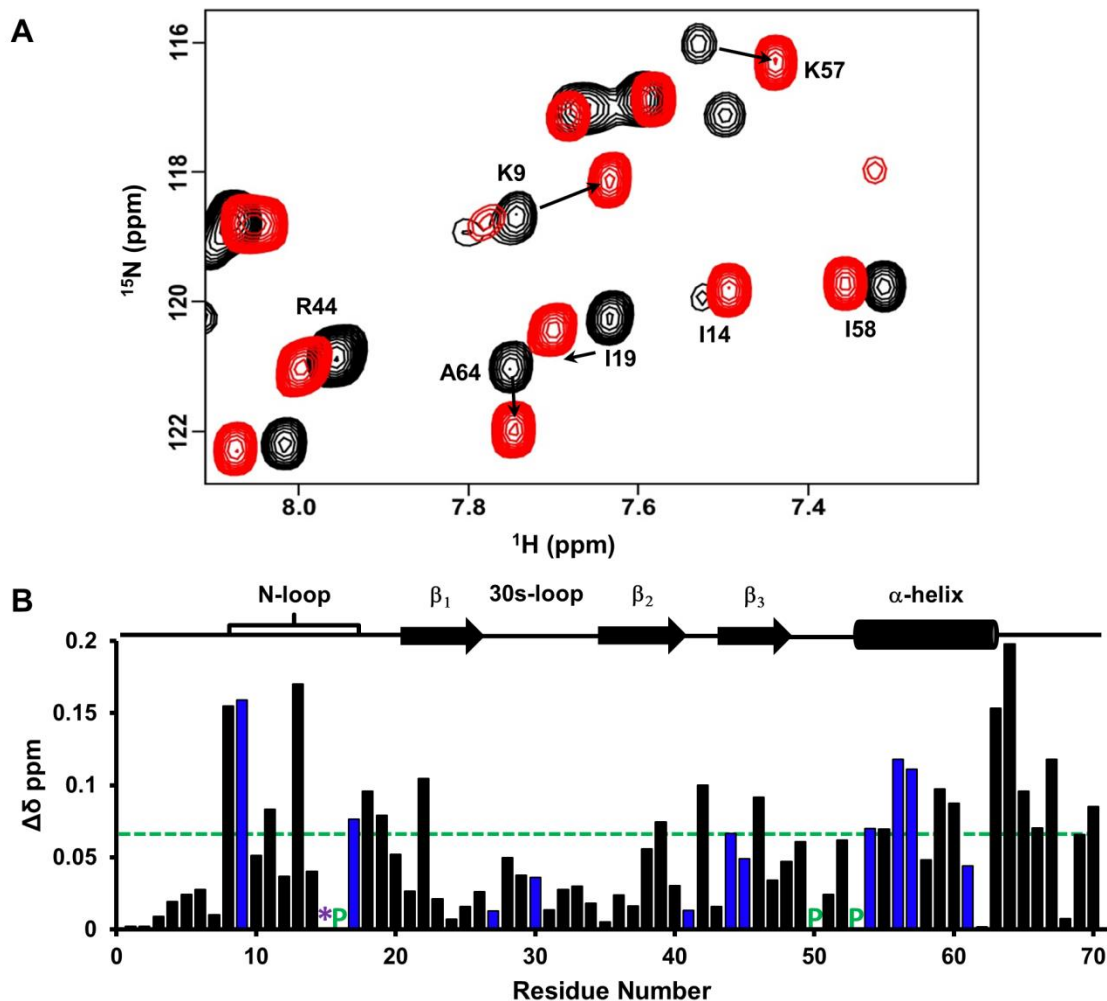


Figure 2.6: **CXCL7 monomer binding to heparin dp8.** (A) Portion of the HSQC spectrum showing the overlay of CXCL7 in the free (black) and in the presence of heparin dp8 at a 1:4 molar ratio (red). Residues that show significant perturbation are labeled. (B) Histogram plot of binding-induced chemical shift changes in CXCL7 monomer as a function of amino acid sequence. Residues that show CSP above the threshold (dashed line) are considered perturbed. Basic residues Arg, Lys, and His are shown in blue. Residue H15 is broadened out in the free spectra and is represented by a '*'. Prolines are shown by a green 'P'. Secondary structural elements are given for reference.

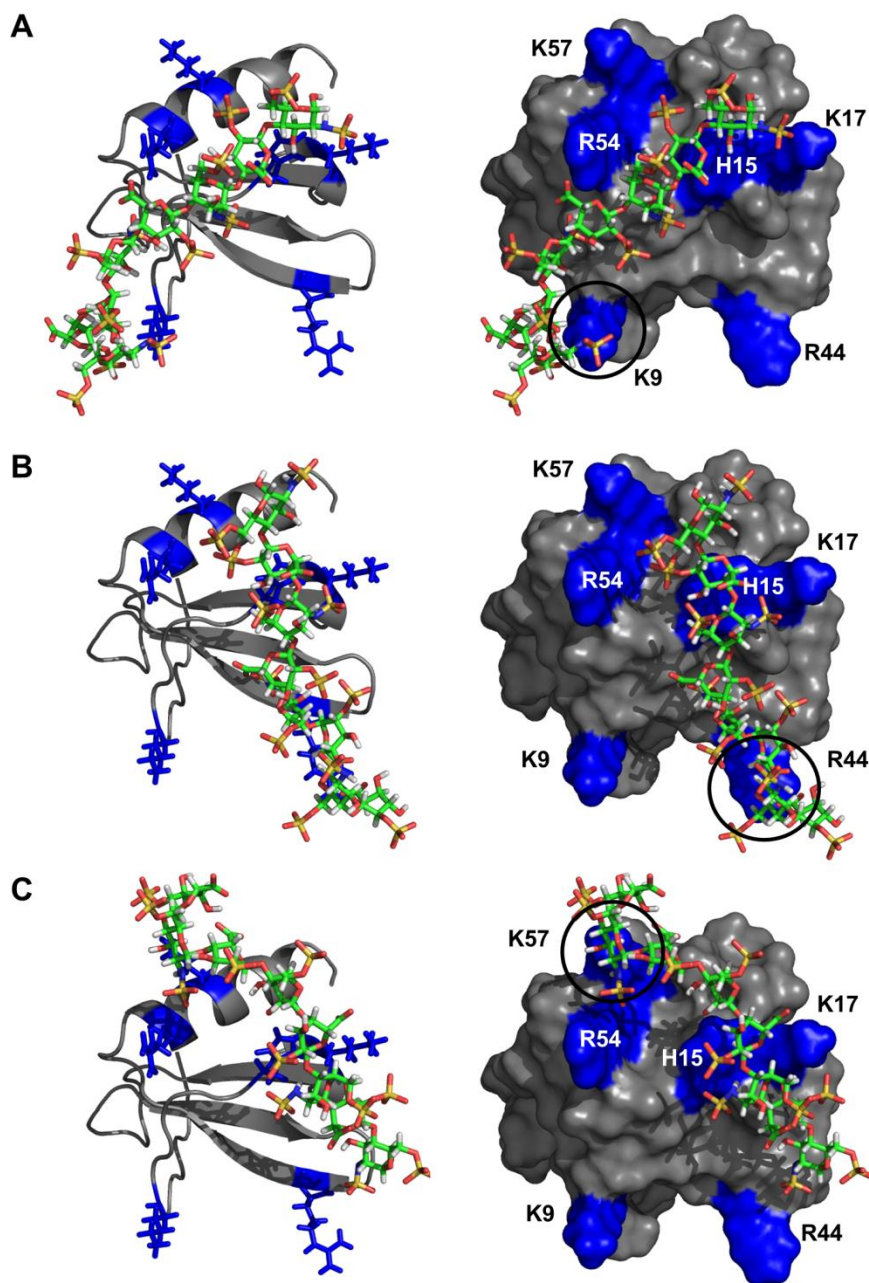


Figure 2.7: **Models of the CXCL7-GAG heparin complexes.** Different binding geometries that arise due to differences in peripheral interactions are shown in panels A to C, respectively. Left column shows the ribbon diagram of the CXCL7 monomer, with GAG and positively charged side chains shown as sticks. Right column shows the surface plots. Arg, Lys, and His residues are highlighted in blue and labeled.

DISCUSSION

CXCL7 plays a critical role in recruiting neutrophils to a variety of tissues, and dysregulation in this process has been implicated in inflammatory diseases such as rheumatoid arthritis, acute lung injury, and COPD¹⁸⁹⁻¹⁹¹, as well as a variety of cancers^{192,193}. One of its primary functions involves neutrophil-platelet crosstalk during vascular injury, as it is released at relatively high concentrations from activated platelets and provides cues for directed neutrophil migration to the injury site⁹⁴. However, nothing is known regarding the molecular level interactions between CXCL7 and its target receptor CXCR2 and GAGs.

As a member of the neutrophil activating chemokine family, CXCL7 shares several properties such as a similar tertiary structure and activation of CXCR2 via the conserved 'ELR' motif. However, CXCL7 is unique, as it alone forms a weak dimer and also a tetramer at high concentrations, whereas other members form stronger dimers and no tetramers. Previous NMR studies have characterized binding interactions for native CXCL1, CXCL5, and CXCL8 dimers and engineered CXCL1 and CXCL8 monomers as only dimers could be studied at concentrations used for NMR^{148,150,185,187,188}. In this study, for the very first time, the binding interactions of a native neutrophil activating chemokine monomer have been characterized. By exploiting the weaker dimerization propensity and carefully varying solution conditions and protein concentration, the monomer chemical shifts could be assigned that allowed mapping of the binding interactions and the generation of structural models.

In addition to the ligand structure, knowledge of the receptor and ligand-receptor complex structures is also essential to fully describe residue-specific relationships between structural features, conformational changes, and function. In recent years, structures of the free CXCR1 receptor and of other chemokine receptors bound with an antagonist and small molecule inhibitors have been reported^{116,117}. However, structures of

CXCR2 or the agonist-CXCR2 complex are not available. Therefore, our approach using the isolated N-domain and NMR chemical shift perturbation experiments can provide critical structural information that is otherwise difficult to obtain. Further, NMR CSP-based methods have been shown to be extremely useful for describing residue-specific GAG interactions, as protein-GAG complexes are notoriously difficult to crystallize. The CXCL7 monomer chemical shift assignments were previously reported in the presence of 2-chloroethanol^{56,194}. Chemical shifts from this study were similar but not identical, and interestingly, heteronuclear relaxation data of the monomer showed a structured 30s loop whereas previous studies carried out in the presence of chloroethanol showed substantial dynamics similar to those observed for terminal residues. These observations highlight that dynamic studies carried out in the presence of reagents that disrupt native H-bonding interactions must be interpreted with caution.

NMR and modeling studies suggest that the N-loop and adjacent β -strand residues of CXCL7 mediate CXCR2 Site-I interactions. The binding mode and the nature of these interactions are similar to that observed for other CXCR2-activating chemokines CXCL1, CXCL5, and CXCL8^{77,148,150,188}. Binding is principally mediated by hydrophobic packing interactions that are conserved across the NAC family (Figure 2.1). However, charged residues unique to CXCL7 such as K9 and R54 also mediate binding, suggesting that such interactions finetune receptor activation and confer chemokine-specific function to what at first glance seems a redundant chemokine system. High resolution X-ray or NMR structures are essential to confirm and better describe the binding interactions at a single residue level.

Another important aspect of CXCL7 function is its interaction with GAGs. It is now well established that GAG binding plays a pivotal role in regulating chemokine signaling and establishing chemotactic/haptotactic gradients. Chemokines in solution form chemotactic and in GAG-bound form haptotactic gradients, but whether it is the GAG-bound or free chemokine that activates the receptor is not well understood. Our

results indicate that GAG binding to the CXCL7 monomer is highly plastic and that GAG adopts multiple geometries. Independent of the binding models, a number of residues that mediate GAG interactions are also involved in receptor interactions indicating that the GAG-bound CXCL7 monomer cannot bind the receptor (Figure 2.8). Both monomer and dimer bound heparin dp8 with similar affinity and hence binding had no effect on the monomer-dimer equilibrium. During active neutrophil recruitment and tissue injury, it is very likely that local concentrations can vary by orders of magnitude, and so it is possible that the levels of different oligomeric states and their GAG interactions are highly coupled and regulate *in vivo* function. We conclude that GAG interactions provide spatial and temporal control of monomer receptor activity by modulating the amount of free chemokine and that the interplay between monomer-receptor and monomer-GAG plays an important role in mediating neutrophil recruitment in response to vascular injury.

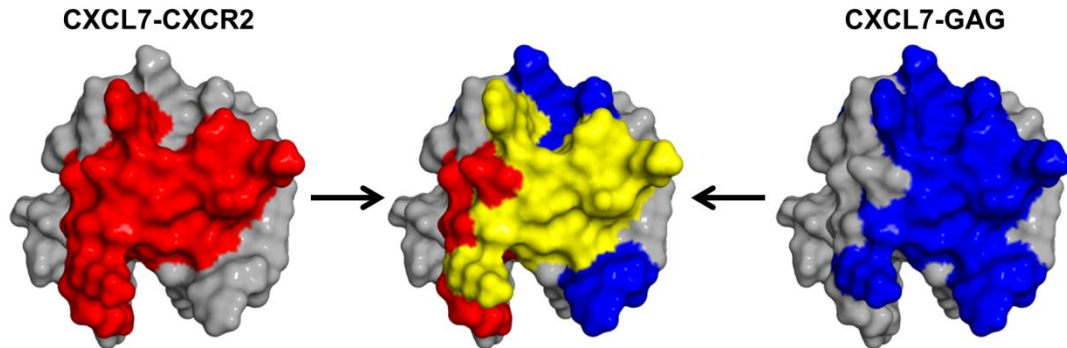


Figure 2.8: **Overlap between GAG and CXCR2 binding domains.** A schematic showing the CXCR2 binding domain (red), GAG binding domain (blue), and the overlap between the two domains (yellow).

MATERIALS AND METHODS

REAGENTS AND PROTEIN EXPRESSION

CXCL7 was expressed in *E. coli* cultured in either LB or $^{15}\text{N}/^{13}\text{C}$ enriched minimal medium and purified using a combination of nickel column and reverse phase high-performance liquid chromatography as described previously¹³⁹. Purified protein was then lyophilized and stored at -20 °C until further use. The recombinant CXCR2 N-domain (residues 1-43) peptide was expressed using the same protocol as described above. Heparin dp8 oligosaccharide was purchased from Iduron. According to the manufacturer, the oligosaccharides were purified using high resolution gel filtration chromatography, consist mainly of the disaccharide unit IdoA,2S-GlcNS,6S (~75%), show some variation in sulfation pattern, and contain uronic acid at the non-reducing end and a C4-C5 double bond as a result of the heparinase endolytic action.

CHEMICAL SHIFT ASSIGNMENTS OF THE CXCL7 MONOMER

NMR spectra were acquired using Bruker Avance III 600 and 800 MHz spectrometers equipped with cryoprobes and processed and analyzed using either Bruker Topspin 3.2 or Sparky programs¹⁹⁵. Monomer chemical shift assignments were determined at 30 °C using a 300 μM protein sample in 50 mM phosphate, pH 4.0 containing 1 mM 2,2-dimethyl-2-silapentanesulfonic acid (DSS), 1 mM sodium azide, and 10% D_2O . The ^1H and ^{15}N chemical shifts were assigned using 3D ^1H - ^{15}N heteronuclear NOESY and TOCSY experiments with mixing times of 150 and 80 msec, respectively. The carbon chemical shifts assigned from HNCA and CBCACONH experiments at pH 6.0 also helped in resolving some of the ambiguous assignments. The chemical shifts are shown in the supplementary material (Table S2). 2D ^1H - ^{15}N HSQC spectra collected from pH 4.0 to 7.5 in 0.5 increments were used to assign the backbone chemical shifts over this pH range.

NMR TITRATIONS

Binding interactions of CXCR2 N-terminal domain and heparin dp8 to WT CXCL7 were characterized using solution NMR spectroscopy. A series of ^1H - ^{15}N HSQC spectra were collected upon titrating either CXCR2 N-domain peptide or heparin to WT CXCL7 until no change in the chemical shifts were observed. The protein concentrations selected were high enough to obtain good quality spectra in a reasonable period. In the case of CXCR2 N-domain, we titrated 320 μM CXCR2 N-domain to 77 μM WT CXCL7 in 50 mM phosphate buffer at pH 6.0 and 35 °C. The final molar ratio of CXCL7: CXCR2 N-domain was 1:3.5. For CXCL7-GAG interactions, we titrated 10 mM heparin dp8 to a 50 μM sample in 50 mM phosphate pH 7.4 at 35 °C. The final molar ratio for CXCL7: octasaccharide was 1:4. For all titrations, chemical shift perturbations were calculated as a weighted average of changes in the ^1H and ^{15}N chemical shifts as described⁷⁷.

MODEL OF THE MONOMER STRUCTURE

The monomer structure was generated using CS-Rosetta, a robust tool for generating *de novo* structures from NMR chemical shifts^{196,197}. The program uses the PDB database to select protein fragments based on the given backbone C_α , C_β , N, and NH chemical shifts and then assembles and relaxes these fragments into a converged structure using a ROSETTA Monte Carlo approach. Disulfide bonds were absent in the initial structure and subsequently added using PyMol¹⁹⁸. The structure was subjected to constrained energy minimization to allow the disulfides to adopt proper geometry, followed by global energy minimization and structural analysis using the AMBER 12 suite and VADAR^{199,200}.

MOLECULAR DOCKING USING HADDOCK

Molecular docking of CXCR2Nd and heparin to the CXCL7 monomer was carried out using the High Ambiguity Driven biomolecular DOCKing (HADDOCK) approach as described previously^{185,187,201,202}. The CXCL7 monomer structure determined using CS-Rosetta, the unstructured CXCR2 N-terminal peptide generated in Pymol, and the NMR structure of heparin (PDB ID: 1HPN)²⁰³ were used for docking. Ambiguous Interaction Restraints (AIRs) were selected based on NMR chemical shift perturbation results. The pair-wise “ligand interface RMSD matrix” over all structures was calculated and the final structures were clustered using an RMSD cut-off value of 7.5 Å for CXCR2Nd and 4 Å for heparin. The clusters were then prioritized using RMSD and ‘HADDOCK score’ (weighted sum of a combination of energy terms).

Chapter 3

CXCL7 Homodimer: Structural Insights, CXCR2 Receptor Function, and Glycosaminoglycan Interactions

ABSTRACT

Platelet-derived chemokine CXCL7 (also known as NAP-2) plays a critical role in mediating the crosstalk between platelets and neutrophils for initiating repair during vascular injury. CXCL7 function is coupled to CXCR2 receptor activation and interactions with sulfated glycosaminoglycans (GAG) that regulate receptor activity. Previous studies have established that CXCL7 dimer always exists in the presence of monomer or tetramer and that the monomer dominates at lower and tetramer at higher concentrations. These observations then raise the question: what, if any, is the role of the dimer? In this study, we make a striking observation that dimer is actually favored in the GAG-bound form. Further, we successfully characterized the structural basis of dimer-GAG interactions using solution NMR spectroscopy. The chemical shift assignments, though challenging, were accomplished using a multi-prong strategy that included a disulfide-linked obligate dimer and exploiting heparin binding-induced NMR spectral changes in the WT monomer and dimer. We also observe that the receptor interactions of the dimer are similar to the monomer and that GAG-bound dimer is occluded from receptor interactions. We conclude that the dimer does play an important role, and that GAG-bound dimer regulates the levels of free monomer available for CXCR2 activation and neutrophil recruitment.

INTRODUCTION

Chemokines, a large family of signaling proteins, mediate diverse biological functions including inflammation, development, and tissue repair^{4,5,32}. Common to all of these functions is the directed movement of cells to their desired targets. Directed trafficking must be tightly controlled, as dysregulation leads to collateral tissue damage and disease^{8,16,160}. Chemokines mediate their function by activating seven transmembrane G-protein coupled receptors (GPCRs) and binding glycosaminoglycans (GAGs) that regulate receptor function^{78,169}. Another key feature of chemokines is their ability to reversibly exist as monomers and dimers. Animal model studies have shown that the property of existing as monomers and dimers and GAG interactions are coupled and is fundamental to function^{72,204}.

CXCL7 is a member of a subset of seven chemokines, characterized by their N-terminal ELR motif, that function as agonists for the CXCR2 receptor. CXCR2 is expressed in neutrophils and in other cell types including cancer cells, and so these chemokines have been implicated in cellular trafficking in response to bacterial and viral infections and tissue injury as well as in various cancer models^{8,16,25,192,193,205}. These chemokines also share the property of reversibly existing as monomers and dimers and interacting with GAGs. CXCL7, specifically, plays a prominent role in recruiting neutrophils to the injury site during thrombosis⁹⁴. Previous studies have established that CXCL7 exists as monomers, dimers, and tetramers, but the dimer levels are low and the monomer dominates at lower and the tetramer dominates at higher concentrations. These observations raise the question: what, if any, is the role of the dimer?

In this study, we make a striking observation that dimer is actually the favored form in the GAG-bound state. Further, we successfully characterized the structural basis of dimer-GAG interactions using solution NMR spectroscopy. As native CXCL7 dimer is the minor species in the free form, we engineered a trapped disulfide-linked dimer. This

dimer was used for NMR characterization, chemical shift assignments, and characterizing GAG interactions. We subsequently used results from the trapped dimer to elucidate native dimer interactions. Chemical shift assignments for the native dimer were challenging but could be accomplished using a multi-pronged strategy including use of the disulfide-linked obligate dimer and exploiting heparin binding-induced NMR spectral changes in the WT monomer and dimer. In addition to GAG interactions, we report the structural characterization of the native CXCL7 dimer binding to the CXCR2 N-terminal domain (N-domain) using NMR spectroscopy. We observe that the receptor interactions of the dimer are similar to the monomer, and that GAG-bound dimer is occluded from receptor interactions. On the basis of these data, considering the local CXCL7 concentration can vary by orders of magnitude during active neutrophil recruitment, we propose that the dimer actually plays a prominent role through its GAG interactions and regulating the levels of free monomer for receptor activation. We further propose, in the context of platelet-neutrophil crosstalk, that the relative ratios of the monomer and dimer in the free and GAG-bound form could be critical to maximize repair and minimize collateral tissue damage and disease.

RESULTS

Various cellular, ex vivo, and biophysical studies for a wide variety of chemokines have shown that dimers and higher order oligomers bind GAGs with much higher affinity compared to monomer²⁰⁶⁻²⁰⁹. Our lab's recent NMR studies of GAG heparin binding using WT CXCL1 and CXCL5 have shown that the dimer is the high affinity GAG ligand and that the differences in affinities can be clearly observed with longer GAGs^{187,188}. Moreover, longer GAGs better represent the length of the physiological GAGs. With this in mind, the binding of heparin dp26 to a 120 μ M sample of WT CXCL7 at pH 6.0 was characterized. Under these conditions, 70% of the protein exists as the monomer and the remaining as the dimer (Table 1.1). Based on chemical

shift intensities under these conditions, we also estimate the monomer-dimer equilibrium constant to be $\sim 150 \mu\text{M}$. In principle, four different species will exist in solution due to coupled equilibria – monomer and dimer in both the free and 26mer-bound forms. The intensities of peaks are a direct reflection of relative populations and binding constants. During the course of the titration, the peaks corresponding to the monomer disappear and the weak peaks corresponding to the dimer gain intensity, indicating that the dimer binds the 26mer with much higher affinity (Figure 3.1A). In addition to peak intensity changes, the shape and magnitude of CSP profiles for the dimer compared to the monomer also indicates that the dimer is the high affinity ligand (Fig. 3.1B,C).

CXCL7 Dimer Chemical Shift Assignments

Chemical shifts are exquisitely sensitive to local changes in the electronic environment, and as such, serve as useful probes for mapping the binding interface of macromolecular interactions. Therefore, knowledge of the CXCL7 dimer chemical shifts is essential to describe the molecular basis of receptor and GAG interactions. However, unlike for the CXCL7 monomer (discussed in Chapter 2), there is no solution condition at which the dimer population dominates. This makes chemical shift assignments for the native dimer extremely challenging, as there will always be interference from either the monomer or tetramer. To overcome these challenges, a multi-pronged strategy was used that included chemical shift assignments of a disulfide-linked trapped homodimer, GAG binding-induced chemical shift changes of the trapped and WT dimers, and tracking intensity and chemical shift changes of WT monomer and dimer upon heparin titrations. These collectively allowed assignment of $\sim 80\%$ of the residues including all of the residues that showed perturbation during GAG binding.

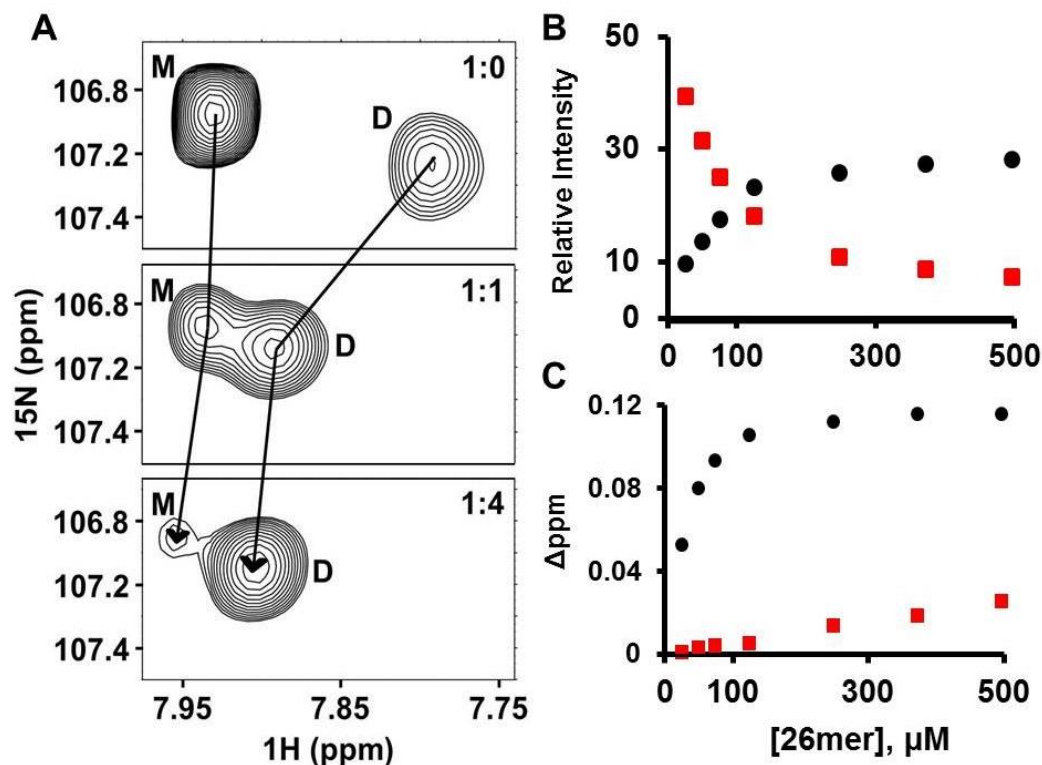


Figure 3.1: **CXCL7 dimer is the high-affinity GAG ligand.** (A) A section of HSQC spectrum showing dp26-binding induced transition from a predominantly monomeric to predominantly dimeric state for residue G65. (B) Plot showing the relative change in peak intensity for monomer (red squares) and dimer (black circles). (C) Plot showing the change in chemical shifts for monomer (red squares) vs. dimer (black circles). These data indicate the CXCL7 dimer binds dp26 with much higher affinity than the monomer.

For the disulfide-linked trapped dimer, we assigned chemical shifts of fifty residues. The remaining residues could not be assigned due to chemical shift degeneracy or lack of sequential NOEs. These chemical shifts were assigned based on a combination of NOESY, TOCSY, HNCA, and CBCACONH experiments. Many of these assignments corresponded to residues in the N-loop and β -sheet along with a few C-terminal residues (Figure 3.2). These assignments could be transferred to WT dimer residues that showed similar chemical shifts as the trapped dimer, especially those of well dispersed peaks, in a straightforward manner. Additional assignments were obtained by comparing binding-

induced NMR spectral changes of the WT and trapped dimer upon GAG titration. During these titrations, weak dimer peaks become strong, and monomer peaks become weak. This makes tracking the dimer chemical shifts much simpler. In addition to intensity changes, binding also resulted in chemical shift perturbations. On the basis of similar binding-induced chemical shift perturbations to the trapped dimer, we could confirm the authenticity of all of the WT dimer assignments assigned above. In addition, these data allowed assigning a few more residues whose peaks were too weak in the WT spectra but became stronger on GAG binding. These data collectively allowed for 48 assignments of the WT dimer. We also observed that the intensity of 29 peaks did not change during the WT titration, indicating the dimer and monomer chemical shifts of these residues are identical. Therefore, the dimer residues were assigned on the basis of monomer chemical shifts. 23 of these residues matched previously assigned chemical shifts from the trapped dimer, resulting in six new assignments bringing the total to 54 WT dimer assignments. The remaining 13 residues could not be assigned, but lack of this knowledge was not limiting as these residues showed minimal to no perturbation in GAG-binding experiments.

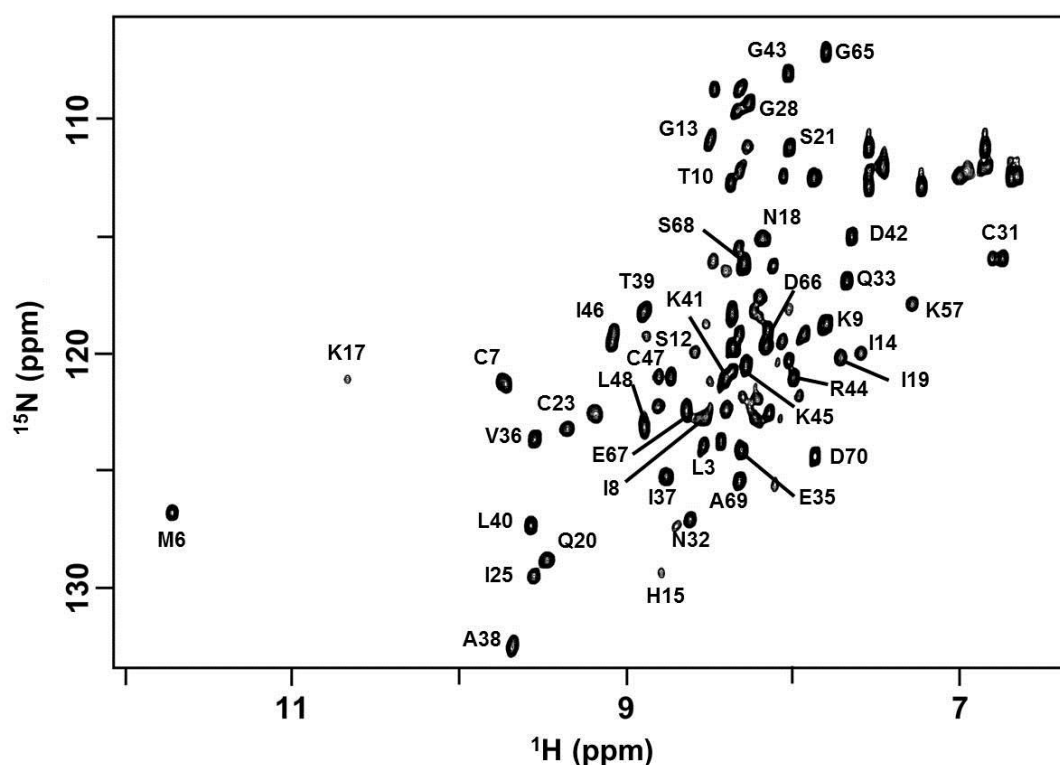


Figure 3.2: ^1H - ^{15}N HSQC spectrum of a trapped CXCL7 dimer. Spectrum displays a single species corresponding to the trapped dimer. Well dispersed peaks for residues whose chemical shifts were determined are labeled.

CXCL7 Dimer-GAG Interactions

Analysis of the chemical shift perturbations (CSP) on heparin binding revealed five basic residues H15, K17, R44, R54, and K57 as showing significant perturbation (Fig. 3.3). Our previous studies characterizing heparin dp8 binding to the monomer also showed perturbation of these residues. In the case of monomer, perturbations were also observed for residues K9, K45, and K56 (Chapter 2)²¹⁰. Another interesting difference from the monomer was the C-terminal helical residues L63 to D70. With the exception of S68, these residues were all perturbed in the monomer. In the dimer, L63 and S68-D70 showed no perturbation, while A64-E67 showed large perturbations. These differences may be explained by a more defined helix, or more restricted dynamics, in the dimer, and

therefore, GAG binding resulting in less structural changes and consequently less or no chemical shift changes. We also observed that the same basic residues that mediate binding in the WT dimer (H15, K17, R44, R54, and K57) are also involved in binding to the trapped dimer (Fig. 3.4).

To gain insight into the binding geometry, we performed four independent HADDOCK-based calculations to ensure that both 1:1 and 1:2 stoichiometries were covered and to avoid any inherent bias in the docking process. In run I, restraints were given between one GAG and to only one monomer of the dimer. In run II, restraints were given between one GAG and both monomers of the dimer. In run III, restraints were given from each of the two GAGs to only one monomer of the dimer. Finally, in run IV, restraints were given from each of the two GAGs to both monomers of the dimer.

Run I essentially resulted in a single geometry, which could be divided into two major clusters, with structures in one cluster interacting with all residues implicated in binding from NMR studies (defined as Model-I), and the second cluster missing interactions from R44 (Figure 3.5). Comparison of the two clusters reveals that H15, K17, R54, and K57 function as a core domain and R44 functions as a peripheral residue, suggesting that interactions with R44 are more transient. Interestingly, run II resulted in a single geometry in which GAG spans both monomers of the dimer. In this geometry (defined as Model-II), all residues except R44 from both monomers of the dimer mediate binding for a single GAG. Both runs III and IV indicated that two GAGs bound each monomer of the dimer with geometries observed for run I. These observations indicate that a two GAG stoichiometry does not allow a geometry spanning the dimer interface (Model-II) and/or that it is less favored.

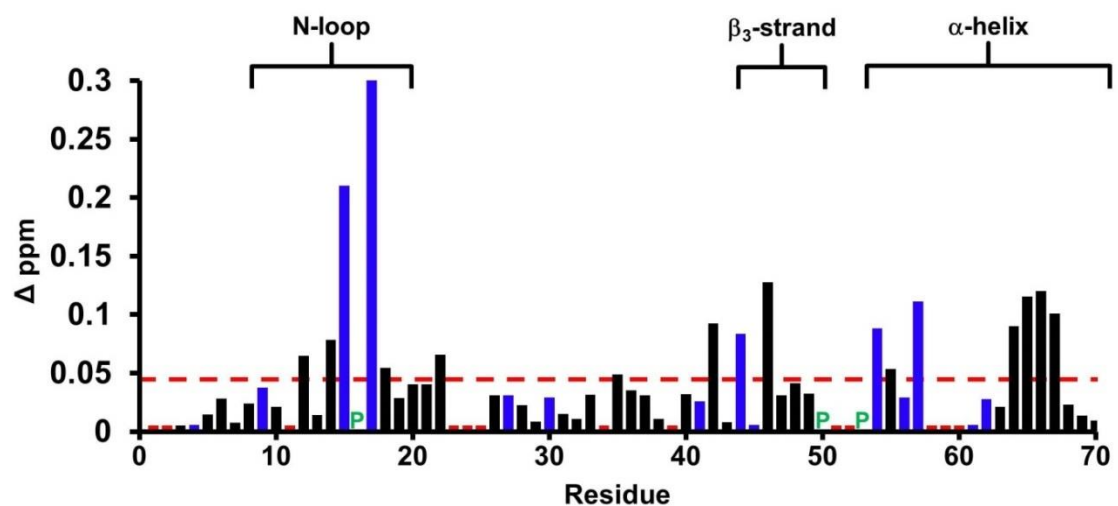


Figure 3.3: **CXCL7 dimer binding to heparin dp26.** Histogram plot of binding-induced chemical shift changes in CXCL7 dimer as a function of amino acid sequence is shown. Residues that show CSP above the threshold (dashed line) are considered involved in binding. Basic residues Arg, Lys, and His are shown in blue and unassigned residues that show no perturbation are shown in red. Proline is represented by a green 'P'.

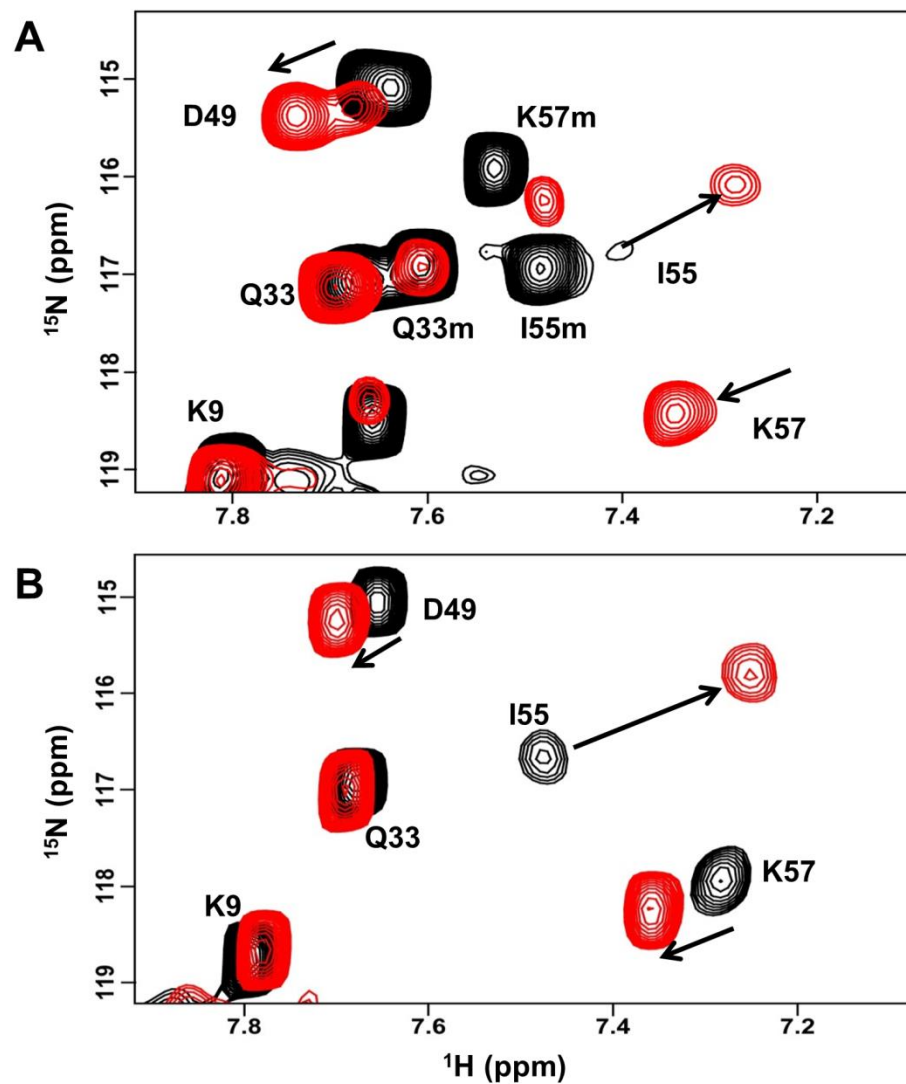


Figure 3.4: **WT vs Trapped Dimer GAG Binding.** (A) Portion of the ^1H - ^{15}N HSQC spectra showing the overlay of native CXCL7 in the free (black) and heparin dp26 bound form at a 1:4 molar ratio (red). (B) Portion of the ^1H - ^{15}N HSQC spectra showing the overlay of the trapped CXCL7 homodimer in the free (black) and heparin dp26 bound form at a 1:4 molar ratio (red). In both spectra the dimer peaks are labeled for reference. Monomer peaks are indicated with an 'm.' Arrows indicate the direction of peak movement.

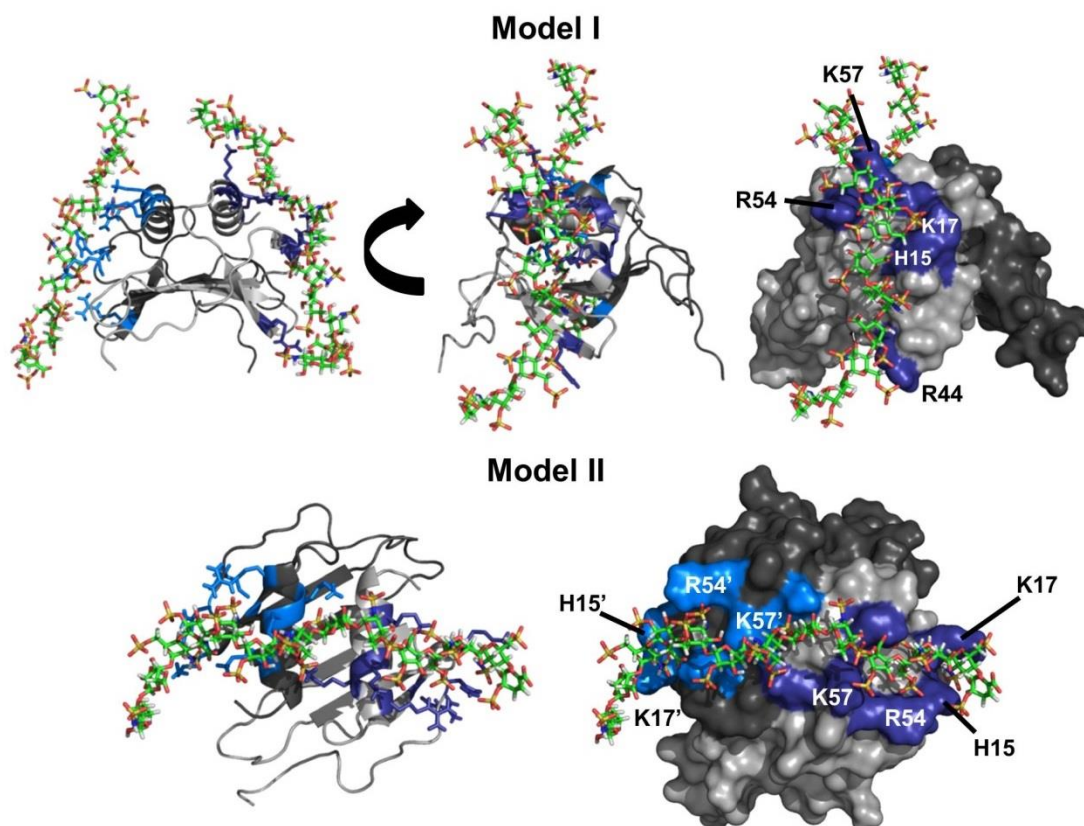


Figure 3.5: **CXCL7 dimer-GAG binding models.** Schematic showing the two primary models for GAG binding to the CXCL7 dimer. Each monomer of the dimer is shaded differently for clarity. GAG binding residues Arg, Lys, and His are highlighted in blue and labeled. Model-I depicts binding of two GAG-chains to each monomer of the dimer, and two different views are shown to highlight the binding geometry. Model-II depicts binding of a single GAG across the dimer interface and is shown from a top-down view.

CXCL7 Dimer Binding to the CXCR2 N-domain

Currently nothing is known regarding the structural basis of how CXCL7 dimer binds the CXCR2 receptor. In Chapter 2, the structural basis of CXCL7 monomer binding the Site-1 N-terminal domain peptide was characterized using solution NMR spectroscopy. However, the questions still remain what is the receptor activity of the dimer and what is the structural basis for these interactions? We used the same divide and conquer approach as for the monomer to characterize these interactions. Such an

approach has been extensively used to characterize Site-I interactions for a number of chemokines using different biophysical techniques including solution NMR spectroscopy^{148-152,187,211}.

We performed NMR HSQC titration experiments to characterize the Site-I CXCR2 N-domain interactions. Under our experimental conditions, CXCL7 exists as ~70% monomer and ~30% dimer. Armed with our dimer chemical shifts, we could thus track CSPs for the dimer and the monomer simultaneously. Similar to the monomer, significant CSPs are observed for residues I8 to T11, I14, H15, I46, and C47. Many of these residues were shown to have overlapping peaks with the monomer, thus simplifying evaluation of CSPs. These residues constitute a continuous surface along the N-loop and β_3 -strand. Following the analysis from the monomer, binding is mediated by a hydrophobic pocket consisting of residues T11-I14 and I46. The receptor is oriented about this pocket via ionic interactions between CXCL7 K9 and N-domain D30 and between CXCL7 H15 or R54 and N-domain F27. We also note that the relative intensities of monomer and dimer remain similar throughout the titration, indicating that the monomer and dimer bind the receptor N-domain with similar affinity.

A central question in determining the role of dimer is how GAG binding relates to receptor activation. Independent of any binding models, there is considerable overlap between the GAG and CXCR2 binding domains in the dimer, suggesting the GAG-bound CXCL7 dimer cannot bind the receptor (Figure 3.6B). In order to test whether this is the case, we carried out NMR titrations of the CXCR2 N-domain peptide to the heparin dp26-bound CXCL7 dimer. We observe that the spectra are unaltered, indicating that the GAG-bound CXCL7 dimer cannot bind the receptor and that GAG-binding occludes the receptor binding sites (Figure 3.6A).

DISCUSSION

In the event of vascular injury, crosstalk between activated platelets and neutrophils is essential for initiating repair and successful restoration of homeostasis. However, any dysregulation in this process also aggravates the course of various thrombus-related cardiovascular and inflammatory diseases. Chemokine CXCL7, released by activated platelets, plays a prominent role in recruiting neutrophils to the injury site. CXCL7 elicits its function by binding GAG and the CXCR2 receptor. CXCL7 is unique for the reason that it is the only neutrophil-activating chemokine (NAC) that is almost exclusively present only in platelets, and it is also unusual for the reason that it forms a weak dimer. Therefore, the functional relevance of the dimeric state for *in vivo* function was not clear. Evidence from this dissertation provides compelling evidence that the dimeric form does play a crucial role in regulating neutrophil trafficking by regulating the levels of free monomer available for chemotactic gradients and receptor interactions.

In this chapter, we successfully characterized how the CXCL7 dimer binds GAG and the CXCR2 receptor N-domain using solution NMR spectroscopy. Characterization requires chemical shift assignments of the dimer that were not trivial to come by due to its low population. A combination of several strategies was used, including assigning chemical shifts of a disulfide-linked dimer and characterizing its GAG heparin interactions. We also exploited the higher binding affinities of the native dimer for heparin dp26. By using heparin dp26, the relative populations switched from monomer being dominant in the free to dimer being dominant in the GAG-bound form. This allowed identification of key GAG binding residues and also describing the GAG binding geometries in the dimer. The structural models carried out with one GAG, or with two GAGs each binding one monomer of the dimer, indicate that the binding geometries are also dependent on the stoichiometry. In the case of one GAG, two distinct geometries could be observed, one involved interactions within a monomer of the dimer (Model-I)

and the other involved interactions across both monomers of the dimer (Model-II) (Figure 3.5). In the case of two GAGs, only geometries corresponding to Model-I were seen indicating this geometry is favored over one or two GAGs binding across the dimer. Moreover, only Model-I satisfied all of the NMR restraints, as Model-II was completely missing R44 interactions. Considering the binding interface is likely highly plastic, it is possible that both binding geometries mediate binding. However, the two GAG binding model (Model I) could be the preferred mode of interaction due to the inclusion of R44 interactions, which are absent in Model II. Additionally, GAG levels are much higher in vivo compared to chemokine levels, further supporting the Model-I binding geometry. Two GAGs were also observed to bind CXCL1, CXCL5, and CXCL8 dimers, though the geometries and interactions were different^{185,187,188,212}.

A comparison of GAG-binding residues between CXCL7 and other NACs reveals both highly conserved and unique interactions (Fig. 3.6). For instance, highly conserved residues H15, K17, and K57 mediate GAG binding in all NACs studied to date. On the other hand, R54 is unique to CXCL7 and serves as a core binding residue. This likely contributes unique binding interactions compared to related chemokines. Another unique binding feature is a lack of interactions for K61 in CXCL7, whose corresponding residues play a prominent role in CXCL1, CXCL5, and CXCL8 GAG interactions^{185,187,188}. Interestingly, molecular dynamics (MD) studies have shown that K61 could be involved in intramolecular electrostatic interactions with the carboxylate group of D70, thus shielding this residue from GAG-binding¹⁸².

In addition to specific residues, the binding geometries for the CXCL7 dimer to GAG also vary compared to other NACs, indicating that conserved residues in the context of structure determine geometries that could not have been predicted from sequence alignment alone. For example, characterization of CXCL8-GAG interactions revealed multiple binding geometries with GAG binding parallel to the helices on either side of the dimer or across both helices¹⁸⁵. In CXCL7, GAG binds across a similar

interface to the so called parallel model of CXCL8, however, the GAGs in CXCL7 are instead oriented perpendicular to the helices. The binding geometry for the CXCL1 dimer is also unique, with two GAGs binding across the dimer interface on opposite faces of the protein¹⁸⁷. This geometry is similar to Model-II in CXCL7, except that interactions to an additional domain are missing in CXCL7. The binding geometry of CXCL5 is the most similar to that of the CXCL7 dimer, except for differences due to CXCL7 R54 directing GAG towards the N-terminal end of the helix and additional C-terminal helical residues dominating CXCL5 interactions¹⁸⁸. These observations speak to the rich diversity of chemokine-GAG interactions that likely play a role in fine-tuning neutrophil recruitment.

NMR studies for the CXCL7 dimer binding to the CXCR2 N-domain reveal that the N-loop and adjacent β -strand residues mediate these interactions. The binding mode and the nature of these interactions are similar to that observed for other CXCR2-activating chemokines CXCL1, CXCL5, and CXCL8^{148,187,188}. Independent of the binding geometry and stoichiometry, comparison of the GAG and receptor binding domains reveals a number of residues play dual roles by binding both (Fig. 3.7B), indicating GAG-bound CXCL7 dimer is precluded from interacting and activating the receptor. This is corroborated by the observation that CXCR2 N-domain is unable to bind the dp26-bound CXCL7 dimer (Fig. 3.7A). These results are consistent with what has been observed for other CXCR2-activating chemokines^{148,185,187,213}.

The importance of the monomer-dimer equilibrium for neutrophil trafficking has been clearly demonstrated using animal models^{72,204}. During neutrophil recruitment into the thrombus, CXCL7 is released at high concentrations from α -granules of activated platelets. This results in CXCL7 being present over a large concentration range as a function of space and time, wherein CXCL7 can exist as monomers, dimers, and possibly even tetramers either in the free and/or GAG-bound forms. Our data indicate that the monomer exists predominantly in the free and the dimer in the GAG-bound form. Our observation for the dimer was unexpected and interesting considering free dimer levels

are low at all concentrations. Therefore, GAG binding must neutralize or overcome interactions that disfavor dimerization, and knowledge of the solution or crystal structure of the complex is necessary to understand the structural basis for the higher affinity of the dimer for GAG.

In summary, these studies indicate that distribution of monomers and dimers is intimately linked to CXCL7-GAG interactions and that unique GAG binding geometries likely play a role in mediating function through occluding receptor binding and influencing the steepness and duration of gradients in a context dependent manner. The makeup of the gradients could be critical in the context of platelet-neutrophil crosstalk to maximize repair and minimize collateral tissue damage and disease.

	1	6	11	15	20	25	30	35	40	45	50	55	60	65																																																														
CXCL7	-----	<u>A</u>	<u>ELR</u>	CMCI	<u>I</u>	<u>TTSG</u>	-I	<u>H</u>	<u>P</u>	<u>K</u>	<u>N</u>	<u>I</u>	<u>Q</u>	<u>S</u>	<u>L</u>	<u>E</u>	<u>V</u>	<u>I</u>	<u>G</u>	<u>K</u>	<u>G</u>	<u>T</u>	<u>H</u>	<u>C</u>	<u>N</u>	<u>Q</u>	<u>V</u>	<u>E</u>	<u>I</u>	<u>A</u>	<u>T</u>	<u>L</u>	<u>K</u>	<u>D</u>	<u>G</u>	<u>R</u>	<u>K</u>	<u>I</u>	<u>C</u>	<u>L</u>	<u>D</u>	<u>P</u>	<u>D</u>	<u>A</u>	<u>P</u>	<u>I</u>	<u>K</u>	<u>K</u>	<u>I</u>	<u>V</u>	<u>Q</u>	<u>K</u>	<u>K</u>	<u>L</u>	<u>A</u>	<u>G</u>	<u>D</u>	<u>E</u>	<u>S</u>	<u>A</u>	<u>D</u>															
CXCL1	----	A	S	V	A	T	E	L	R	C	Q	C	L	Q	T	L	Q	G	-I	H	P	K	N	I	Q	S	V	N	V	K	S	P	G	P	H	C	A	Q	T	E	V	I	A	T	L	K	N	G	R	K	A	C	L	N	P	A	S	P	I	V	K	K	I	E	K	M	L	N	S	D	K	S	N			
CXCL2	----	A	P	L	A	T	E	L	R	C	Q	C	L	Q	T	L	Q	G	-I	H	L	K	N	I	Q	S	V	K	V	K	S	P	G	P	H	C	A	Q	T	E	V	I	A	T	L	K	N	G	Q	K	A	C	L	N	P	A	S	P	M	V	K	K	I	E	K	M	L	K	N	G	K	S	N			
CXCL3	----	A	S	V	V	T	E	L	R	C	Q	C	L	Q	T	L	Q	G	-I	H	L	K	N	I	Q	S	V	N	V	R	S	P	G	P	H	C	A	Q	T	E	V	I	A	T	L	K	N	G	K	K	A	C	L	N	P	A	S	P	M	V	Q	K	I	E	K	I	L	N	K	G	S	T	N			
CXCL5	AGP	A	A	A	V	L	R	E	L	R	C	V	C	L	Q	T	T	Q	G	-V	H	P	K	M	I	S	N	L	Q	V	F	A	I	G	P	Q	C	S	K	V	E	V	V	A	S	L	K	N	G	K	E	I	C	L	D	P	E	A	P	F	L	K	K	V	I	Q	K	I	L	D	G	G	N	K	E	N
CXCL6	-GP	V	S	A	V	L	T	E	L	R	C	T	C	L	R	V	T	L	R	-V	N	P	K	T	I	G	K	L	Q	V	F	P	A	G	P	Q	C	S	K	V	E	V	V	A	S	L	K	N	G	K	Q	V	C	L	D	P	E	A	P	F	L	K	K	V	I	Q	K	I	L	D	S	G	N	K	K	N
CXCL8	-----	S	A	K	E	L	R	C	Q	C	I	K	T	Y	S	K	P	F	H	P	K	F	I	K	E	L	R	V	I	E	S	G	P	H	C	A	N	T	E	I	I	V	K	L	S	D	G	R	E	L	C	L	D	P	K	E	N	W	V	Q	R	V	V	E	K	F	L	K	R	A	E	N	S			

Figure 3.6: **Sequence alignment of neutrophil activating chemokines.** Conserved 'ELR' motif is shown in green, and potential GAG-binding residues from CXCL7 are shown in blue. GAG binding residues unique to CXCL7 are underlined and italicized.

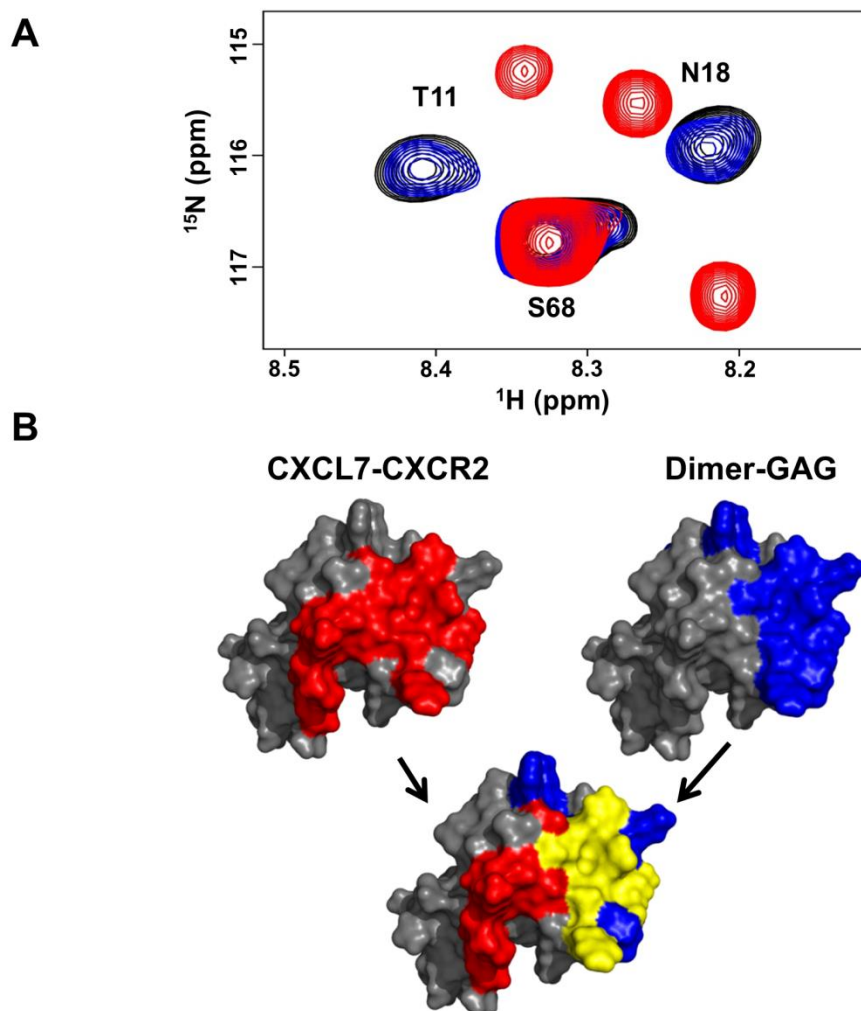


Figure 3.7: **Overlap between GAG and CXCR2 binding domains.** (A) Section of the ^1H - ^{15}N HSQC spectrum showing peaks corresponding to the CXCL7:dp26 complex (black), the CXCL7: CXCR2 N-domain complex (red) and the CXCL7:dp26 complex upon titrating CXCR2 N-domain peptide up to a 1:7 molar ratio (blue). (B) A schematic showing the CXCR2 binding domain (red), GAG binding domain (blue), and the overlap between the two domains (yellow) for the CXCL7 dimer. Monomer structure is used for clarity. Extensive overlap between the GAG and receptor domains suggests that GAG-bound CXCL7 cannot activate the receptor.

MATERIALS AND METHODS

REAGENTS AND PROTEIN EXPRESSION

WT and disulfide-linked trapped CXCL7 were expressed in *E. coli* cultured in either LB or $^{15}\text{N}/^{13}\text{C}$ enriched minimal medium and purified using a combination of nickel column and reverse phase high-performance liquid chromatography as described previously¹³⁹. Purified protein was then lyophilized and stored at -20 °C until further use. The recombinant CXCR2 N-domain (residues 1-43) peptide was expressed using the same protocol as described above. Heparin dp26 oligosaccharide was purchased from Iduron.

CHEMICAL SHIFT ASSIGNMENTS OF THE CXCL7 MONOMER

NMR samples were prepared in a 50 mM phosphate, pH 6.0 or 7.4, containing 1 mM 2,2-dimethyl-2-silapentanesulfonic acid (DSS), 1 mM sodium azide, and 10% D₂O. NMR spectra were acquired on a Bruker Avance III 600 (with a QCI cryoprobe) or 800 MHz (with a TXI cryoprobe) spectrometer and processed and analyzed using either Bruker Topspin 3.2 or Sparky programs¹⁹⁵. Trapped dimer chemical shift assignments were determined at 30 °C using a 400 μM sample. The ^1H and ^{15}N chemical shifts were assigned using 3D ^1H - ^{15}N heteronuclear NOESY and TOCSY experiments with mixing times of 150 and 80 msec, respectively. The carbon chemical shifts assignments were obtained from HNCA and CBCACONH experiments at pH 6.0.

NMR TITRATIONS

Binding interactions of CXCR2 N-terminal domain and heparin dp8 to WT CXCL7 were characterized using solution NMR spectroscopy. A series of ^1H - ^{15}N HSQC spectra were collected upon titrating either CXCR2 N-domain peptide or heparin dp26 to WT CXCL7 until no change in the chemical shifts were observed. The protein concentrations selected were high enough to obtain good quality spectra in a reasonable

period. In the case of CXCR2 N-domain, we titrated 320 μ M CXCR2 N-domain to 77 μ M WT CXCL7 in 50 mM phosphate buffer at pH 6.0 and 35 °C. The final molar ratio of CXCL7: CXCR2 N-domain was 1:3.5. For CXCL7-GAG interactions, we titrated 2.5 mM heparin dp26 to a 124 μ M sample in 50 mM phosphate pH 6.0 at 35 °C. The final molar ratio for CXCL7:dp26 was 1:4. For all titrations, chemical shift perturbations were calculated as a weighted average of changes in the ^1H and ^{15}N chemical shifts as described⁷⁷.

MOLECULAR DOCKING USING HADDOCK

Molecular docking of heparin to the CXCL7 dimer was carried out using the High Ambiguity Driven biomolecular DOCKing (HADDOCK) approach as described previously^{185,187,201,202}. The CXCL7 dimer structure consisted of chains A and B from the tetramer structure (PDB ID: 1NAP)⁵⁷ and the NMR structure of heparin (PDB ID: 1HPN)²⁰³ were used for docking. Ambiguous Interaction Restraints (AIRs) were selected based on NMR chemical shift perturbation results. The pair-wise “ligand interface RMSD matrix” over all structures was calculated and the final structures were clustered using an RMSD cut-off value of either 4 or 7 Å. The clusters were then prioritized using RMSD and ‘HADDOCK score’ (weighted sum of a combination of energy terms).

Chapter 4

Chemokine CXCL7 Heterodimers: Structural Insights, CXCR2 Receptor Function, and Glycosaminoglycan Interactions

ABSTRACT

Chemokines mediate diverse fundamental biological processes including combating infection. Multiple chemokines are expressed at the site of infection and so chemokine synergy by heterodimer formation could play a role in determining function. Chemokine function involves interactions with G-protein-coupled receptors and sulfated glycosaminoglycans (GAG). However, very little is known regarding heterodimer's structural features and receptor and GAG interactions. Solution NMR and MD characterization of platelet-derived chemokine CXCL7 heterodimerization with chemokines CXCL1, CXCL4, and CXCL8 indicated packing interactions promote CXCL7-CXCL1 and CXCL7-CXCL4 heterodimers and electrostatic repulsive interactions disfavor CXCL7-CXCL8 heterodimer. As characterizing the native heterodimer is challenging due to interference from monomers and homodimers, we engineered a 'trapped' disulfide-linked CXCL7-CXCL1 heterodimer. NMR and modeling studies indicated that GAG heparin binding to the heterodimer is distinctly different from the CXCL7 monomer and that the GAG-bound heterodimer is unlikely to bind the receptor. Interestingly, the trapped heterodimer showed potent receptor activity comparable to the native proteins. These data collectively suggest that GAG interactions play a prominent role in determining heterodimer in vivo function. Further, this study provides proof-of-concept that the disulfide trapping strategy can serve as a valuable tool for characterizing the structural and functional features of a chemokine heterodimer.

INTRODUCTION

Chemokines, a large family of signaling proteins, mediate diverse biological processes including innate and adaptive immunity, organogenesis, and tissue repair^{4,8,214}. Common to these functions is the directed trafficking of various cell types through interactions with seven transmembrane G-protein coupled receptors. Chemokine-chemokine receptor interactions form an intricate network of crosstalk with a given chemokine binding either a single or multiple receptors, and a given receptor binding either a single or multiple chemokines^{13,14}. Additional layers of complexity arise from chemokines existing in multiple states — from monomers, dimers, and tetramers to oligomers and polymers — and from their interactions with sulfated glycosaminoglycans (GAG)^{78,93,170}. During active inflammation, local chemokine concentrations both in the free and GAG-bound forms could vary by orders of magnitude, which in turn could regulate the steepness and duration of chemotactic and haptotactic gradients^{155,215}. Further, several lines of evidence indicate that chemokines also form heterodimers suggesting yet another layer of complexity in regulating function.

Humans express ~50 different chemokines, which can be classified into subfamilies on the basis of the first two conserved cysteine residues as CXC, CC, CX₃C, and XC^{169,216}. Despite sequence identity that can be as low as 20%, chemokines share a similar structure at the monomer level. Considering they are small (~ 8 to 10 kDa), they show a remarkable array of oligomeric states and binding interfaces. At the simplest level, chemokines share similar dimeric structures within a subfamily. The CXC-family forms globular dimers with the first β -strand constituting the dimer interface, while the CC-family forms elongated dimers with the N-loop constituting the dimer interface. However, this classification is not stringent, as some CC chemokines form CXC dimers⁶⁴ and some do not form dimers even at mM concentrations^{48,217}. Chemokines that form tetramers exhibit both CXC and CC dimer interfaces^{57,66,67}. Some chemokines form

elongated polymers that have a completely different interface^{70,208}. Further, lymphotactin, the only member of the C family, shows a typical chemokine fold and yet a completely different fold as a function of pH and solution conditions³⁹. These properties speak to the inherent plasticity of the chemokine dimer interface. Considering many chemokines are co-expressed under conditions of insult or co-exist in granules, it follows that chemokines are capable of forming heterodimers.

Functional studies have provided evidence for chemokine ‘synergy,’ wherein the presence of multiple chemokines results in enhanced or altered activity⁹⁵⁻⁹⁸. Synergy is thought to play an important role at the onset of inflammatory signaling, and has been attributed to altered receptor signaling¹⁰² and/or heterodimer formation^{104,105}. As an example, the functional potential of chemokine synergy was demonstrated in vivo by using peptides that inhibit the CXCL4/CCL5 heterodimer in a mouse atherosclerosis model¹¹⁰. Many of the chemokines known to exist in platelets, as well as those that mediate neutrophil recruitment, form heterodimers. Several studies have provided evidence for heterodimers^{106,108,109}, but very little is known regarding the structural features, the molecular mechanisms underlying heterodimerization, or how heterodimers interact with their cognate receptors and GAGs. Such knowledge is essential to describe how the interplay between heterodimers, GAGs, and receptors mediates crosstalk between platelets and neutrophils towards successful resolution of disease.

In this study, we investigated the molecular basis of heterodimer formation for chemokine CXCL7 with chemokines CXCL1, CXCL4, and CXCL8. These chemokines co-exist in platelet granules, and their release upon platelet activation orchestrates neutrophils to the tissue injury site. CXCL7, CXCL1, and CXCL8, characterized by the conserved N-terminal ‘ELR’ motif, direct neutrophil trafficking by activating the CXCR2 receptor¹⁷⁴. CXCL4 is not a CXCR2 agonist as it lacks the ELR motif but plays an important role in promoting neutrophil adhesion²¹⁸. In this study, we show that favorable packing and ionic interactions promote CXCL7-CXCL1 and CXCL7-CXCL4

heterodimers and repulsive ionic interactions disfavor CXCL7-CXCL8 heterodimer. Using a ‘trapped’ disulfide-linked CXCL7-CXCL1 heterodimer, we provide definitive insights into GAG and receptor binding interactions. Interestingly, we observe the trapped heterodimer was as active as the native proteins for CXCR2 function. Further, GAG heparin interactions of the heterodimer are distinctly different from the CXCL7 monomer, and the GAG-bound heterodimer is unlikely to bind the receptor. Our observation that GAG binding interactions of a heterodimer could be quite different from the monomer suggests these differences could play important roles in fine-tuning in vivo neutrophil recruitment and function. To our knowledge, this is the very first report of receptor and GAG interactions that could be unambiguously attributed to a chemokine heterodimer.

RESULTS

NMR Characterization of CXCL7 Heterodimers

CXCL7, compared to CXCL1 and CXCL8, forms weak dimers, and actually forms a tetramer at high concentrations. CXCL4, on the other hand, forms an even stronger tetramer. Tetramer structures of CXCL7 and CXCL4 reveal both CXC and CC type dimer interfaces^{57,68}. CXC-type homodimers are stabilized by six H-bonds across the dimer interface β -strands and inter-subunit packing interactions between helical and β -sheet residues^{28,51,52,57,66}. Sequences and the structures reveal that many of the hydrophobic dimer interface residues are conserved and that polar and charged dimer interface residues are not (Figure 4.1A). Comparing dimer interface residues of CXCL7 to CXCL1, CXCL4, and CXCL8 reveals ~ 40% to 60% similarity, suggesting the propensity to form heterodimers could vary between each chemokine pair.

Solution NMR spectroscopy is ideally suited for characterizing CXCL7 heterodimers compared to other techniques. In chapters two and three, we assigned the chemical shifts of the monomer and dimer and extensively characterized dimerization

propensity as a function of solution conditions such as pH and buffer²¹⁰. The spectrum of ¹⁵N-labeled CXCL7 shows essentially a monomer along with some weak homodimer peaks. On titrating unlabeled CXCL1 or CXCL4 to ¹⁵N-CXCL7, the monomer and homodimer peaks gradually weaken and new peaks appear that must correspond to the heterodimer (Figures 4.1B and 4.1C). These new peaks are in slow exchange in the NMR timescale with the CXCL7 monomer and homodimer. No changes were observed on titrating CXCL8 to ¹⁵N-CXCL7 indicating absence of heterodimer formation (Figure 4.1D). We also carried out reverse titrations by titrating unlabeled CXCL7 to ¹⁵N-labeled CXCL1 or CXCL8. Titrating CXCL7 to ¹⁵N-CXCL1 resulted in disappearance of monomer peaks and appearance of new peaks confirming heterodimer formation. Conversely, titrating CXCL7 to ¹⁵N-CXCL8 resulted in no spectral changes as observed before.

Appearance of a new peak during the course of a titration indicates that the environment of the particular residue in the heterodimer is different compared to the monomer or homodimer. On titrating CXCL1 to ¹⁵N-CXCL7, new peaks are observed that correspond to CXCL7 β_1 -strand residues S21, L22, V24, β_2 -strand residues V34, E35, V36, and I37, and C-terminal helical residues K56, K62, A64, and G65. These residues are located either at the dimer interface or proximal to the dimer interface. In the reverse titration of adding CXCL7 to ¹⁵N-CXCL1, new peaks corresponding to residues I23 to S30 of the dimer-interface β_1 -strand, T38 to L44 of the adjacent β_2 -strand, and C-terminal helical residues I58 to S69 are observed. These data collectively indicate that CXCL7-CXCL1 forms a CXC-type heterodimer and that the residues involved in packing interactions that stabilize the homodimers also stabilize the heterodimer. We also explored whether side chain chemical shifts of glutamine and asparagine can serve as probes for heterodimer formation. In CXCL1, a glutamine and an asparagine are located at the CXC dimer interface as well as a pair of glutamines in the CC dimer interface (Figure 4.2A). Upon titrating CXCL7, chemical shift changes were observed for CXC

dimer-interface Q24 and N27 but not for CC interface Q10 and Q13 (Figure 4.2B), providing further structural evidence for a CXC-type dimer.

Peak intensities can provide valuable information on the relative populations of the monomer, homodimer, and heterodimer. We could track intensity changes for a number of residues upon titrating CXCL1 into ^{15}N -CXCL7 and vice versa. During the course of the titration, populations of both CXCL7 monomer and homodimer decrease and populations of the heterodimer increases. On adding excess CXCL1, heterodimer and monomer populations become comparable and homodimer population becomes negligible (Figure 4.2C). However, in the case of CXCL1, heterodimer population continues to increase but the homodimer levels remain high and the monomer population becomes negligible (Figure 4.2D). The relative populations from both titrations indicate that the heterodimer is more favored than the CXCL7 homodimer but less favored than the CXCL1 homodimer. Considering the equilibrium constants (K_d) for CXCL7 and CXCL1 are $\sim 150\ \mu\text{M}$ and $\sim 5\ \mu\text{M}$, respectively, we estimate the K_d for the heterodimer to be $\sim 25\text{-}50\ \mu\text{M}$ based on the relative chemical shift peak intensities of the monomer, homodimer, and heterodimer.

We briefly describe our findings for the CXCL7-CXCL4 heterodimer. Considering the tetramer structures of CXCL7 and CXCL4 reveal both CXC and CC dimer interfaces^{57,66}, heterodimerization could occur via one or both interfaces. However, similar to the CXCL7-CXCL1 heterodimer, most of the new peaks lie in proximity to the first and second β -strand residues and none were found close to the N-loop residues indicating a CXC-type dimer interface. Side chain chemical shifts of Asn and Gln residues of the CXC dimer interface were also perturbed providing further evidence for a CXC-type dimer.

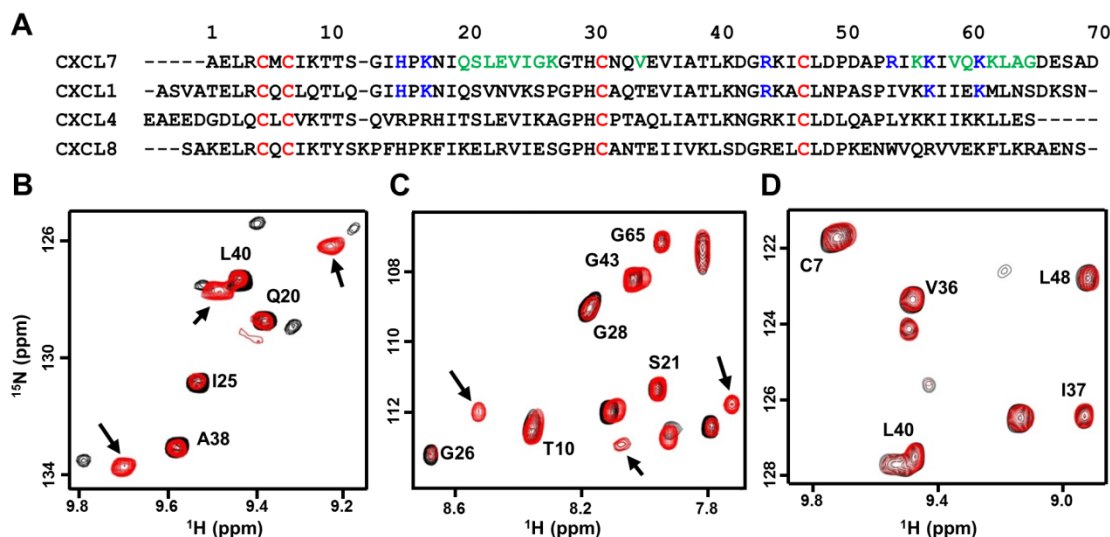


Figure 4.1: **NMR characterization of chemokine heterodimers.** (A) Sequence alignment of platelet-derived CXC chemokines. GAG binding residues identified from this study are in blue, dimer interface residues for CXCL7 are in green, and conserved Cys residues are in red. (B to D) Portions of the ^1H - ^{15}N HSQC spectra showing the overlay of CXCL7 in the free (black) and in the presence of CXCL1 (B, red), CXCL4 (C, red), and CXCL8 (D, red). Arrows indicate new peaks corresponding to the heterodimer. No new peaks were observed in the case of the CXCL8 titration.

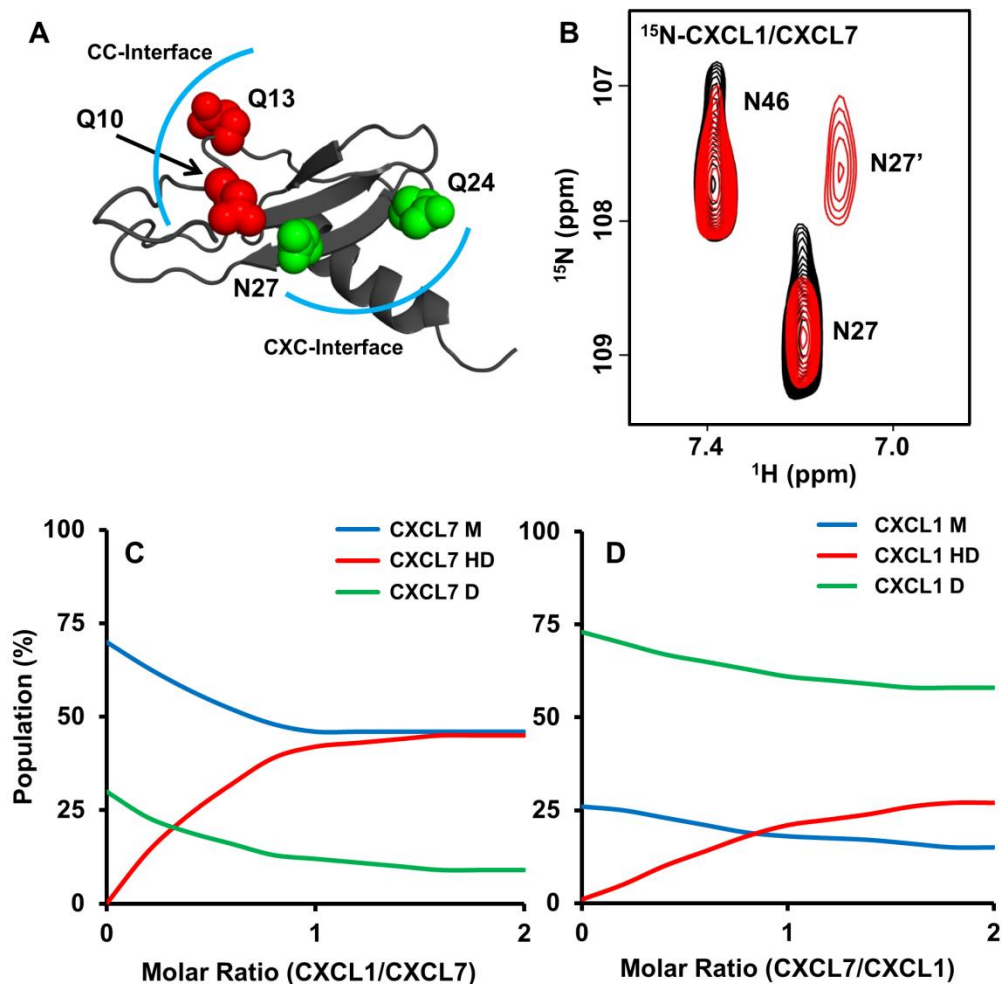


Figure 4.2: **Characterization of the native CXCL7-CXCL1 heterodimer.** (A) Structure of CXCL1 highlighting the CXC (green) and CC (red) dimer-interface asparagine and glutamine residues. The CXC and CC dimer interfaces are outlined with a blue arc. (B) Section of the spectra showing the side chain peaks for N27 and N46. On adding CXCL1, only N27 shows reduced intensity and a new peak corresponding to the heterodimer (labeled as N27'). (C,D) Plots showing the relative populations of monomer (M), homodimer (D), and heterodimer (HD) based on NMR peak intensities during the course of the titration. Panel C shows the relative populations on adding CXCL1 to ^{15}N -CXCL7 and panel D shows the populations on adding CXCL7 to ^{15}N -CXCL1.

Molecular Dynamics of Chemokine Heterodimers

We utilized a molecular dynamics-based approach to gain insight into the molecular basis for heterodimer formation. Energy minimized heterodimer structures were subjected to 180ns molecular dynamics (MD) simulations in order to arrive at a stable structure that had minimal fluctuations in backbone RMSD. To gain insight into the relative stabilities and better understand the structural features that mediate heterodimer formation, we examined several parameters during the course of the simulation — H-bonds and packing interactions of the dimer-interface residues, backbone ϕ - ψ angles, and charge-charge interactions. The MD simulations collectively indicated that a combination of favorable H-bonding, packing, and electrostatic interactions, similar to what drives any complex formation, dictate heterodimer formation.

In the case of CXCL7-CXCL1, both monomer structures retained their tertiary fold. The H-bond network across the dimer interface β -strands remained intact for the CXCL7 residues L22 and V24 to CXCL1 residues V26 and V28, while peripheral H-bonds between CXCL7 G26 and Q20 to CXCL1 Q24 and S30 are transient and fluctuated throughout the run (Figure 4.3B). Backbone ϕ - ψ angles fall in the allowed region of the Ramachandran plot throughout the simulation. The dimer interface is stabilized by a number of favorable intermolecular packing interactions — between M66 and L67 of CXCL1 and V24, G26, K56, and V59 of CXCL7, and between K62 and L63 of CXCL7 and V28, S30, V40, and I63 of CXCL1 (Figures 4.3C and 4.3D). Further, as is the case for the respective homodimer structures, the relative orientation of the helices remained parallel and in register (Figure 4.3A).

For the CXCL7-CXCL4 heterodimer, the final MD structure revealed that the monomer structures maintained their tertiary fold (Figure 4.3E). The dimer interface H-bonds across the β_1 -strands remain intact for CXCL7 residues L22 and V24 to CXCL4

residues L27 and V29, whereas the edge H-bonds (between CXCL7 Q20 and CXCL4 K31 and between CXCL7 G26 and CXCL4 T25) are more transient (Figure 4.3F). The dimer is stabilized by favorable packing interactions between K62 and L63 of CXCL7 and V29, L41, Y60, and I64 of CXCL4, and between L67 and L68 of CXCL4 and V24, V34, V36, K56, V59, and L63 of CXCL7 (Figures 4.3G and 4.3H). Many of these residues are similar in the corresponding homodimers indicating conserved interactions (Figure 4.1A). However, there are unique structural differences in the heterodimer. For instance, E69 of CXCL4 (corresponding to A64 in CXCL7) is involved in ionic interactions with K56 from the opposite helix in CXCL7 (Figure 4.3H), and CXCL4 L67 and L68 are now involved in additional packing interactions with CXCL7 L63 and V59. These new interactions result in realignment of the helix and partial unwinding of the terminal helical residues.

For CXCL7-CXCL8 heterodimer, despite favorable H-bonding and packing interactions, there was significant disruption of the tertiary fold due to unfavorable ionic interactions. The structure reveals that CXCL7 K27 and CXCL8 R68 are positioned across the dimer interface resulting in electrostatic repulsion (Figure A3). In the CXCL8 homodimer, R68 is involved in favorable ionic interactions with E29 across the dimer interface. This swap from favorable to unfavorable interactions provides a molecular basis as to why CXCL7-CXCL8 fails to form a heterodimer.

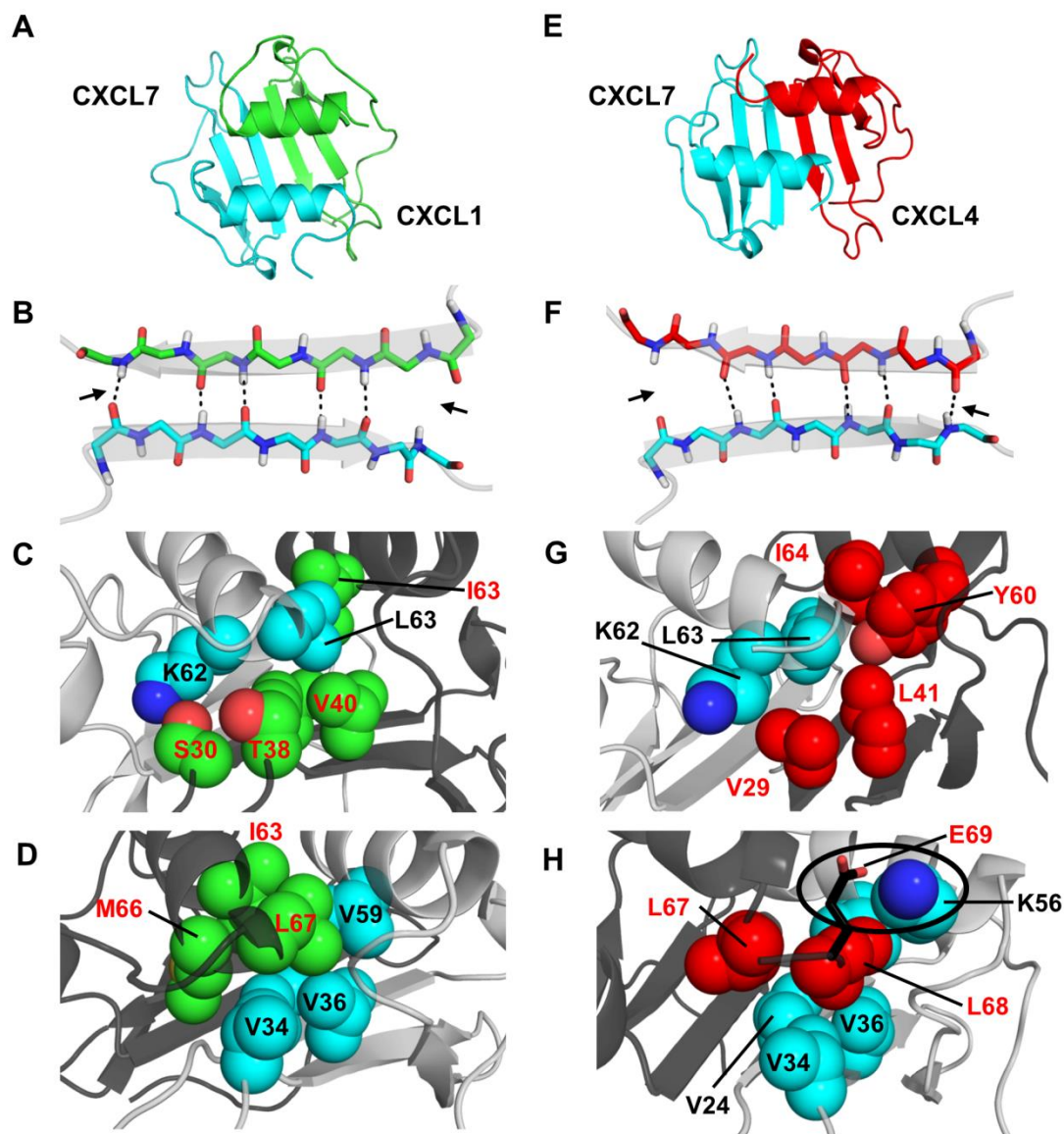


Figure 4.3: **Structural features of the CXCL7 heterodimers.** (A and E) Snap shots of the structural models of CXCL7-CXCL1 and CXCL7-CXCL4 heterodimers from the last 5ns of the MD simulations. (B and F) A schematic showing the β_1 -strand dimer interface H-bonds (dashed line) from the final 5ns of the MD run. Arrows indicate transient H-bonds. (C,D) Packing interactions involving CXCL7 helical and CXCL1 β -sheet residues and CXCL1 helical and CXCL7 β -sheet residues, respectively. CXCL1 residues are labeled in red. (G and H) Packing interactions involving CXCL7 helical and CXCL4 β -sheet residues and the CXCL4 helical and CXCL7 β -sheet residues. CXCL4 residues are labeled in red. The circle highlights the potential ionic interaction between CXCL4 E69 and CXCL7 K56.

Design and Characterization of a Trapped Heterodimer

Characterizing the structural and functional features of the native heterodimer is challenging due to contributions from two native homodimers and two native monomers. In principle, the solution contains as many as ten species, two monomers in the free and bound form, two dimers in the free and bound form, and heterodimer in the free and bound form. NMR experiments reduce this complexity by selective labeling one of the monomers of the heterodimer that simplifies the spectra to six species. In reality, we observe three sets of peaks due to fast exchange between the free and the bound form. Nevertheless, interpretation of such spectra is still challenging due to challenges in unambiguously assigning the chemical shifts of the newly formed heterodimer and tracking CSPs of multiple species. This was evident when we initially attempted to characterize GAG binding to a WT heterodimer mixture of ^{15}N -CXCL7/CXCL1 or CXCL7/ ^{15}N -CXCL1 at a 1:1 molar ratio. In order to overcome these limitations, we designed a disulfide-linked ‘trapped’ CXCL7-CXCL1 heterodimer.

We used our heterodimer structural models from MD simulations to examine potential mutation sites in the CXCL7-CXCL1 heterodimer. To ensure formation of only the disulfide-linked heterodimer and no disulfide-linked homodimers, we looked for residues that are away from the 2-fold symmetry axis. Other criteria considered were that these residues should minimally contribute to dimerization and/or influence the native fold. Our analysis pinpointed the solvent exposed β_1 -strand residues as likely candidates (Figure 4.4A and 4.4B). From this group, we chose the pair S21 from CXCL7 and K29 from CXCL1. The individual cysteine mutants (CXCL7 S21C and CXCL1 K29C) were recombinantly expressed, purified, and trapped heterodimer was allowed to form by simple mixing of the proteins. Trapped heterodimer formation was confirmed using SDS-PAGE gel electrophoresis. Bands corresponding to the heterodimer were observed only under non-reducing conditions indicating a disulfide-linked heterodimer (Figure 4.4C).

Further characterization using NMR revealed that the trapped heterodimer spectra had well dispersed peaks characteristic of a folded protein (Figures 4.5A and 4.5B). NMR spectra of the trapped heterodimer were also compared to the WT heterodimer (Figure 4.5C). The spectra were essentially similar except for residues in and around the mutation, indicating that the introduction of the disulfide does not perturb the native fold and that the trapped heterodimer retains the structural characteristics of the native heterodimer.

Knowledge of the chemical shifts is essential for NMR characterization of the trapped heterodimer GAG interactions. Towards this, we carried out ^{15}N -edited NOESY and TOCSY experiments on ^{15}N -CXCL7-CXCL1 and ^{15}N -CXCL1-CXCL7 trapped heterodimer samples. We could assign the backbone ^1H and ^{15}N chemical shifts of all CXCL1 residues and ~80% of CXCL7 residues. Some of the CXCL7 residues could not be assigned due to overlap or lack of sequential NOEs, but was not limiting, as most of the unassigned residues play no role in GAG interactions.

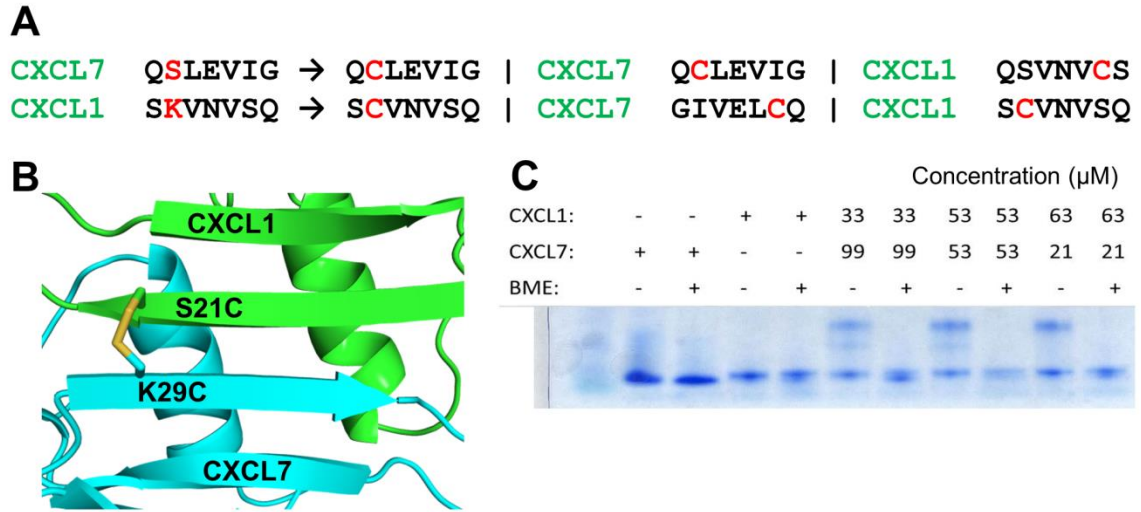


Figure 4.4: **Characterization of the CXCL7-CXCL1 Trapped Heterodimer.** (A) Trapping strategy showing cysteine mutations that will result only in a trapped heterodimer. Cysteines are too far away in the homodimer for disulfide formation. (B) A schematic of the heterodimer showing the location of the disulfide across the heterodimer interface. CXCL7 is in cyan and CXCL1 is in green. Cys residues are labeled for reference. (C) SDS-PAGE gel demonstrating the formation of the disulfide bond. The higher molecular weight heterodimer band is observed only under non-reducing conditions. BME stands for β -mercaptoethanol.

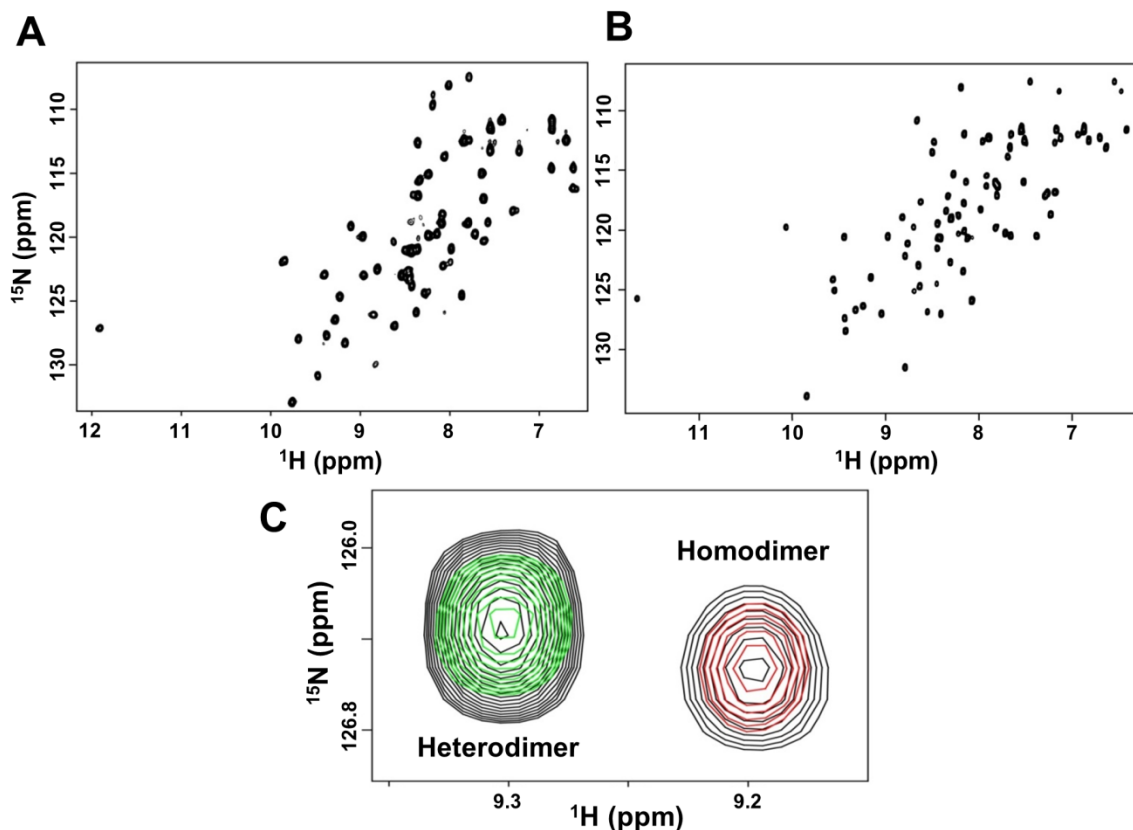


Figure 4.5: **NMR structural features of the trapped heterodimer.** ^1H - ^{15}N HSQC spectra of the (A) ^{15}N -CXCL7: CXCL1 and (B) ^{15}N -CXCL1: CXCL7 trapped heterodimer. Spectra demonstrate a properly folded heterodimer with no evidence of monomer or homodimer. (C) Structure of the trapped heterodimer is similar to the native heterodimer. A section of the superimposed HSQC spectra of ^{15}N -labeled CXCL7 (red), trapped heterodimer (green), and a mixture of CXCL7 and CXCL1 where both native heterodimer and native homodimer are present (black). Trapped heterodimer alone exists as a single species, free CXCL7 exists as monomers and homodimers, and native heterodimer is present along with native monomer and homodimer (Figure 2C). The trapped and native heterodimers have similar chemical shifts as evident from superimposed peaks. Please note the absence of a green peak superimposed on the homodimer peak. The peak corresponding to the monomer is not seen as it resonates out of the spectral window.

Heterodimer-GAG Interactions

We characterized binding interactions of GAG heparin octasaccharide (dp8) by individual titrations to ^{15}N -CXCL7-CXCL1 and CXCL7- ^{15}N -CXCL1 trapped heterodimer samples. In the ^{15}N -CXCL7-CXCL1 trapped heterodimer, significant perturbations were observed for N-loop, β_3 -strand, and α -helical residues. Of particular interest are the basic residues H15 and K17 of the N-loop, R44 and K45 from the β_3 -strand, and K56 and K57 from the helix (Figure 4.6A). CSPs for hydrophobic or acidic residues located proximal to these basic residues are likely due to indirect interactions. In the case of ^{15}N -CXCL1-CXCL7 trapped heterodimer, significant perturbations were observed for residues along the N-loop, β_3 -strand, and α -helix. These include the basic residues H19 and K21 of the N-loop, K45 and R48 of the 40s loop and β_3 -strand, and K61, K65, and K71 of the α -helix (Figure 4.6B).

Interestingly, the CSP profiles of CXCL1 vs. CXCL7 residues were strikingly different (Figures 4.7A and 4.7B). Whereas all CXCL1 residues showed similar hyperbolic profiles, CXCL7 showed three distinctly different profiles. A subset of residues showed hyperbolic profiles (Figure 4.7C), a subset showed an initial delay in perturbation followed by a hyperbolic profile (Figure 4.7D), and a subset showed sigmoidal like profiles (Figure 4.7E). These residues are defined as belonging to Set-I, Set-II, and Set-III, respectively.

Set-I residues include K27, C31 to V34 of the 30s-loop, and K56 of the helix (Figure 4.6A). These residues lie along the dimer interface across from the CXCL1 β -sheet and helical residues. Considering these residues show hyperbolic perturbation profiles similar to CXCL1 residues, it is likely that their CSPs are due to indirect interactions of dp8 binding to CXCL1. For example, our structural model reveals that the CXCL7 K27 side chain is oriented towards the CXCL1 helix, likely making it sensitive

to any structural changes in the CXCL1 helix, such as those often associated with dp8 binding.

Set-II residues include G13 to I19 of the N-loop, D42 to I46 of the β_3 -strand, and V59 to A64 of the helix (Figure 4.6A). These residues are located away from the dimer interface and thus are not influenced by CXCL1 binding. These perturbations can therefore be attributed to direct dp8 binding to CXCL7.

Set-III residues include Q20 to I25 of the β_1 -strand, helical residues K57 and I58, and G65 to A69, and L48 to A52 that precede the helix (Figure 4.6A). In addition to sigmoidal binding profiles, these peaks showed non-linear chemical shift perturbations (Figure 4.7B). These residues are located at the crossroad between the CXCL7-GAG binding interface and the dimer interface. Therefore, their perturbations are likely a composite of both CXCL1 and CXCL7 dp8-binding. Residues K56, K57, and I58 are prominent examples. K56 side chain is pointed towards the dimer interface, while K57 points out towards the N-loop. K56 shows a linear perturbation similar to CXCL1 residues, suggesting its perturbation is due to direct or indirect interactions from dp8 binding to CXCL1. The initial perturbation of residues K57 and I58 can thus be attributed to a proximity effect of K56. However, the perturbation profile of K57 and I58 is altered upon further addition of dp8 indicating these changes must be due to direct dp8 binding to CXCL7. Thus the sigmoidal profiles are a composite of CXCL1 and CXCL7 binding (Figures 4.7B and 4.7E). These data collectively indicate two independent binding sites, with one heparin binding one monomer and the second heparin binding the other monomer of the heterodimer, and that heparin first binds to CXCL1 due to higher affinity and then to CXCL7.

As discussed above, characterizing GAG binding to the WT heterodimer is challenging. However, using the trapped heterodimer titration spectrum as a template, we explored whether it was possible to characterize heparin binding to the native heterodimer. Indeed, we could track heparin binding to a few well-dispersed heterodimer

peaks. For instance, upon titration, a heterodimer peak was observed, which showed significant CSP, a non-linear sigmoidal profile, and similar chemical shifts as K57 and I58 in the trapped heterodimer. Additionally, heterodimer peaks that could be assigned to Q20, L48, and G65 showed sigmoidal profiles similar to what was observed in the trapped heterodimer. These observations provide compelling evidence that binding interactions of the trapped heterodimer captures the complexity of the native heterodimer.

To gain insight into the binding geometries, we generated models of the GAG heparin dp8 bound CXCL1-CXCL7 heterodimer complex using HADDOCK-based docking. We performed two independent runs. In run-I, restraints were given between one dp8 and CXCL7 and between another dp8 and CXCL1. In run-II, restraints were given between two GAGs and both monomers of the heterodimer. Both runs showed essentially the same binding geometry, with one GAG binding to each monomer of the heterodimer (Figure 4.8A). In CXCL7, the GAG-binding interface spans the β_3 -strand, the N-loop, and the helix, and is mediated by H15 and K17 of the N-loop, R44 of the β_3 -strand, and R54, K57, and K61 of the helix (Figure 4.8B). In CXCL1, the GAG-binding interface also spans the β_3 -strand, the N-loop, and the helix and is mediated by H19 and K21 of the N-loop, R48 of the β_3 -strand, and K61 and K65 of the helix (Figure 4.8C). Note that CXCL1 K45 and CXCL7 K27 were not involved in binding though both showed significant CSP indicating their CSP is most likely due to indirect interactions. We also carried out modeling of one GAG to either CXCL1 or CXCL7 and observed the same binding interactions as observed for two GAGs. Our models provide the structural basis for stepwise and non-overlapping binding geometry that is consistent with the NMR titrations. Further, the GAG-binding geometry is distinct from that observed in CXCL1 dimer, where GAG binds across the β -sheet dimer interface¹⁸⁷.

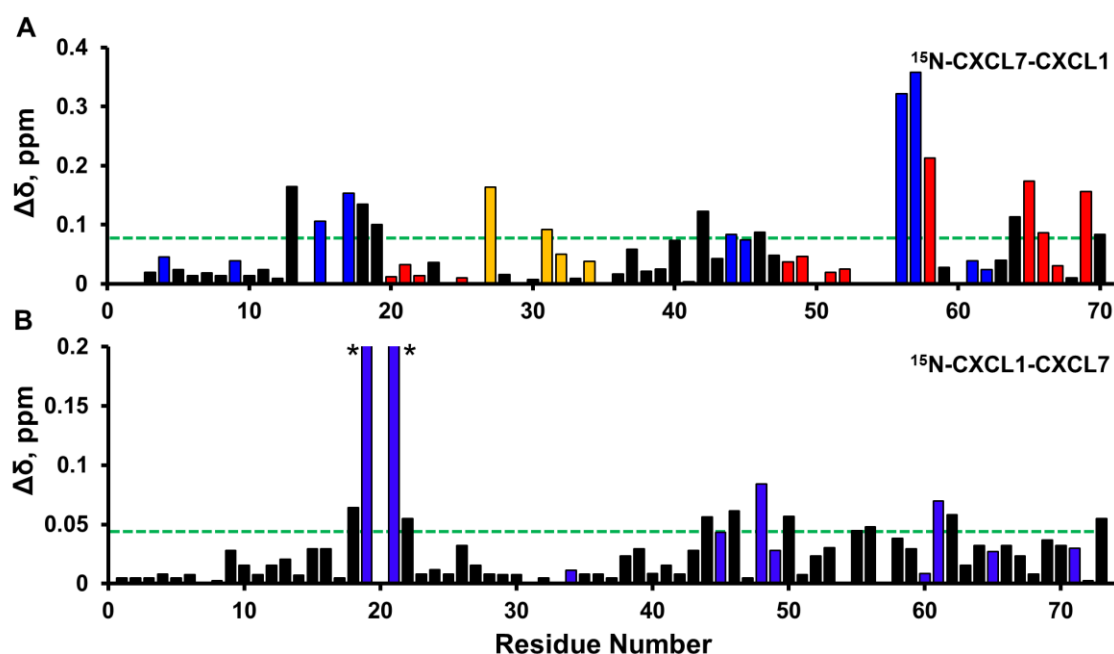


Figure 4.6: **Histogram plots of chemical shift changes on Heparin binding to trapped heterodimer.** Heparin binding-induced chemical shift changes in CXCL7 (A) and CXCL1 (B) of the CXCL7-CXCL1 trapped heterodimer. Residues that show CSP above the threshold (dashed line) are considered involved in binding. Basic residues Arg, Lys, and His are shown in blue. CXCL7 residues that show sigmoidal binding profiles are shown in red and residues showing normal hyperbolic profiles are shown in gold. Residues H19 and K21 (highlighted by *) show much higher CSPs (0.26 and 0.71 ppm, respectively).

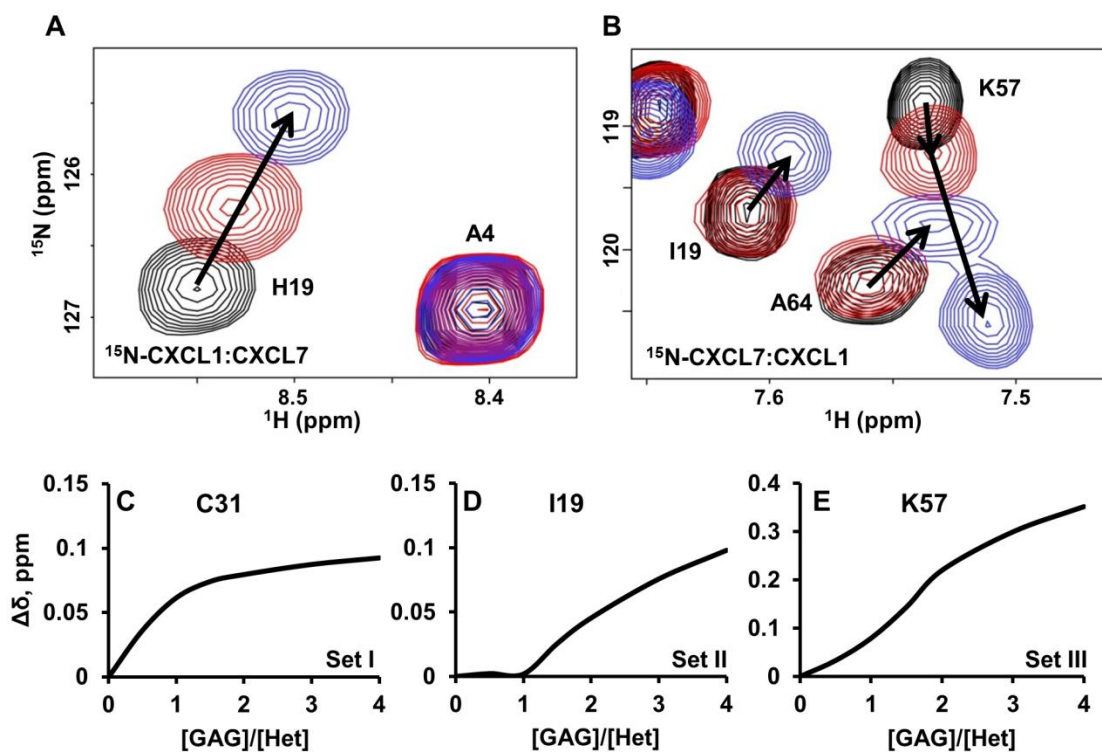


Figure 4.7: **NMR characteristics of trapped heterodimer-heparin interactions.** Sections of the ^1H - ^{15}N HSQC spectra showing the overlay of CXCL7-CXCL1 trapped heterodimer in the free (black) and heparin dp8 bound form at 1:1 (red) and 1:4 (blue) molar ratios. Arrows indicate direction of movement. (A) For CXCL1, only linear chemical shifts are observed. (B) In the case of CXCL7, both non-linear chemical shifts (K57) and delayed linear chemical shifts (I19 and A64) are observed. (C-E) Plots of binding-induced chemical shift changes on adding heparin. For CXCL7, hyperbolic (C), hyperbolic after a delay (D), and sigmoidal (E) profiles are observed.

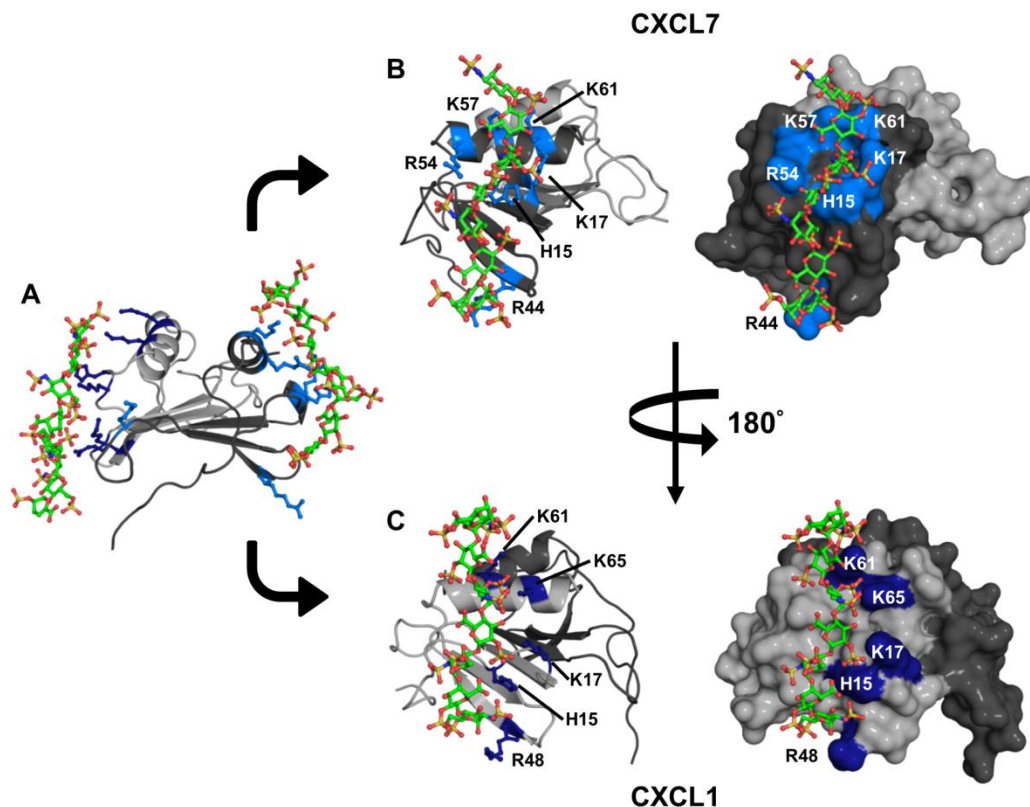


Figure 4.8: **A model of heparin-bound CXCL7-CXCL1 heterodimer complex.** (A) Ribbon diagram showing heparin binds to both monomers of the heterodimer. CXCL7 is shown in dark gray and CXCL1 light gray. (B and C) Cartoon and surface plots showing side views of the CXCL7 and CXCL1 monomer faces interacting with heparin dp8, respectively. Basic residues involved in binding are labeled and shown in blue.

Heterodimer Receptor Binding Activity

We characterized receptor activity by measuring Ca^{2+} release using HL60 cells stably transfected with CXCR2 receptor¹⁵⁰. We compared receptor activities of WT CXCL1, WT CXCL7, a mixture of both chemokines (CXCL7 and CXCL1), and our trapped heterodimer (CXCL7-CXCL1). The trapped heterodimer was as potent as the WT chemokines, and the activity of the mixture of CXCL1 and CXCL7 (that corresponds to the native heterodimer) was no different from the trapped heterodimer or WT proteins (Figure 4.9). These data indicate that there is no synergy and that essentially one of the

monomers of the heterodimer binds and activates the receptor. Previous studies using a trapped homodimer have also shown that the activity of the homodimer was no different from the monomer^{76,150,219}.

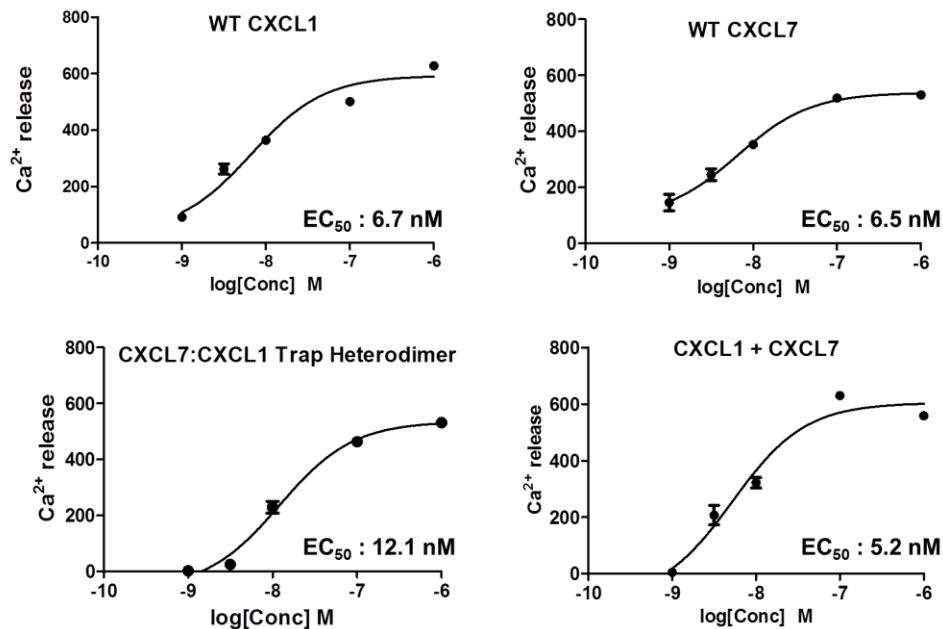


Figure 4.9: **CXCR2 activity of the heterodimer.** A plot showing the activity curves for WT CXCL1, WT CXCL7, 1:1 CXCL7/CXCL1 mixture, and the trapped CXCL7-CXCL1 heterodimer. The EC₅₀ values indicate that the heterodimer binds and activates the receptor like the WT proteins.

DISCUSSION

Animal model and in vitro studies have shown enhanced or altered activity for a wide variety of CXC, CC, and CXC/CC chemokine pairs⁹⁵⁻¹⁰¹. For instance, high levels of CXCL1 (KC) and CXCL2 (MIP-2) have been observed in a number of murine disease models, virus-infected epithelial cells release multiple chemokines that direct neutrophil chemotaxis, peptides that inhibit CCL5/CXCL4 heterodimer formation alleviate atherosclerosis in a mouse model, and CXCL7/CXCL4 pair compared to CXCL7 alone

shows differential activity for neutrophil adhesion and transendothelial migration^{110,220-222}. However, whether altered activity is due to non-additive receptor activity of two chemokines or to distinct heterodimer receptor activity is lacking.

Knowledge of the structural basis and molecular mechanisms by which chemokines form heterodimers is essential to understanding how heterodimers mediate function. In this study, using solution NMR spectroscopy, the structural features and molecular basis by which CXCL7 is able to form heterodimers with some chemokines but not with others are described. Further, using NMR spectroscopy, the molecular basis of heparin GAG binding to the CXCL7-CXCL1 heterodimer is also described. NMR detects direct binding and does not require exogenous tagging as do the fluorescence-based FRET/BRET methods, and so does not suffer from potential artifacts. Popular techniques for distinguishing between monomers and dimers such as gel filtration and native gel electrophoresis cannot distinguish between heterodimers and homodimers due to their similar size and molecular weight. Mass spectrometry and co-immunoprecipitation techniques have been used to detect chemokine heterodimers^{107,109,223}, but these techniques do not provide any insight into the molecular basis of heterodimer formation. NMR chemical shifts of the backbone amide (¹H and ¹⁵N) are sensitive to secondary, tertiary, and quaternary structures. Therefore, under ideal conditions, NMR could distinguish heterodimers from homodimers and monomers. Previous NMR studies have shown heterodimer formation between CXCL4 and CXCL8¹⁰⁶ and that CCL2-CCL8 heterodimer is favored compared to CCL2 homodimer¹⁰⁷, but did not describe the structural features of the heterodimer. This is challenging and requires chemical shift assignments not only of the monomer and homodimer but also of the heterodimer.

The role of heterodimer function in vivo is dependent on receptor and/or GAG interactions. GAG interactions play multiple roles that include determining the makeup of the chemotactic/haptotactic gradients, influencing whether it is the free or GAG-bound

chemokine that activates the receptor, and regulating the levels of the free monomer and homodimer. Further, free and GAG-bound heterodimer levels will depend on the GAG affinities, the equilibrium constants (K_d) of the heterodimer and of the two homodimers, and the relative amounts of the two chemokines. Our findings indicate that for CXCL7 and CXCL1 the heterodimer K_d falls between the two homodimers. Using trapped homodimers, it has been shown that the dimer could be as active as the monomer for CXCR2 function in cellular assays¹⁵⁰. However, the in vivo recruitment activity of the monomers and dimers are distinctly different, indicating that the monomer-dimer equilibrium and GAG binding are coupled and regulate in vivo recruitment^{72,93,186}. Therefore, any novel activity of the heterodimer can be inferred only under conditions where heterodimer dominates and its activity is different from monomers and homodimers, and becomes challenging if its levels are not high and/or its activity is not very different from monomers and homodimers.

In this study, using a disulfide-trapping strategy, heparin dp8 binding and CXCR2 activity of the CXCL7-CXCL1 heterodimer were successfully characterized. To our knowledge, this is the very first study that describes the GAG interactions and receptor activity of a heterodimer without interference from the monomers or homodimers. The GAG interactions of the heterodimer were strikingly different from the monomer and CXCL1 homodimer^{187,210}, and most interestingly, the receptor activity was no different compared to the native proteins. We conclude that differences in heterodimer-GAG interactions could play a role in fine-tuning chemotactic/haptotactic gradients and also control the amount of free chemokine available to activate the receptor. Finally, our strategy of engineering a disulfide-linked, trapped chemokine heterodimer opens up new avenues to characterize in vivo heterodimer function, the role of differential receptor signaling pathways, and elucidate heterodimer's role for a variety of chemokine pairs in health and disease.

MATERIALS AND METHODS

MOLECULAR DYNAMICS SIMULATIONS OF HETERODIMERS

Initial structures were prepared using NMR or X-ray coordinates available from the protein data bank (PDB). The PDB IDs used were 1NAP (CXCL7)⁵⁷, 1MSG (CXCL1)⁵², 1PFM (CXCL4)⁶⁸, and 1IL8 (CXCL8)²⁸. Structures were generated by alignment of homodimer backbones and then removing one of the monomers of each homodimer using PyMol¹⁹⁸. In the heterodimer the monomer structures were adjusted by translational and rotational motions about the two fold symmetry axis to align the hydrogen bond network across the β -strands of the dimer interface. The modelled heterodimer structures were then subjected to constrained energy minimization to eliminate any steric clashes, followed by free minimization using the AMBER 12 suite software and the ff03 force field^{199,224}. The energy-minimized structures were subjected to an equilibration protocol in explicit solvent²²⁵, followed by ~180 ns of MD production runs were carried out using the PMEMD (Particle mesh Ewald molecular dynamics) module of the AMBER 12 software suite on the Lonestar Dell Linux Cluster at the Texas Advanced Computing Center (TACC, UT Austin, TX). The trajectories were analyzed using AMBERtools 12, VMD, and PyMol^{198,199,226}.

EXPRESSION AND PURIFICATION OF CHEMOKINES

Chemokines were expressed in *E. coli* cultured in either LB or ¹⁵N-enriched minimal medium and purified using a combination of nickel column and reverse phase high-performance liquid chromatography as previously described¹³⁹. The CXCL7-CXCL1 trapped heterodimer was prepared by introducing a disulfide across the dimer interface. CXCL7 S21C and CXCL1 K29C mutants were purified using Ni-NTA column, cleaved using Factor Xa, and were combined without further purification and left overnight at 35 °C. Heterodimer formation was confirmed using SDS-PAGE and was

purified using high performance liquid chromatography. Purified proteins were then lyophilized and stored at -20 °C until further use.

NMR CHARACTERIZATION OF HETERODIMER

Samples were prepared in a 50 mM sodium phosphate buffer pH 7.4 at 25°C containing 1 mM 2,2-dimethyl-2-silapentanesulfonic acid (DSS), 1 mM sodium azide, and 10% D₂O. Heterodimer formation between two chemokines can be inferred from changes in the HSQC spectra on titrating an unlabeled chemokine to a ¹⁵N-labeled chemokine prepared in the same buffer. Initial ¹⁵N-labeled chemokine concentrations varied between 30 and 150 μM. The final molar ratios of labeled to unlabeled chemokine varied from 1:2 to 1:4. For these experiments, titrations were carried out until essentially no change in the spectra was observed. NMR experiments were performed on a Bruker Avance III 600 (with a QCI cryoprobe) or 800 MHz (with a TXI cryoprobe) spectrometer. All spectra were processed and analyzed using Bruker Topspin 3.2 or Sparky software¹⁹⁵.

The ¹H and ¹⁵N chemical shifts of the trapped CXCL7-CXCL1 heterodimer were assigned using ¹⁵N-CXCL1-CXCL7 and ¹⁵N-CXCL7-CXCL1 samples prepared in 50 mM phosphate pH 6.0 and 35 °C. The concentrations of ¹⁵CXCL7-CXCL1 and CXCL7-¹⁵CXCL1 were 300 and 670 μM, respectively, and assignments were obtained from analysis of ¹H-¹⁵N heteronuclear NOESY and TOCSY experiments with mixing times of 150 and 80 ms, respectively.

CHARACTERIZATION OF HEPARIN GAG AND HETERODIMER

Binding of heparin dp8 to CXCL7-CXCL1 heterodimer was characterized using solution NMR spectroscopy in 50 mM phosphate buffer at pH 6.0 and 30 °C. The protein concentration for the titrations varied between 50 and 70 μM. Heparin dp8 was purchased from Iduron (Manchester, UK) and prepared in the same buffer (10 mM stock) and a

series of ^1H - ^{15}N HSQC spectra were collected upon titrating GAG until no changes in the spectra are observed. The final molar ratio of heterodimer to GAG was 1:4. For the trapped heterodimer, both ^{15}N -CXCL7-CXCL1 and ^{15}N -CXCL1-CXCL7 samples were used. For native heterodimer interactions, a mixture of CXCL7 and CXCL1 at 1:1 molar ratio was used. The final molar ratio of heterodimer to GAG was \sim 1:3 to 1:4. For all titrations, chemical shift perturbations were calculated as a weighted average of changes in the ^1H and ^{15}N chemical shifts as described previously⁷⁷.

HETERODIMER-GAG DOCKING

Molecular docking of heparin to the CXCL7-CXCL1 heterodimer was carried out using High Ambiguity Driven biomolecular DOCKing (HADDOCK) approach as described previously^{185,201,202}. The CXCL7-CXCL1 heterodimer structure from MD studies and the NMR structure of heparin (PDB ID: 1HPN)²⁰³ were used for docking. Ambiguous interaction restraints (AIRs) were selected based on NMR chemical shift perturbation data. The pair-wise “ligand interface RMSD matrix” over all structures was calculated and final structures were clustered using an RMSD cut-off value of 4 Å. The clusters were then prioritized using RMSD and ‘HADDOCK score’ (weighted sum of a combination of energy terms).

RECEPTOR ACTIVITY OF THE HETERODIMER

The CXCR2 receptor activity of the heterodimer was determined using a Ca^{2+} release assay as described previously¹⁵⁰. Ca^{2+} levels were measured using a FlexStation III microplate reader using the Calcium 5 assay kit (FLIPR, Molecular Devices). Differentiated HL60 cells expressing CXCR2 were incubated with varying concentrations of either WT CXCL1, WT CXCL7, a mixture of both WTs, or the trapped CXCL7-CXCL1 heterodimer. Changes in fluorescence of the Calcium 5 dye upon addition of chemokine were measured every 5 s for up to 500 s, and the agonist response

was determined from the maximum change in fluorescence. EC_{50} values were calculated based on the response over a range of concentrations.

Chapter 5

Conclusions and Future Directions

The platelet chemokine CXCL7 plays an important role in neutrophil-platelet crosstalk during vascular injury. It is one of the most abundant chemokines released from platelets, and activates the CXCR2 receptor on circulating neutrophils^{227,228}. These interactions provide cues that direct neutrophils to the site of injury in the form of chemotactic and haptotactic gradients. Both our current and previous studies reveal a prominent role for monomer-dimer equilibrium and GAG interactions in controlling the steepness and duration of these gradients. In addition, in the context of vascular injury, CXCL7 is secreted with multiple other chemokines, and the formation of heterodimers likely plays a role in mediating recruitment. Considering that repair of injury and resolution of inflammation occur over a period of hours to days, the local CXCL7 concentration can vary by orders of magnitude. Accordingly, the relative ratios of the monomers, dimers, and heterodimers will vary, which dictate the makeup of the gradients. The gradients, in turn, determine the recruitment and the neutrophil phenotype from proinflammatory to repair. Disruption of any of these interactions at any point could result in collateral tissue damage and disease. However, nothing is known regarding the molecular mechanisms that mediate these interactions. In this dissertation, we provide for the first time, valuable structural insights into these interactions.

In this study, the molecular level interactions of the CXCL7 monomer, homodimer, and heterodimer with both GAG and the CXCR2 receptor N-domain were characterized. By utilizing the weak dimer potential of CXCL7 in the first study of its kind, we characterized the structural features of the CXCL7 monomer. The CXCL7 monomer binds GAG with multiple geometries, indicating the binding interface is highly plastic. The CXCR2 N-domain binds a conserved hydrophobic pocket flanked between

the N-loop and the β_3 -strand of the monomer. Comparison of the GAG and receptor binding domains reveals that the GAG-bound monomer cannot bind the receptor N-domain. In the context of neutrophil recruitment, these interactions indicate that GAG-binding regulates the amount of free monomer available to activate the receptor.

To date, the role of CXCL7 homodimer has never been addressed in the literature because it is present only as a minor species at any concentration or solution condition. However, quite strikingly, we observed that GAG-bound CXCL7 exists as a dimer. This indicates that the importance of the homodimer can be fully appreciated only when GAG interactions are taken into consideration. Utilizing this property, the molecular level interactions of the homodimer with both GAG and CXCR2 were investigated. GAG binds to each monomer unit of the CXCL7 dimer in a two GAG to one dimer stoichiometry, and the CXCR2 N-domain binds the CXCL7 dimer as it does for the monomer. Similar to what was observed for the monomer, the GAG-binding and receptor-binding domains overlap, indicating that the GAG-bound dimer cannot activate the receptor.

In this study, the potential for heterodimer formation of CXCL7 with the other platelet chemokines CXCL1 and CXCL4 was demonstrated. Interestingly, the CXCL7-CXCL1 heterodimer was more favored than the CXCL7 homodimer, but less favored than the CXCL1 homodimer. Further, we also observe that the heterodimer binds GAG with high affinity, indicating the role of heterodimer is intimately linked to GAG binding. To structurally characterize the GAG and receptor interactions of the heterodimer, we developed a novel disulfide-trapped heterodimer. Using this trapped heterodimer, the receptor activity of the heterodimer was observed to be the same as the WT protein as measured in a Ca^{2+} release assay. These findings suggest that any differential activity of the heterodimer is likely due to GAG interactions²²⁹.

At this time, there are no technologies or methodologies available to measure in vivo local chemokine concentrations, so providing a quantitative description of how

different CXCL7 variants mediate trafficking is not possible. Therefore, we propose models and scenarios that are semi-quantitative at best. We have determined the monomer-dimer equilibrium constant (K_d) for CXCL7 and CXCL1 homodimers as $\sim 150 \mu\text{M}$ and $\sim 5 \mu\text{M}$ ^{73,187}, and the K_d for the CXCL7-CXCL1 heterodimer as $\sim 25\text{-}50 \mu\text{M}$ on the basis of relative intensities of the monomer, dimer, and heterodimer peaks. The availability of dimer and heterodimer formation equilibrium constants, receptor binding affinities, and relative GAG binding affinities for the monomer, dimer, and heterodimer allows better description of how different CXCL7 species regulate neutrophil function (Figures 5.1 to 5.3).

The observations from this dissertation reveal the importance of homodimer and heterodimer in relation to GAG binding (Figure 5.1). Upon release from activated platelets, CXCL7 diffuses through the blood resulting in gradient formation. Gradient formation at a given time is impacted by multiple factors such as shear forces, crowding effects, and the distribution of GAGs (Figure 5.2). Serum concentrations of CXCL7 have been measured as $\sim 5 \mu\text{M}$, which is several orders of magnitude higher compared to other chemokines. It is likely that dimers and heterodimers dominate during early time points and near the thrombus. As CXCL7 diffuses away from the injury site, its local concentration will drop, and accordingly, the population will shift predominantly to a monomer. It must also be remembered that gradients, both along the blood flow (say x-axis) and away from the endothelial cell wall (say y- and z-axis), must be taken into consideration (Figure 5.3). Neutrophils respond to the soluble monomer chemotactic gradients and move towards the injury site. However, the steepness and duration of the chemotactic gradient will vary as a function of time, which in turn will regulate the neutrophil levels to the injury site (Figure 5.1). Our findings indicate that removal or dysregulation of dimer or GAG would result in disruption of ideal gradients and subsequently the directional cues that mediate neutrophil recruitment (Figure 5.2).

This work has provided valuable insights into the molecular mechanisms that dictate CXCL7 mediated platelet-neutrophil crosstalk. However, this is still just the tip of the iceberg. Future studies on the role of CXCL7 tetramer and its GAG interactions, heterodimer in activating β -arrestin pathways and receptor internalization need to be elucidated in order to fully describe CXCL7 function in the thrombus. Such studies are now feasible thanks to the development of a disulfide linked trapped heterodimer. Further, in vivo studies investigating the recruitment activity of monomers, homodimers, and heterodimers in a thrombus injury model would provide a more complete overview to put further context into the findings discussed here. Most importantly, methods and technologies must be developed that can provide snapshots of local concentrations and their changes with time, in order to develop mathematical models to better describe chemokine levels, neutrophil function, and successful resolution.

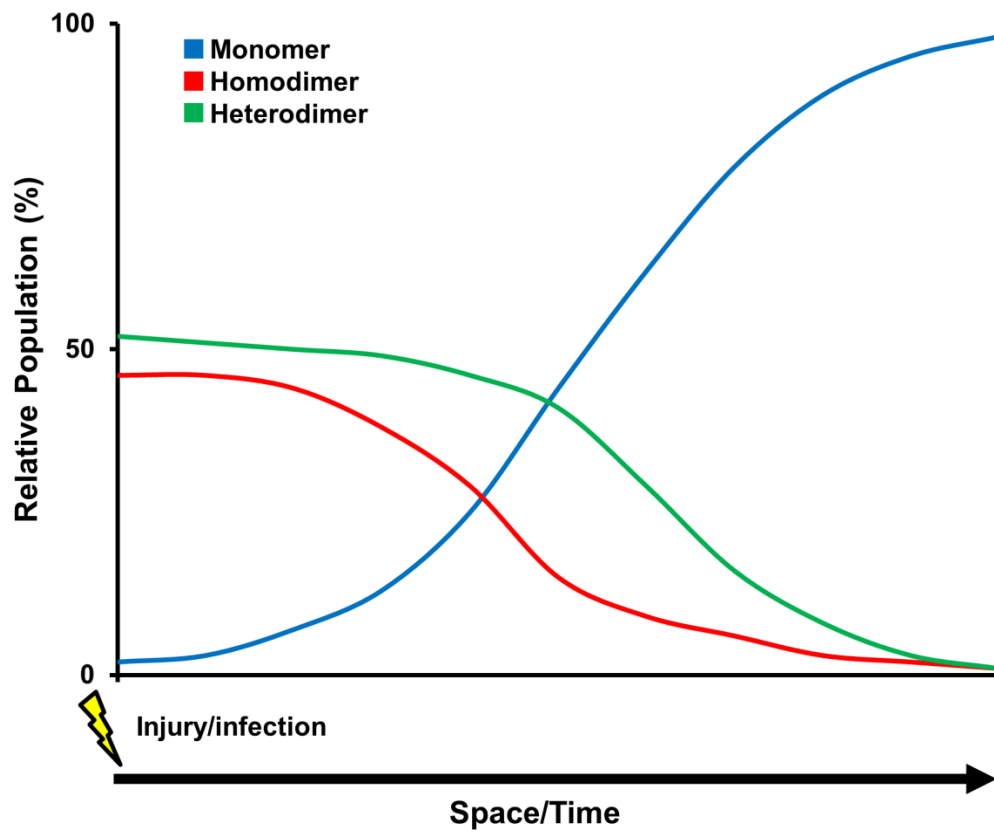


Figure 5.1: **Relative populations of monomer, homodimers, and heterodimers.** Populations are based on equilibrium constants and GAG-binding affinities. Homodimers and heterodimers in the presence of GAG initially dominate. As CXCL7 moves away from the injury site and becomes diluted, monomer begins to populate.

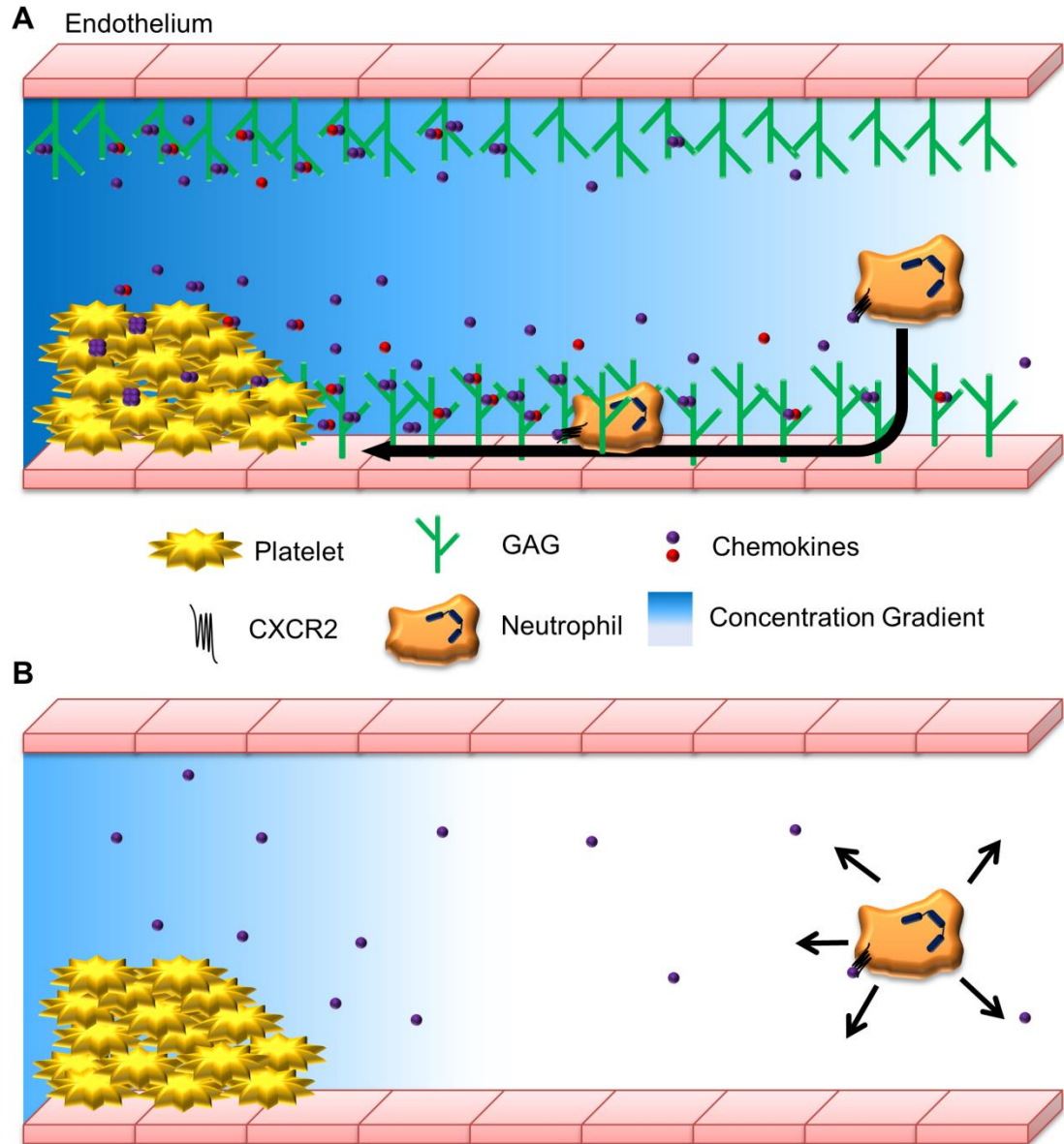


Figure 5.2: **Schematic of CXCL7-mediated neutrophil recruitment.** (A) Platelets release CXCL7 along with other chemokines during thrombus formation. Homodimers and heterodimers are shown predominantly in the GAG bound form. The blue background illustrates the chemotactic gradient and the black arrow indicates the direction of neutrophil migration. (B) Disruption of GAG interactions or dimer formation results in reduced gradient formation as illustrated by the blue color gradient. Arrows indicate directional cues are lost under these circumstances, resulting in reduced recruitment to the thrombus.

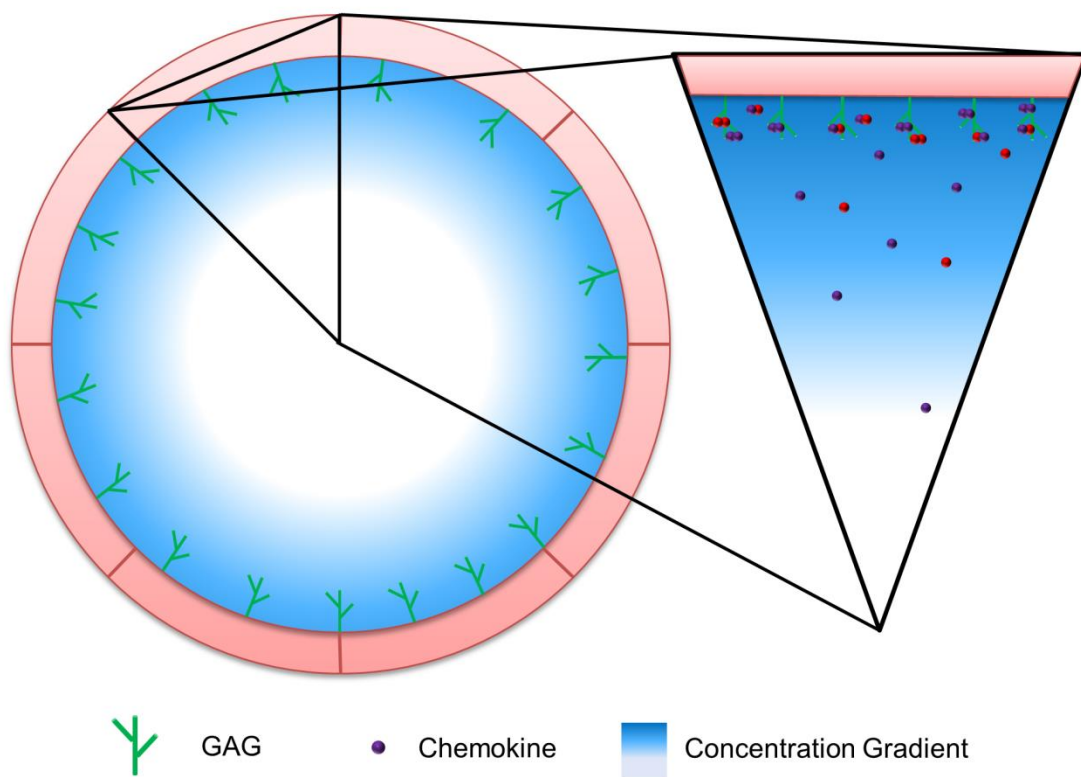


Figure 5.3: **Gradient formation in the vasculature.** Cross section of a blood vessel demonstrating the chemotactic gradient also occurs in the radial dimension. A zoomed in slice is shown to further illustrate the role of GAG binding and dimer formation in mediating gradient formation that facilitates neutrophil recruitment to the thrombus in the proximity of the endothelium.

Appendix A Tables and Figures

Table A1: Assignments for CXCL7 monomer in 50 mM phosphate at pH 4.0, 30°C

CXCL7 Sequence Assignments							
Residue	NH	H α	H β	others	N	C α	C β
1. Ala							
2. Glu	8.66	4.43	2.02	γ H 2.39	120.63	53.71	28.84
3. Leu	8.44	4.38	1.62	γ H 1.62, δ H 0.84	124.47	52.45	43.93
4. Arg	8.28	4.65	2.03, 1.81	γ H 1.59 δ H 3.16	120.71	52.37	29.65
5. Cys	8.36	4.65	3.50, 2.88		119.42	52.78	37.72
6. Met	9.36	4.40	2.11	γ H 2.61	123.88	54.28	32.50
7. Cys	8.41	4.90	3.06, 2.92		118.17	52.00	40.36
8. Ile	8.44	4.19	1.98	γ H 1.27 δ H 0.99	122.63	59.69	36.68
9. Lys	7.91	4.66	1.94, 1.80	γ H 1.49 δ H 2.93	119.97	52.50	33.22
10. Thr	8.31	4.68	4.03	γ H 1.13	113.15	57.63	69.90
11. Thr	8.38	4.73	4.05	γ H 1.23	115.77	58.73	69.04
12. Ser	8.58	4.74	4.01		119.51	55.17	62.81
13. Gly	8.58	3.99			110.36	43.87	
14. Ile	7.50	4.25	1.82	γ H 1.15 δ H 0.79	118.94	56.11	36.70
15. His	8.64	5.06	3.39, 3.21		124.66	52.32	
16. Pro						62.60	30.33
17. Lys	8.65	4.27	1.90	γ H 1.46	116.99	55.63	29.81
18. Asn	8.20	4.88	3.18, 2.86		115.28	50.73	37.99
19. Ile	7.68	3.90	1.94	γ H 1.68 δ H 0.76	120.19	60.38	37.21
20. Gln	9.48	4.48	1.90	γ H 2.29	128.30	54.33	28.96
21. Ser	7.94	4.68	3.90		111.31	54.98	63.60
22. Leu	8.50	5.21	1.49	δ H 0.82	122.00	51.76	44.69
23. Glu	8.85	4.72	2.06, 1.93	γ H 2.34	124.29	52.46	31.19
24. Val	9.42	4.32	1.98	γ H 1.11	129.96	59.09	31.18
25. Ile	8.67	4.72	2.00	γ H 1.50 δ H 0.88	125.33	58.28	36.70
26. Gly	8.59	4.14, 3.86			112.40	42.60	
27. Lys	8.22	4.16	1.77	γ H 1.25, δ H 1.39	119.92	54.57	31.71
28. Gly	8.41	4.35, 4.14			110.31	43.07	
29. Thr	8.35	4.68	4.07	γ H 1.09	114.23	62.27	67.05
30. His	8.53	4.80	3.40, 3.17		115.71	53.94	28.80
31. Cys	7.56	4.80	3.15		116.24	54.08	39.62
32. Asn	8.70	4.87	2.96		126.38	51.17	36.25
33. Gln	7.63	4.68	2.16, 1.92	γ H 2.37	116.81	51.49	41.14
34. Val	8.34	4.18	1.94	γ H 1.08, 0.86	122.60	60.42	29.70
35. Glu	8.71	4.80	2.02	γ H 2.55	124.20	53.19	30.80
36. Val	9.47	4.82	2.11	γ H 0.84	124.05	57.93	30.96
37. Ile	9.01	4.79	1.85	γ H 1.50, 1.17, δ H 0.80	126.39	57.65	37.83
38. Ala	9.63	5.27	1.30		132.89	47.47	19.16
39. Thr	8.87	4.94	4.12	γ H 1.28	119.17	59.84	67.29
40. Leu	9.48	5.09	2.27	γ H 1.75, δ H 0.96	127.70	51.48	40.37
41. Lys	8.48	4.03	1.86	γ H 1.47	120.96	56.90	30.51

CXCL7 Sequence Assignments							
Residue	NH	H α	H β	others	N	C α	C β
42. Asp	7.66	4.61	3.19, 2.65		114.81	50.73	38.60
43. Gly	8.09	4.4, 3.58			108.32	42.33	
44. Arg	7.89	4.27	2.04	γ H 1.71	120.90	54.78	30.11
45. Lys	8.19	5.53	1.72	γ H 1.50, ϵ H 3.01	120.02	52.48	32.50
46. Ile	9.01	4.70	1.80	δ H 0.84	119.35	56.44	40.30
47. Cys	8.73	5.62	3.79, 3.31		121.81	54.10	44.73
48. Leu	8.99	5.04	1.68	γ H 1.51, δ H 0.80	123.31	49.91	42.12
49. Asp	8.19	4.72	2.88, 2.60		121.85	48.97	
50. Pro						61.35	30.54
51. Asp	8.08	4.70	2.90, 2.69		114.30	51.30	40.16
52. Ala	7.50	4.64	1.59		126.18	48.14	
53. Pro						63.64	30.50
54. Arg	8.78	4.14	2.02	γ H 1.82	115.40	56.51	28.31
55. Ile	7.44	4.05	2.27	γ H 1.47, δ H 0.82	117.01	58.36	40.44
56. Lys	8.48	4.04	1.91	γ H 1.52	122.50	57.76	30.75
57. Lys	7.52	4.13	1.91	γ H 1.62	115.92	56.49	30.59
58. Ile	7.37	3.82	2.04	γ H 1.23, δ H 0.86	120.17	62.12	40.45
59. Val	8.33	3.50	2.27	γ H 0.99	120.61	64.22	30.07
60. Gln	8.18	4.02	2.21	γ H 2.55	117.15	56.27	26.73
61. Lys	7.68	4.18	2.21, 2.00	γ H 1.61	118.45	56.49	29.64
62. Lys	8.11	4.24	1.98	γ H 1.60	118.95	55.43	
63. Leu	8.25	4.30	1.82	γ H 1.60, δ H 0.88	118.99	53.93	39.86
64. Ala	7.74	4.38	1.55		121.78	50.19	17.61
65. Gly	8.02	4.04			106.93	43.17	
66. Asp	8.15	4.72	2.82		119.68	51.52	40.46
67. Glu	8.39	4.45	2.26, 2.03	γ H 2.47	121.05	53.88	28.21
68. Ser	8.26	4.45	3.95		116.34	56.06	62.72
69. Ala	8.22	4.46	1.45		125.91	49.94	17.94
70. Asp	7.96	4.53	2.79		122.99	53.41	
Side Chain					N		
4. Arg				7.19	121.22		
18. Asn				7.10, 7.67	112.30		
20. Gln				6.86, 7.40	111.85		
32. Asn				6.86, 7.55	111.30		
33. Gln				6.79, 7.48	112.00		
44. Arg				7.87	121.92		
54. Arg				7.35	120.75		
60. Gln				6.81, 7.44	111.20		

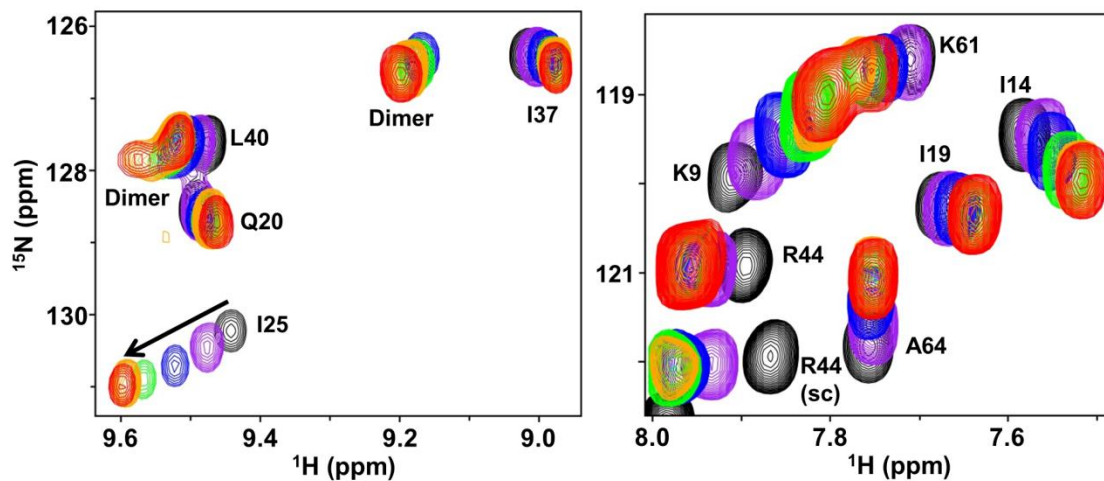


Figure A1: **HSQC spectra of the pH titration from pH 4.0 to 7.0.** Titration points go from pH 4.0 (black), 4.4 (purple), 5.0 (blue), 5.5 (green), 6.0 (orange), and pH 7.0 (red). Monomer peaks are labeled. Dimer peaks become visible at higher pH as indicated.

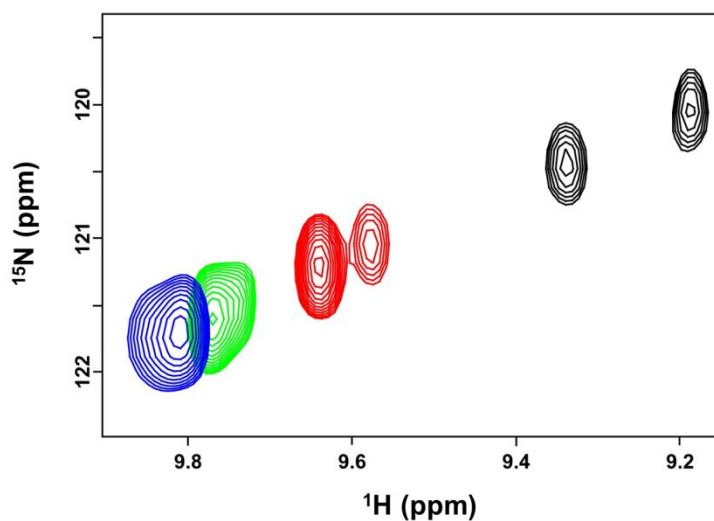


Figure A2: **HSQC spectrum of the C7 peak splitting.** Titration points go from pH 5.0 (black), 5.5 (red), 6.0 (green), and 7.0 (blue).

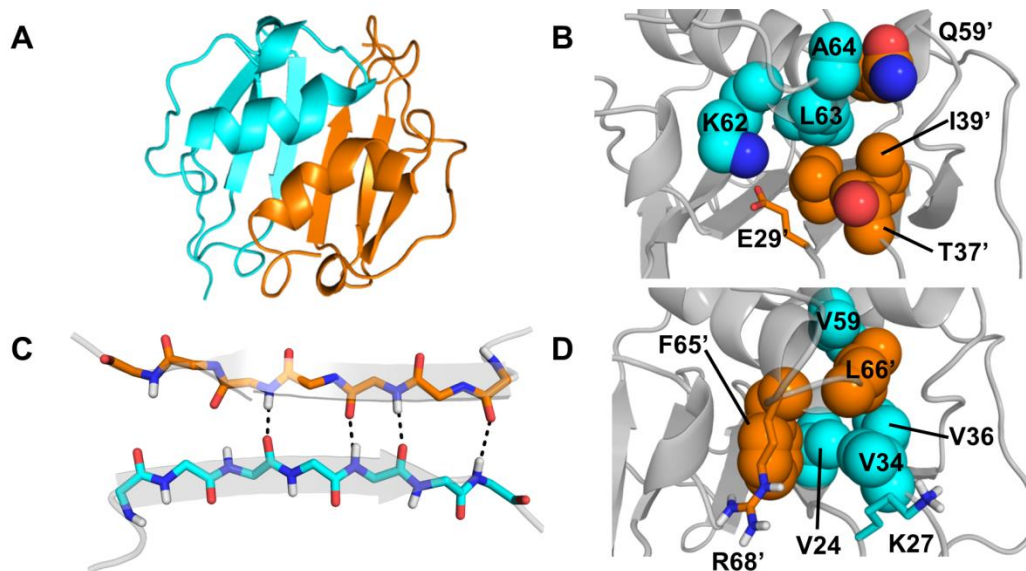


Figure A3: **Structural features of the CXCL7-CXCL8 heterodimer.** (A) Snap shot of the structural model of CXCL7-CXCL8 heterodimer from the last 5ns of the MD simulation. (C) A schematic showing the β_1 -strand dimer interface H-bonds (dashed line) from the final 5ns of the MD run. (B,D) Packing interactions involving CXCL7 helical and CXCL8 β -sheet residues and CXCL8 helical and CXCL7 β -sheet residues, respectively. CXCL8 residues are labeled with an prime (').

References

1. Esche C, Stellato C, Beck LA. Chemokines: key players in innate and adaptive immunity. *J Invest Dermatol* 2005;125(4):615-28.
2. Allen SJ, Crown SE, Handel TM. Chemokine: receptor structure, interactions, and antagonism. *Annu Rev Immunol* 2007;25:787-820.
3. Luster AD, Alon R, von Andrian UH. Immune cell migration in inflammation: present and future therapeutic targets. *Nat Immunol* 2005;6(12):1182-90.
4. Griffith JW, Sokol CL, Luster AD. Chemokines and chemokine receptors: positioning cells for host defense and immunity. *Annu Rev Immunol* 2014;32:659-702.
5. Bonecchi R, Galliera E, Borroni EM, Corsi MM, Locati M, Mantovani A. Chemokines and chemokine receptors: an overview. *Front Biosci* 2009;14:540-51.
6. Kiefer F, Siekmann AF. The role of chemokines and their receptors in angiogenesis. *Cell Mol Life Sci* 2011;68(17):2811-30.
7. Nguyen LT, Vogel HJ. Structural perspectives on antimicrobial chemokines. *Front Immunol* 2012;3:384.
8. Raman D, Sobolik-Delmaire T, Richmond A. Chemokines in health and disease. *Exp Cell Res* 2011;317(5):575-89.
9. Dimberg A. Chemokines in angiogenesis. *Curr Top Microbiol Immunol* 2010;341:59-80.
10. Speyer CL, Ward PA. Role of endothelial chemokines and their receptors during inflammation. *J Invest Surg* 2011;24(1):18-27.
11. Luther SA, Cyster JG. Chemokines as regulators of T cell differentiation. *Nat Immunol* 2001;2(2):102-7.
12. Gerdes N, Zhu L, Ersoy M, Hermansson A, Hjemdahl P, Hu H, Hansson GK, Li N. Platelets regulate CD4⁺ T-cell differentiation via multiple chemokines in humans. *Thromb Haemost* 2011;106(2):353-62.
13. Rajagopalan L, Rajarathnam K. Structural basis of chemokine receptor function--a model for binding affinity and ligand selectivity. *Biosci Rep* 2006;26(5):325-39.
14. Stone MJ, Hayward JA, Huang C, E Huma Z, Sanchez J. Mechanisms of Regulation of the Chemokine-Receptor Network. *Int J Mol Sci* 2017;18(2).
15. Rajarathnam K. Designing decoys for chemokine-chemokine receptor interaction. *Curr Pharm Des* 2002;8(24):2159-69.
16. Gerard C, Rollins BJ. Chemokines and disease. *Nat Immunol* 2001;2(2):108-15.
17. Plater-Zyberk C, Hoogewerf AJ, Proudfoot AE, Power CA, Wells TN. Effect of a CC chemokine receptor antagonist on collagen induced arthritis in DBA/1 mice. *Immunol Lett* 1997;57(1-3):117-20.
18. De Benedetti F, Pignatti P, Bernasconi S, Gerloni V, Matsushima K, Caporali R, Montecucco CM, Sozzani S, Fantini F, Martini A. Interleukin 8 and monocyte chemoattractant protein-1 in patients with juvenile rheumatoid arthritis. Relation

- to onset types, disease activity, and synovial fluid leukocytes. *J Rheumatol* 1999;26(2):425-31.
19. Boisvert WA, Curtiss LK, Terkeltaub RA. Interleukin-8 and its receptor CXCR2 in atherosclerosis. *Immunol Res* 2000;21(2-3):129-37.
 20. Gu L, Okada Y, Clinton SK, Gerard C, Sukhova GK, Libby P, Rollins BJ. Absence of monocyte chemoattractant protein-1 reduces atherosclerosis in low density lipoprotein receptor-deficient mice. *Mol Cell* 1998;2(2):275-81.
 21. Boring L, Gosling J, Cleary M, Charo IF. Decreased lesion formation in CCR2^{-/-} mice reveals a role for chemokines in the initiation of atherosclerosis. *Nature* 1998;394(6696):894-7.
 22. Hancock WW, Gao W, Faia KL, Csizmadia V. Chemokines and their receptors in allograft rejection. *Curr Opin Immunol* 2000;12(5):511-6.
 23. McManus C, Berman JW, Brett FM, Staunton H, Farrell M, Brosnan CF. MCP-1, MCP-2 and MCP-3 expression in multiple sclerosis lesions: an immunohistochemical and in situ hybridization study. *J Neuroimmunol* 1998;86(1):20-9.
 24. Balashov KE, Rottman JB, Weiner HL, Hancock WW. CCR5(+) and CXCR3(+) T cells are increased in multiple sclerosis and their ligands MIP-1 α and IP-10 are expressed in demyelinating brain lesions. *Proc Natl Acad Sci U S A* 1999;96(12):6873-8.
 25. Berger EA, Murphy PM, Farber JM. Chemokine receptors as HIV-1 coreceptors: roles in viral entry, tropism, and disease. *Annu Rev Immunol* 1999;17:657-700.
 26. Ying S, Meng Q, Zeibecoglou K, Robinson DS, Macfarlane A, Humbert M, Kay AB. Eosinophil chemotactic chemokines (eotaxin, eotaxin-2, RANTES, monocyte chemoattractant protein-3 (MCP-3), and MCP-4), and C-C chemokine receptor 3 expression in bronchial biopsies from atopic and nonatopic (Intrinsic) asthmatics. *J Immunol* 1999;163(11):6321-9.
 27. Luster AD. Chemokines--chemotactic cytokines that mediate inflammation. *N Engl J Med* 1998;338(7):436-45.
 28. Clore GM, Appella E, Yamada M, Matsushima K, Gronenborn AM. Three-dimensional structure of interleukin 8 in solution. *Biochemistry* 1990;29(7):1689-96.
 29. Clubb RT, Omichinski JG, Clore GM, Gronenborn AM. Mapping the binding surface of interleukin-8 complexed with an N-terminal fragment of the type 1 human interleukin-8 receptor. *FEBS Lett* 1994;338(1):93-7.
 30. Fernando H, Nagle GT, Rajarathnam K. Thermodynamic characterization of interleukin-8 monomer binding to CXCR1 receptor N-terminal domain. *FEBS J* 2007;274(1):241-51.
 31. Clore GM, Gronenborn AM. Three-dimensional structures of alpha and beta chemokines. *FASEB J* 1995;9(1):57-62.
 32. Kufareva I, Salanga CL, Handel TM. Chemokine and chemokine receptor structure and interactions: implications for therapeutic strategies. *Immunol Cell Biol* 2015;93(4):372-383.
 33. Clark-Lewis I, Kim KS, Rajarathnam K, Gong JH, Dewald B, Moser B, Baggiolini M, Sykes BD. Structure-activity relationships of chemokines. *J Leukoc Biol* 1995;57(5):703-11.

34. Clark-Lewis I, Dewald B, Loetscher M, Moser B, Baggiolini M. Structural requirements for interleukin-8 function identified by design of analogs and CXC chemokine hybrids. *J Biol Chem* 1994;269(23):16075-81.
35. Legendre B, Tokarski C, Chang Y, De Freitas Caires N, Lortat-Jacob H, Nadaï PD, Rolando C, Duez C, Tsicopoulos A, Lassalle P. The disulfide bond between cysteine 10 and cysteine 34 is required for CCL18 activity. *Cytokine* 2013;64(1):463-70.
36. Rajagopalan L, Chin CC, Rajarathnam K. Role of intramolecular disulfides in stability and structure of a noncovalent homodimer. *Biophys J* 2007;93(6):2129-34.
37. Escher SE, Sticht H, Forssmann WG, Rösch P, Adermann K. Synthesis and characterization of the human CC chemokine HCC-2. *J Pept Res* 1999;54(6):505-13.
38. Sticht H, Escher SE, Schweimer K, Forssmann WG, Rösch P, Adermann K. Solution structure of the human CC chemokine 2: A monomeric representative of the CC chemokine subtype. *Biochemistry* 1999;38(19):5995-6002.
39. Tuinstra RL, Peterson FC, Kutlesa S, Elgin ES, Kron MA, Volkman BF. Interconversion between two unrelated protein folds in the lymphotactin native state. *Proc Natl Acad Sci U S A* 2008;105(13):5057-62.
40. Rajasekaran D, Fan C, Meng W, Pflugrath JW, Lolis EJ. Structural insight into the evolution of a new chemokine family from zebrafish. *Proteins* 2014;82(5):708-16.
41. Williams G, Borkakoti N, Bottomley GA, Cowan I, Fallowfield AG, Jones PS, Kirtland SJ, Price GJ, Price L. Mutagenesis studies of interleukin-8. Identification of a second epitope involved in receptor binding. *J Biol Chem* 1996;271(16):9579-86.
42. Baldwin ET, Weber IT, St Charles R, Xuan JC, Appella E, Yamada M, Matsushima K, Edwards BF, Clore GM, Gronenborn AM. Crystal structure of interleukin 8: symbiosis of NMR and crystallography. *Proc Natl Acad Sci U S A* 1991;88(2):502-6.
43. Clore GM, Gronenborn AM. NMR and X-ray analysis of the three-dimensional structure of interleukin-8. *Cytokines* 1992;4:18-40.
44. Lodi PJ, Garrett DS, Kuszewski J, Tsang ML, Weatherbee JA, Leonard WJ, Gronenborn AM, Clore GM. High-resolution solution structure of the beta chemokine hMIP-1 beta by multidimensional NMR. *Science* 1994;263(5154):1762-7.
45. Skelton NJ, Aspiras F, Ogez J, Schall TJ. Proton NMR assignments and solution conformation of RANTES, a chemokine of the C-C type. *Biochemistry* 1995;34(16):5329-42.
46. Chung CW, Cooke RM, Proudfoot AE, Wells TN. The three-dimensional solution structure of RANTES. *Biochemistry* 1995;34(29):9307-14.
47. Crump MP, Rajarathnam K, Kim KS, Clark-Lewis I, Sykes BD. Solution structure of eotaxin, a chemokine that selectively recruits eosinophils in allergic inflammation. *J Biol Chem* 1998;273(35):22471-9.

48. Rajarathnam K, Li Y, Rohrer T, Gentz R. Solution structure and dynamics of myeloid progenitor inhibitory factor-1 (MPIF-1), a novel monomeric CC chemokine. *J Biol Chem* 2001;276(7):4909-16.
49. Keizer DW, Crump MP, Lee TW, Slupsky CM, Clark-Lewis I, Sykes BD. Human CC chemokine I-309, structural consequences of the additional disulfide bond. *Biochemistry* 2000;39(20):6053-9.
50. Covell DG, Smythers GW, Gronenborn AM, Clore GM. Analysis of hydrophobicity in the alpha and beta chemokine families and its relevance to dimerization. *Protein Sci* 1994;3(11):2064-72.
51. Fairbrother WJ, Reilly D, Colby TJ, Hesselgesser J, Horuk R. The solution structure of melanoma growth stimulating activity. *J Mol Biol* 1994;242(3):252-70.
52. Kim KS, Clark-Lewis I, Sykes BD. Solution structure of GRO/melanoma growth stimulatory activity determined by ¹H NMR spectroscopy. *J Biol Chem* 1994;269(52):32909-15.
53. Shao W, Jerva LF, West J, Lolis E, Schweitzer BI. Solution structure of murine macrophage inflammatory protein-2. *Biochemistry* 1998;37(23):8303-13.
54. Qian YQ, Johanson KO, McDevitt P. Nuclear magnetic resonance solution structure of truncated human GRObeta [5-73] and its structural comparison with CXC chemokine family members GROalpha and IL-8. *J Mol Biol* 1999;294(5):1065-72.
55. Sepuru KM, Poluri KM, Rajarathnam K. Solution structure of CXCL5--a novel chemokine and adipokine implicated in inflammation and obesity. *PLoS One* 2014;9(4):e93228.
56. Young H, Roongta V, Daly TJ, Mayo KH. NMR structure and dynamics of monomeric neutrophil-activating peptide 2. *Biochem J* 1999;338 (Pt 3):591-8.
57. Malkowski MG, Wu JY, Lazar JB, Johnson PH, Edwards BF. The crystal structure of recombinant human neutrophil-activating peptide-2 (M6L) at 1.9-A resolution. *J Biol Chem* 1995;270(13):7077-87.
58. Crump MP, Gong JH, Loetscher P, Rajarathnam K, Amara A, Arenzana-Seisdedos F, Virelizier JL, Baggiolini M, Sykes BD, Clark-Lewis I. Solution structure and basis for functional activity of stromal cell-derived factor-1; dissociation of CXCR4 activation from binding and inhibition of HIV-1. *Embo J* 1997;16(23):6996-7007.
59. Lubkowski J, Bujacz G, Boqué L, Dommaille PJ, Handel TM, Wlodawer A. The structure of MCP-1 in two crystal forms provides a rare example of variable quaternary interactions. *Nat Struct Biol* 1997;4(1):64-9.
60. Handel TM, Dommaille PJ. Heteronuclear (¹H, ¹³C, ¹⁵N) NMR assignments and solution structure of the monocyte chemoattractant protein-1 (MCP-1) dimer. *Biochemistry* 1996;35(21):6569-84.
61. Ye J, Mayer KL, Mayer MR, Stone MJ. NMR solution structure and backbone dynamics of the CC chemokine eotaxin-3. *Biochemistry* 2001;40(26):7820-31.
62. Meunier S, Bernassau JM, Guillemot JC, Ferrara P, Darbon H. Determination of the three-dimensional structure of CC chemokine monocyte chemoattractant protein 3 by ¹H two-dimensional NMR spectroscopy. *Biochemistry* 1997;36(15):4412-22.

63. Kim KS, Rajarathnam K, Clark-Lewis I, Sykes BD. Structural characterization of a monomeric chemokine: monocyte chemoattractant protein-3. *FEBS Lett* 1996;395(2-3):277-82.
64. Hoover DM, Boulegue C, Yang D, Oppenheim JJ, Tucker K, Lu W, Lubkowski J. The structure of human macrophage inflammatory protein-3alpha /CCL20. Linking antimicrobial and CC chemokine receptor-6-binding activities with human beta-defensins. *J Biol Chem* 2002;277(40):37647-54.
65. Murphy JW, Yuan H, Kong Y, Xiong Y, Lolis EJ. Heterologous quaternary structure of CXCL12 and its relationship to the CC chemokine family. *Proteins* 2010;78(5):1331-7.
66. St Charles R, Walz DA, Edwards BF. The three-dimensional structure of bovine platelet factor 4 at 3.0-A resolution. *J Biol Chem* 1989;264(4):2092-9.
67. Liang WG, Ren M, Zhao F, Tang WJ. Structures of human CCL18, CCL3, and CCL4 reveal molecular determinants for quaternary structures and sensitivity to insulin-degrading enzyme. *J Mol Biol* 2015;427(6 Pt B):1345-58.
68. Mayo KH, Roongta V, Ilyina E, Milius R, Barker S, Quinlan C, La Rosa G, Daly TJ. NMR solution structure of the 32-kDa platelet factor 4 ELR-motif N-terminal chimera: a symmetric tetramer. *Biochemistry* 1995;34(36):11399-409.
69. Ren M, Guo Q, Guo L, Lenz M, Qian F, Koenen RR, Xu H, Schilling AB, Weber C, Ye RD and others. Polymerization of MIP-1 chemokine (CCL3 and CCL4) and clearance of MIP-1 by insulin-degrading enzyme. *EMBO J* 2010;29(23):3952-66.
70. Wang X, Watson C, Sharp JS, Handel TM, Prestegard JH. Oligomeric structure of the chemokine CCL5/RANTES from NMR, MS, and SAXS data. *Structure* 2011;19(8):1138-48.
71. Fernando H, Chin C, Rösger J, Rajarathnam K. Dimer dissociation is essential for interleukin-8 (IL-8) binding to CXCR1 receptor. *J Biol Chem* 2004;279(35):36175-8.
72. Gangavarapu P, Rajagopalan L, Kolli D, Guerrero-Plata A, Garofalo RP, Rajarathnam K. The monomer-dimer equilibrium and glycosaminoglycan interactions of chemokine CXCL8 regulate tissue-specific neutrophil recruitment. *J Leukoc Biol* 2012;91(2):259-65.
73. Rajarathnam K, Kay CM, Dewald B, Wolf M, Baggiolini M, Clark-Lewis I, Sykes BD. Neutrophil-activating peptide-2 and melanoma growth-stimulatory activity are functional as monomers for neutrophil activation. *J Biol Chem* 1997;272(3):1725-9.
74. Rajarathnam K, Sykes BD, Kay CM, Dewald B, Geiser T, Baggiolini M, Clark-Lewis I. Neutrophil activation by monomeric interleukin-8. *Science* 1994;264(5155):90-2.
75. Paolini JF, Willard D, Consler T, Luther M, Krangel MS. The chemokines IL-8, monocyte chemoattractant protein-1, and I-309 are monomers at physiologically relevant concentrations. *J Immunol* 1994;153(6):2704-17.
76. Rajarathnam K, Prado GN, Fernando H, Clark-Lewis I, Navarro J. Probing receptor binding activity of interleukin-8 dimer using a disulfide trap. *Biochemistry* 2006;45(25):7882-8.

77. Ravindran A, Joseph PR, Rajarathnam K. Structural basis for differential binding of the interleukin-8 monomer and dimer to the CXCR1 N-domain: role of coupled interactions and dynamics. *Biochemistry* 2009;48(37):8795-805.
78. Salanga CL, Handel TM. Chemokine oligomerization and interactions with receptors and glycosaminoglycans: the role of structural dynamics in function. *Exp Cell Res* 2011;317(5):590-601.
79. Iozzo RV, Schaefer L. Proteoglycan form and function: A comprehensive nomenclature of proteoglycans. *Matrix Biol* 2015;42:11-55.
80. Li L, Ly M, Linhardt RJ. Proteoglycan sequence. *Mol Biosyst* 2012;8(6):1613-25.
81. Prabhakar V, Capila I, Sasisekharan R. The structural elucidation of glycosaminoglycans. *Methods Mol Biol* 2009;534:147-56.
82. Perrimon N, Bernfield M. Specificities of heparan sulphate proteoglycans in developmental processes. *Nature* 2000;404(6779):725-8.
83. Scarpellini A, Germack R, Lortat-Jacob H, Muramatsu T, Billett E, Johnson T, Verderio EA. Heparan sulfate proteoglycans are receptors for the cell-surface trafficking and biological activity of transglutaminase-2. *J Biol Chem* 2009;284(27):18411-23.
84. Chen Y, Maguire T, Hileman RE, Fromm JR, Esko JD, Linhardt RJ, Marks RM. Dengue virus infectivity depends on envelope protein binding to target cell heparan sulfate. *Nat Med* 1997;3(8):866-71.
85. Shukla D, Liu J, Blaiklock P, Shworak NW, Bai X, Esko JD, Cohen GH, Eisenberg RJ, Rosenberg RD, Spear PG. A novel role for 3-O-sulfated heparan sulfate in herpes simplex virus 1 entry. *Cell* 1999;99(1):13-22.
86. Sasisekharan R, Shriver Z, Venkataraman G, Narayanasami U. Roles of heparan-sulphate glycosaminoglycans in cancer. *Nat Rev Cancer* 2002;2(7):521-8.
87. Liu D, Shriver Z, Venkataraman G, El Shabrawi Y, Sasisekharan R. Tumor cell surface heparan sulfate as cryptic promoters or inhibitors of tumor growth and metastasis. *Proc Natl Acad Sci U S A* 2002;99(2):568-73.
88. Khan S, Fung KW, Rodriguez E, Patel R, Gor J, Mulloy B, Perkins SJ. The solution structure of heparan sulfate differs from that of heparin: implications for function. *J Biol Chem* 2013;288(39):27737-51.
89. Xu D, Esko JD. Demystifying heparan sulfate-protein interactions. *Annu Rev Biochem* 2014;83:129-57.
90. Bishop JR, Schuksz M, Esko JD. Heparan sulphate proteoglycans fine-tune mammalian physiology. *Nature* 2007;446(7139):1030-7.
91. Bernfield M, Götte M, Park PW, Reizes O, Fitzgerald ML, Lincecum J, Zako M. Functions of cell surface heparan sulfate proteoglycans. *Annu Rev Biochem* 1999;68:729-77.
92. Shioiri T, Tsuchimoto J, Watanabe H, Sugiura N. Sequence determination of synthesized chondroitin sulfate dodecasaccharides. *Glycobiology* 2016.
93. Das ST, Rajagopalan L, Guerrero-Plata A, Sai J, Richmond A, Garofalo RP, Rajarathnam K. Monomeric and dimeric CXCL8 are both essential for in vivo neutrophil recruitment. *PLoS One* 2010;5(7):e11754.
94. Ghasemzadeh M, Kaplan ZS, Alwis I, Schoenwaelder SM, Ashworth KJ, Westein E, Hosseini E, Salem HH, Slattery R, McColl SR and others. The CXCR1/2

- ligand NAP-2 promotes directed intravascular leukocyte migration through platelet thrombi. *Blood* 2013;121(22):4555-66.
95. von Hundelshausen P, Koenen RR, Sack M, Mause SF, Adriaens W, Proudfoot AE, Hackeng TM, Weber C. Heterophilic interactions of platelet factor 4 and RANTES promote monocyte arrest on endothelium. *Blood* 2005;105(3):924-30.
 96. Gijsbers K, Gouwy M, Struyf S, Wuyts A, Proost P, Opdenakker G, Penninckx F, Ectors N, Geboes K, Van Damme J. GCP-2/CXCL6 synergizes with other endothelial cell-derived chemokines in neutrophil mobilization and is associated with angiogenesis in gastrointestinal tumors. *Exp Cell Res* 2005;303(2):331-42.
 97. Gouwy M, Schiraldi M, Struyf S, Van Damme J, Uguccioni M. Possible mechanisms involved in chemokine synergy fine tuning the inflammatory response. *Immunol Lett* 2012;145(1-2):10-4.
 98. Proudfoot AE, Uguccioni M. Modulation of Chemokine Responses: Synergy and Cooperativity. *Front Immunol* 2016;7:183.
 99. Kuscher K, Danelon G, Paoletti S, Stefano L, Schiraldi M, Petkovic V, Locati M, Gerber BO, Uguccioni M. Synergy-inducing chemokines enhance CCR2 ligand activities on monocytes. *Eur J Immunol* 2009;39(4):1118-28.
 100. Sebastiani S, Danelon G, Gerber B, Uguccioni M. CCL22-induced responses are powerfully enhanced by synergy inducing chemokines via CCR4: evidence for the involvement of first beta-strand of chemokine. *Eur J Immunol* 2005;35(3):746-56.
 101. Vanbervliet B, Bendriss-Vermare N, Massacrier C, Homey B, de Bouteiller O, Brière F, Trinchieri G, Caux C. The inducible CXCR3 ligands control plasmacytoid dendritic cell responsiveness to the constitutive chemokine stromal cell-derived factor 1 (SDF-1)/CXCL12. *J Exp Med* 2003;198(5):823-30.
 102. Krug A, Uppaluri R, Facchetti F, Dorner BG, Sheehan KC, Schreiber RD, Cella M, Colonna M. IFN-producing cells respond to CXCR3 ligands in the presence of CXCL12 and secrete inflammatory chemokines upon activation. *J Immunol* 2002;169(11):6079-83.
 103. Verkaar F, van Offenbeek J, van der Lee MM, van Lith LH, Watts AO, Rops AL, Aguilar DC, Ziarek JJ, van der Vlag J, Handel TM and others. Chemokine cooperativity is caused by competitive glycosaminoglycan binding. *J Immunol* 2014;192(8):3908-14.
 104. Dudek AZ, Nesmelova I, Mayo K, Verfaillie CM, Pitchford S, Slungaard A. Platelet factor 4 promotes adhesion of hematopoietic progenitor cells and binds IL-8: novel mechanisms for modulation of hematopoiesis. *Blood* 2003;101(12):4687-94.
 105. Paoletti S, Petkovic V, Sebastiani S, Danelon MG, Uguccioni M, Gerber BO. A rich chemokine environment strongly enhances leukocyte migration and activities. *Blood* 2005;105(9):3405-12.
 106. Nesmelova IV, Sham Y, Dudek AZ, van Eijk LI, Wu G, Slungaard A, Mortari F, Griffioen AW, Mayo KH. Platelet factor 4 and interleukin-8 CXC chemokine heterodimer formation modulates function at the quaternary structural level. *J Biol Chem* 2005;280(6):4948-58.

107. Crown SE, Yu Y, Sweeney MD, Leary JA, Handel TM. Heterodimerization of CCR2 chemokines and regulation by glycosaminoglycan binding. *J Biol Chem* 2006;281(35):25438-46.
108. Nesmelova IV, Sham Y, Gao J, Mayo KH. CXC and CC chemokines form mixed heterodimers: association free energies from molecular dynamics simulations and experimental correlations. *J Biol Chem* 2008;283(35):24155-66.
109. Carlson J, Baxter SA, Dréau D, Nesmelova IV. The heterodimerization of platelet-derived chemokines. *Biochim Biophys Acta* 2013;1834(1):158-68.
110. Koenen RR, von Hundelshausen P, Nesmelova IV, Zerneck A, Liehn EA, Sarabi A, Kramp BK, Piccinini AM, Paludan SR, Kowalska MA and others. Disrupting functional interactions between platelet chemokines inhibits atherosclerosis in hyperlipidemic mice. *Nat Med* 2009;15(1):97-103.
111. Raghuwanshi SK, Su Y, Singh V, Haynes K, Richmond A, Richardson RM. The chemokine receptors CXCR1 and CXCR2 couple to distinct G protein-coupled receptor kinases to mediate and regulate leukocyte functions. *J Immunol* 2012;189(6):2824-32.
112. Clister T, Mehta S, Zhang J. Single-cell analysis of G-protein signal transduction. *J Biol Chem* 2015;290(11):6681-8.
113. Ma L, Pei G. Beta-arrestin signaling and regulation of transcription. *J Cell Sci* 2007;120(Pt 2):213-8.
114. Palczewski K, Kumasaka T, Hori T, Behnke CA, Motoshima H, Fox BA, Le Trong I, Teller DC, Okada T, Stenkamp RE and others. Crystal structure of rhodopsin: A G protein-coupled receptor. *Science* 2000;289(5480):739-45.
115. Kobilka BK. G protein coupled receptor structure and activation. *Biochim Biophys Acta* 2007;1768(4):794-807.
116. Park SH, Das BB, Casagrande F, Tian Y, Nothnagel HJ, Chu M, Kiefer H, Maier K, De Angelis AA, Marassi FM and others. Structure of the chemokine receptor CXCR1 in phospholipid bilayers. *Nature* 2012;491(7426):779-83.
117. Kufareva I. Chemokines and their receptors: insights from molecular modeling and crystallography. *Curr Opin Pharmacol* 2016;30:27-37.
118. Baldwin JM. Structure and function of receptors coupled to G proteins. *Curr Opin Cell Biol* 1994;6(2):180-90.
119. Han KH, Green SR, Tangirala RK, Tanaka S, Quehenberger O. Role of the first extracellular loop in the functional activation of CCR2. The first extracellular loop contains distinct domains necessary for both agonist binding and transmembrane signaling. *J Biol Chem* 1999;274(45):32055-62.
120. Hammond ME, Shyamala V, Siani MA, Gallegos CA, Feucht PH, Abbott J, Lapointe GR, Moghadam M, Khoja H, Zakel J and others. Receptor recognition and specificity of interleukin-8 is determined by residues that cluster near a surface-accessible hydrophobic pocket. *J Biol Chem* 1996;271(14):8228-35.
121. Clark-Lewis I, Schumacher C, Baggiolini M, Moser B. Structure-activity relationships of interleukin-8 determined using chemically synthesized analogs. Critical role of NH₂-terminal residues and evidence for uncoupling of neutrophil chemotaxis, exocytosis, and receptor binding activities. *J Biol Chem* 1991;266(34):23128-34.

122. Clark-Lewis I, Dewald B, Geiser T, Moser B, Baggiolini M. Platelet factor 4 binds to interleukin 8 receptors and activates neutrophils when its N terminus is modified with Glu-Leu-Arg. *Proc Natl Acad Sci U S A* 1993;90(8):3574-7.
123. Clark-Lewis I, Mattioli I, Gong JH, Loetscher P. Structure-function relationship between the human chemokine receptor CXCR3 and its ligands. *J Biol Chem* 2003;278(1):289-95.
124. Chung IY, Kim YH, Choi MK, Noh YJ, Park CS, Kwon DY, Lee DY, Lee YS, Chang HS, Kim KS. Eotaxin and monocyte chemotactic protein-3 use different modes of action. *Biochem Biophys Res Commun* 2004;314(2):646-53.
125. Brelot A, Heveker N, Montes M, Alizon M. Identification of residues of CXCR4 critical for human immunodeficiency virus coreceptor and chemokine receptor activities. *J Biol Chem* 2000;275(31):23736-44.
126. Bondue A, Jao SC, Blanpain C, Parmentier M, LiWang PJ. Characterization of the role of the N-loop of MIP-1 beta in CCR5 binding. *Biochemistry* 2002;41(46):13548-55.
127. Booth V, Keizer DW, Kamphuis MB, Clark-Lewis I, Sykes BD. The CXCR3 binding chemokine IP-10/CXCL10: structure and receptor interactions. *Biochemistry* 2002;41(33):10418-25.
128. Campanella GS, Lee EM, Sun J, Luster AD. CXCR3 and heparin binding sites of the chemokine IP-10 (CXCL10). *J Biol Chem* 2003;278(19):17066-74.
129. Blanpain C, Lee B, Vakili J, Doranz BJ, Govaerts C, Migeotte I, Sharron M, Dupriez V, Vassart G, Doms RW and others. Extracellular cysteines of CCR5 are required for chemokine binding, but dispensable for HIV-1 coreceptor activity. *J Biol Chem* 1999;274(27):18902-8.
130. Blanpain C, Doranz BJ, Bondue A, Govaerts C, De Leener A, Vassart G, Doms RW, Proudfoot A, Parmentier M. The core domain of chemokines binds CCR5 extracellular domains while their amino terminus interacts with the transmembrane helix bundle. *J Biol Chem* 2003;278(7):5179-87.
131. Blanpain C, Doranz BJ, Vakili J, Rucker J, Govaerts C, Baik SS, Lorthioir O, Migeotte I, Libert F, Baleux F and others. Multiple charged and aromatic residues in CCR5 amino-terminal domain are involved in high affinity binding of both chemokines and HIV-1 Env protein. *J Biol Chem* 1999;274(49):34719-27.
132. Baly DL, Horuk R, Yansura DG, Simmons LC, Fairbrother WJ, Kotts C, Wirth CM, Gillece-Castro BL, Toy K, Hesselgesser J and others. A His19 to Ala mutant of melanoma growth-stimulating activity is a partial antagonist of the CXCR2 receptor. *J Immunol* 1998;161(9):4944-9.
133. Ahuja SK, Lee JC, Murphy PM. CXC chemokines bind to unique sets of selectivity determinants that can function independently and are broadly distributed on multiple domains of human interleukin-8 receptor B. Determinants of high affinity binding and receptor activation are distinct. *J Biol Chem* 1996;271(1):225-32.
134. LaRosa GJ, Thomas KM, Kaufmann ME, Mark R, White M, Taylor L, Gray G, Witt D, Navarro J. Amino terminus of the interleukin-8 receptor is a major determinant of receptor subtype specificity. *J Biol Chem* 1992;267(35):25402-6.

135. Katancik JA, Sharma A, de Nardin E. Interleukin 8, neutrophil-activating peptide-2 and GRO-alpha bind to and elicit cell activation via specific and different amino acid residues of CXCR2. *Cytokine* 2000;12(10):1480-8.
136. Hébert CA, Chuntharapai A, Smith M, Colby T, Kim J, Horuk R. Partial functional mapping of the human interleukin-8 type A receptor. Identification of a major ligand binding domain. *J Biol Chem* 1993;268(25):18549-53.
137. Monteclaro FS, Charo IF. The amino-terminal extracellular domain of the MCP-1 receptor, but not the RANTES/MIP-1alpha receptor, confers chemokine selectivity. Evidence for a two-step mechanism for MCP-1 receptor activation. *J Biol Chem* 1996;271(32):19084-92.
138. Pakianathan DR, Kuta EG, Artis DR, Skelton NJ, Hébert CA. Distinct but overlapping epitopes for the interaction of a CC-chemokine with CCR1, CCR3 and CCR5. *Biochemistry* 1997;36(32):9642-8.
139. Rajagopalan L, Rajarathnam K. Ligand selectivity and affinity of chemokine receptor CXCR1. Role of N-terminal domain. *J Biol Chem* 2004;279(29):30000-8.
140. Shinkai A, Komuta-Kunitomo M, Sato-Nakamura N, Anazawa H. N-terminal domain of eotaxin-3 is important for activation of CC chemokine receptor 3. *Protein Eng* 2002;15(11):923-9.
141. Skelton NJ, Quan C, Reilly D, Lowman H. Structure of a CXC chemokine-receptor fragment in complex with interleukin-8. *Structure* 1999;7(2):157-68.
142. Wells TN, Power CA, Lusti-Narasimhan M, Hoogewerf AJ, Cooke RM, Chung CW, Peitsch MC, Proudfoot AE. Selectivity and antagonism of chemokine receptors. *J Leukoc Biol* 1996;59(1):53-60.
143. Yan Z, Zhang J, Holt JC, Stewart GJ, Niewiarowski S, Poncz M. Structural requirements of platelet chemokines for neutrophil activation. *Blood* 1994;84(7):2329-39.
144. Ye J, Kohli LL, Stone MJ. Characterization of binding between the chemokine eotaxin and peptides derived from the chemokine receptor CCR3. *J Biol Chem* 2000;275(35):27250-7.
145. Zhou N, Luo Z, Luo J, Liu D, Hall JW, Pomerantz RJ, Huang Z. Structural and functional characterization of human CXCR4 as a chemokine receptor and HIV-1 co-receptor by mutagenesis and molecular modeling studies. *J Biol Chem* 2001;276(46):42826-33.
146. Lowman HB, Slagle PH, DeForge LE, Wirth CM, Gillece-Castro BL, Bourell JH, Fairbrother WJ. Exchanging interleukin-8 and melanoma growth-stimulating activity receptor binding specificities. *J Biol Chem* 1996;271(24):14344-52.
147. Proudfoot AE, Power CA, Hoogewerf AJ, Montjovent MO, Borlat F, Offord RE, Wells TN. Extension of recombinant human RANTES by the retention of the initiating methionine produces a potent antagonist. *J Biol Chem* 1996;271(5):2599-603.
148. Joseph PR, Rajarathnam K. Solution NMR characterization of WT CXCL8 monomer and dimer binding to CXCR1 N-terminal domain. *Protein Sci* 2015;24(1):81-92.
149. Joseph PR, Sawant KV, Isley A, Pedroza M, Garofalo RP, Richardson RM, Rajarathnam K. Dynamic conformational switching in the chemokine ligand is

- essential for G-protein-coupled receptor activation. *Biochem J* 2013;456(2):241-51.
150. Ravindran A, Sawant KV, Sarmiento J, Navarro J, Rajarathnam K. Chemokine CXCL1 dimer is a potent agonist for the CXCR2 receptor. *J Biol Chem* 2013;288(17):12244-52.
 151. Veldkamp CT, Seibert C, Peterson FC, De la Cruz NB, Haugner JC, 3rd, Basnet H, Sakmar TP, Volkman BF. Structural basis of CXCR4 sulfotyrosine recognition by the chemokine SDF-1/CXCL12. *Sci Signal* 2008;1(37):ra4.
 152. Millard CJ, Ludeman JP, Canals M, Bridgford JL, Hinds MG, Clayton DJ, Christopoulos A, Payne RJ, Stone MJ. Structural basis of receptor sulfotyrosine recognition by a CC chemokine: the N-terminal region of CCR3 bound to CCL11/eotaxin-1. *Structure* 2014;22(11):1571-81.
 153. Schnur E, Kessler N, Zherdev Y, Noah E, Scherf T, Ding FX, Rabinovich S, Arshava B, Kurbatska V, Leoncijs A and others. NMR mapping of RANTES surfaces interacting with CCR5 using linked extracellular domains. *FEBS J* 2013;280(9):2068-84.
 154. Girrbaach M, Meliciani I, Waterkotte B, Berthold S, Oster A, Brurein F, Strunk T, Wadhvani P, Berensmeier S, Wenzel W and others. A fluorescence polarization assay for the experimental validation of an in silico model of the chemokine CXCL8 binding to receptor-derived peptides. *Phys Chem Chem Phys* 2014;16(17):8036-43.
 155. Blanchet X, Langer M, Weber C, Koenen RR, von Hundelshausen P. Touch of chemokines. *Front Immunol* 2012;3:175.
 156. Lowman HB, Fairbrother WJ, Slagle PH, Kabakoff R, Liu J, Shire S, Hébert CA. Monomeric variants of IL-8: effects of side chain substitutions and solution conditions upon dimer formation. *Protein Sci* 1997;6(3):598-608.
 157. Stillie R, Farooq SM, Gordon JR, Stadnyk AW. The functional significance behind expressing two IL-8 receptor types on PMN. *J Leukoc Biol* 2009;86(3):529-43.
 158. Phillipson M, Heit B, Colarusso P, Liu L, Ballantyne CM, Kubes P. Intraluminal crawling of neutrophils to emigration sites: a molecularly distinct process from adhesion in the recruitment cascade. *J Exp Med* 2006;203(12):2569-75.
 159. Ley K, Laudanna C, Cybulsky MI, Nourshargh S. Getting to the site of inflammation: the leukocyte adhesion cascade updated. *Nat Rev Immunol* 2007;7(9):678-89.
 160. Kolaczowska E, Kubes P. Neutrophil recruitment and function in health and inflammation. *Nat Rev Immunol* 2013;13(3):159-75.
 161. Martins-Green M, Petreaca M, Wang L. Chemokines and Their Receptors Are Key Players in the Orchestra That Regulates Wound Healing. *Adv Wound Care (New Rochelle)* 2013;2(7):327-347.
 162. Nordenfelt P, Tapper H. Phagosome dynamics during phagocytosis by neutrophils. *J Leukoc Biol* 2011;90(2):271-84.
 163. Brinkmann V, Reichard U, Goosmann C, Fauler B, Uhlemann Y, Weiss DS, Weinrauch Y, Zychlinsky A. Neutrophil extracellular traps kill bacteria. *Science* 2004;303(5663):1532-5.

164. Stephan A, Fabri M. The NET, the trap and the pathogen: neutrophil extracellular traps in cutaneous immunity. *Exp Dermatol* 2015;24(3):161-6.
165. Jeyaseelan S, Manzer R, Young SK, Yamamoto M, Akira S, Mason RJ, Worthen GS. Induction of CXCL5 during inflammation in the rodent lung involves activation of alveolar epithelium. *Am J Respir Cell Mol Biol* 2005;32(6):531-9.
166. Chavey C, Lazennec G, Lagarrigue S, Clapé C, Iankova I, Teyssier J, Annicotte JS, Schmidt J, Matakı C, Yamamoto H and others. CXC ligand 5 is an adipose-tissue derived factor that links obesity to insulin resistance. *Cell Metab* 2009;9(4):339-49.
167. O'Hayre M, Salanga CL, Handel TM, Allen SJ. Chemokines and cancer: migration, intracellular signalling and intercellular communication in the microenvironment. *Biochem J* 2008;409(3):635-49.
168. Li A, King J, Moro A, Sugi MD, Dawson DW, Kaplan J, Li G, Lu X, Strieter RM, Burdick M and others. Overexpression of CXCL5 is associated with poor survival in patients with pancreatic cancer. *Am J Pathol* 2011;178(3):1340-9.
169. Fernandez EJ, Lolis E. Structure, function, and inhibition of chemokines. *Annu Rev Pharmacol Toxicol* 2002;42:469-99.
170. Monneau Y, Arenzana-Seisdedos F, Lortat-Jacob H. The sweet spot: how GAGs help chemokines guide migrating cells. *J Leukoc Biol* 2016;99(6):935-53.
171. Sreeramkumar V, Adrover JM, Ballesteros I, Cuartero MI, Rossaint J, Bilbao I, Náchér M, Pitaval C, Radovanovic I, Fukui Y and others. Neutrophils scan for activated platelets to initiate inflammation. *Science* 2014;346(6214):1234-8.
172. von Hundelshausen P, Petersen F, Brandt E. Platelet-derived chemokines in vascular biology. *Thromb Haemost* 2007;97(5):704-13.
173. Yang Y, Mayo KH, Daly TJ, Barry JK, La Rosa GJ. Subunit association and structural analysis of platelet basic protein and related proteins investigated by ¹H NMR spectroscopy and circular dichroism. *J Biol Chem* 1994;269(31):20110-8.
174. Ahuja SK, Murphy PM. The CXC chemokines growth-regulated oncogene (GRO) alpha, GRObeta, GROgamma, neutrophil-activating peptide-2, and epithelial cell-derived neutrophil-activating peptide-78 are potent agonists for the type B, but not the type A, human interleukin-8 receptor. *J Biol Chem* 1996;271(34):20545-50.
175. Rajarathnam K, Clark-Lewis I, Sykes BD. ¹H NMR solution structure of an active monomeric interleukin-8. *Biochemistry* 1995;34(40):12983-90.
176. Rajarathnam K, Clark-Lewis I, Dewald B, Baggiolini M, Sykes BD. ¹H NMR evidence that Glu-38 interacts with the N-terminal functional domain in interleukin-8. *FEBS Lett* 1996;399(1-2):43-6.
177. Hesselgesser J, Chitnis CE, Miller LH, Yansura DG, Simmons LC, Fairbrother WJ, Kotts C, Wirth C, Gillece-Castro BL, Horuk R. A mutant of melanoma growth stimulating activity does not activate neutrophils but blocks erythrocyte invasion by malaria. *J Biol Chem* 1995;270(19):11472-6.
178. Rajarathnam K, Sykes BD, Dewald B, Baggiolini M, Clark-Lewis I. Disulfide bridges in interleukin-8 probed using non-natural disulfide analogues: dissociation of roles in structure from function. *Biochemistry* 1999;38(24):7653-8.

179. Shen Y, Delaglio F, Cornilescu G, Bax A. TALOS+: a hybrid method for predicting protein backbone torsion angles from NMR chemical shifts. *J Biomol NMR* 2009;44(4):213-23.
180. Shen Y, Bax A. Protein backbone and sidechain torsion angles predicted from NMR chemical shifts using artificial neural networks. *J Biomol NMR* 2013;56(3):227-41.
181. Herring CA, Singer CM, Ermakova EA, Khairutdinov BI, Zuev YF, Jacobs DJ, Nesmelova IV. Dynamics and thermodynamic properties of CXCL7 chemokine. *Proteins* 2015;83(11):1987-2007.
182. Nguyen LT, Kwakman PH, Chan DI, Liu Z, de Boer L, Zaat SA, Vogel HJ. Exploring platelet chemokine antimicrobial activity: nuclear magnetic resonance backbone dynamics of NAP-2 and TC-1. *Antimicrob Agents Chemother* 2011;55(5):2074-83.
183. Joseph PR, Sarmiento JM, Mishra AK, Das ST, Garofalo RP, Navarro J, Rajarathnam K. Probing the role of CXC motif in chemokine CXCL8 for high affinity binding and activation of CXCR1 and CXCR2 receptors. *J Biol Chem* 2010;285(38):29262-9.
184. Kofuku Y, Yoshiura C, Ueda T, Terasawa H, Hirai T, Tominaga S, Hirose M, Maeda Y, Takahashi H, Terashima Y and others. Structural Basis of the Interaction between Chemokine Stromal Cell-derived Factor-1/CXCL12 and Its G-protein-coupled Receptor CXCR4. *J Biol Chem* 2009;284(50):35240-50.
185. Joseph PR, Mosier PD, Desai UR, Rajarathnam K. Solution NMR characterization of chemokine CXCL8/IL-8 monomer and dimer binding to glycosaminoglycans: structural plasticity mediates differential binding interactions. *Biochem J* 2015;472(1):121-33.
186. Sawant KV, Poluri KM, Dutta AK, Sepuru KM, Troshkina A, Garofalo RP, Rajarathnam K. Chemokine CXCL1 mediated neutrophil recruitment: Role of glycosaminoglycan interactions. *Sci Rep* 2016;6:33123.
187. Sepuru KM, Rajarathnam K. CXCL1/MGSA Is a Novel Glycosaminoglycan (GAG)-binding Chemokine: STRUCTURAL EVIDENCE FOR TWO DISTINCT NON-OVERLAPPING BINDING DOMAINS. *J Biol Chem* 2016;291(8):4247-55.
188. Sepuru KM, Nagarajan B, Desai UR, Rajarathnam K. Molecular Basis of Chemokine CXCL5-Glycosaminoglycan Interactions. *J Biol Chem* 2016;291(39):20539-50.
189. Di Stefano A, Caramori G, Gnemmi I, Contoli M, Bristot L, Capelli A, Ricciardolo FL, Magno F, D'Anna SE, Zanini A and others. Association of increased CCL5 and CXCL7 chemokine expression with neutrophil activation in severe stable COPD. *Thorax* 2009;64(11):968-75.
190. Yeo L, Adlard N, Biehl M, Juarez M, Smallie T, Snow M, Buckley CD, Raza K, Filer A, Scheel-Toellner D. Expression of chemokines CXCL4 and CXCL7 by synovial macrophages defines an early stage of rheumatoid arthritis. *Ann Rheum Dis* 2016;75(4):763-71.
191. Bdeir K, Gollomp K, Stasiak M, Mei J, Papiewska-Pajak I, Zhao G, Worthen GS, Cines DB, Poncz M, Kowalska MA. Platelet-specific Chemokines Contribute to the Pathogenesis of Acute Lung Injury. *Am J Respir Cell Mol Biol* 2016.

192. Desurmont T, Skrypek N, Duhamel A, Jonckheere N, Millet G, Leteurtre E, Gosset P, Duchene B, Ramdane N, Hebbar M and others. Overexpression of chemokine receptor CXCR2 and ligand CXCL7 in liver metastases from colon cancer is correlated to shorter disease-free and overall survival. *Cancer Sci* 2015;106(3):262-9.
193. Grépin R, Guyot M, Giuliano S, Boncompagni M, Ambrosetti D, Chamorey E, Scoazec JY, Negrier S, Simonnet H, Pagès G. The CXCL7/CXCR1/2 axis is a key driver in the growth of clear cell renal cell carcinoma. *Cancer Res* 2014;74(3):873-83.
194. Mayo KH, Yang Y, Daly TJ, Barry JK, La Rosa GJ. Secondary structure of neutrophil-activating peptide-2 determined by ¹H-nuclear magnetic resonance spectroscopy. *Biochem J* 1994;304 (Pt 2):371-6.
195. Goddard TD, Kneller DG. SPARKY 3. University of California, San Francisco 2008.
196. Shen Y, Lange O, Delaglio F, Rossi P, Aramini JM, Liu G, Eletsky A, Wu Y, Singarapu KK, Lemak A and others. Consistent blind protein structure generation from NMR chemical shift data. *Proc Natl Acad Sci U S A* 2008;105(12):4685-90.
197. Shen Y, Vernon R, Baker D, Bax A. De novo protein structure generation from incomplete chemical shift assignments. *J Biomol NMR* 2009;43(2):63-78.
198. **The PyMOL Molecular Graphics System, Version 1.8 Schrödinger, LLC.**
199. Case DA, Darden TA, Cheatham III TE, Simmerling CL, Wang J, Duke RE, Luo R, Walker RC, Zhang W, Merz KM and others. AMBER 12, University of California, San Francisco. 2012.
200. Willard L, Ranjan A, Zhang H, Monzavi H, Boyko RF, Sykes BD, Wishart DS. VADAR: a web server for quantitative evaluation of protein structure quality. *Nucleic Acids Res* 2003;31(13):3316-9.
201. Dominguez C, Boelens R, Bonvin AM. HADDOCK: a protein-protein docking approach based on biochemical or biophysical information. *J Am Chem Soc* 2003;125(7):1731-7.
202. de Vries SJ, van Dijk AD, Krzeminski M, van Dijk M, Thureau A, Hsu V, Wassenaar T, Bonvin AM. HADDOCK versus HADDOCK: new features and performance of HADDOCK2.0 on the CAPRI targets. *Proteins* 2007;69(4):726-33.
203. Mulloy B, Forster MJ, Jones C, Davies DB. N.m.r. and molecular-modelling studies of the solution conformation of heparin. *Biochem J* 1993;293 (Pt 3):849-58.
204. Sawant KV, Xu R, Cox R, Hawkins H, Sbrana E, Kolli D, Garofalo RP, Rajarathnam K. Chemokine CXCL1-Mediated Neutrophil Trafficking in the Lung: Role of CXCR2 Activation. *J Innate Immun* 2015;7(6):647-58.
205. Chao T, Furth EE, Vonderheide RH. CXCR2-Dependent Accumulation of Tumor-Associated Neutrophils Regulates T-cell Immunity in Pancreatic Ductal Adenocarcinoma. *Cancer Immunol Res* 2016;4(11):968-982.
206. Hoogewerf AJ, Kuschert GS, Proudfoot AE, Borlat F, Clark-Lewis I, Power CA, Wells TN. Glycosaminoglycans mediate cell surface oligomerization of chemokines. *Biochemistry* 1997;36(44):13570-8.

207. Frevert CW, Goodman RB, Kinsella MG, Kajikawa O, Ballman K, Clark-Lewis I, Proudfoot AE, Wells TN, Martin TR. Tissue-specific mechanisms control the retention of IL-8 in lungs and skin. *J Immunol* 2002;168(7):3550-6.
208. Liang WG, Triandafillou CG, Huang TY, Zulueta MM, Banerjee S, Dinner AR, Hung SC, Tang WJ. Structural basis for oligomerization and glycosaminoglycan binding of CCL5 and CCL3. *Proc Natl Acad Sci U S A* 2016;113(18):5000-5.
209. Dyer DP, Salanga CL, Volkman BF, Kawamura T, Handel TM. The dependence of chemokine-glycosaminoglycan interactions on chemokine oligomerization. *Glycobiology* 2016;26(3):312-26.
210. Brown AJ, Sepuru KM, Rajarathnam K. Structural Basis of Native CXCL7 Monomer Binding to CXCR2 Receptor N-Domain and Glycosaminoglycan Heparin. *Int J Mol Sci* 2017;18(3).
211. Mizoue LS, Bazan JF, Johnson EC, Handel TM. Solution structure and dynamics of the CX3C chemokine domain of fractalkine and its interaction with an N-terminal fragment of CX3CR1. *Biochemistry* 1999;38(5):1402-14.
212. Poluri KM, Joseph PR, Sawant KV, Rajarathnam K. Molecular basis of glycosaminoglycan heparin binding to the chemokine CXCL1 dimer. *J Biol Chem* 2013;288(35):25143-53.
213. Sepuru KM, Nagarajan B, Desai UR, Rajarathnam K. Molecular basis of chemokine CXCL5-glycosaminoglycan interactions. *J Biol Chem* 2016.
214. Zlotnik A, Yoshie O. The chemokine superfamily revisited. *Immunity* 2012;36(5):705-16.
215. Massena S, Christoffersson G, Hjertström E, Zcharia E, Vlodavsky I, Ausmees N, Rolny C, Li JP, Phillipson M. A chemotactic gradient sequestered on endothelial heparan sulfate induces directional intraluminal crawling of neutrophils. *Blood* 2010;116(11):1924-31.
216. Zlotnik A, Yoshie O. Chemokines: a new classification system and their role in immunity. *Immunity* 2000;12(2):121-7.
217. LiWang AC, Cao JJ, Zheng H, Lu Z, Peiper SC, LiWang PJ. Dynamics study on the anti-human immunodeficiency virus chemokine viral macrophage-inflammatory protein-II (VMIP-II) reveals a fully monomeric protein. *Biochemistry* 1999;38(1):442-53.
218. Kasper B, Brandt E, Bulfone-Paus S, Petersen F. Platelet factor 4 (PF-4)-induced neutrophil adhesion is controlled by src-kinases, whereas PF-4-mediated exocytosis requires the additional activation of p38 MAP kinase and phosphatidylinositol 3-kinase. *Blood* 2004;103(5):1602-10.
219. Nasser MW, Raghuwanshi SK, Grant DJ, Jala VR, Rajarathnam K, Richardson RM. Differential activation and regulation of CXCR1 and CXCR2 by CXCL8 monomer and dimer. *J Immunol* 2009;183(5):3425-32.
220. Bdeir K, Gollomp K, Stasiak M, Mei J, Papiewska-Pajak I, Zhao G, Worthen GS, Cines DB, Poncz M, Kowalska MA. Platelet-Specific Chemokines Contribute to the Pathogenesis of Acute Lung Injury. *Am J Respir Cell Mol Biol* 2017;56(2):261-270.
221. Zwijnenburg PJ, Polfliet MM, Florquin S, van den Berg TK, Dijkstra CD, van Deventer SJ, Roord JJ, van der Poll T, van Furth AM. CXC-chemokines KC and

- macrophage inflammatory protein-2 (MIP-2) synergistically induce leukocyte recruitment to the central nervous system in rats. *Immunol Lett* 2003;85(1):1-4.
222. Rzepka JP, Haick AK, Miura TA. Virus-infected alveolar epithelial cells direct neutrophil chemotaxis and inhibit their apoptosis. *Am J Respir Cell Mol Biol* 2012;46(6):833-41.
 223. Guan E, Wang J, Norcross MA. Identification of human macrophage inflammatory proteins 1alpha and 1beta as a native secreted heterodimer. *J Biol Chem* 2001;276(15):12404-9.
 224. Duan Y, Wu C, Chowdhury S, Lee MC, Xiong G, Zhang W, Yang R, Cieplak P, Luo R, Lee T and others. A point-charge force field for molecular mechanics simulations of proteins based on condensed-phase quantum mechanical calculations. *J Comput Chem* 2003;24(16):1999-2012.
 225. Lee MC, Deng J, Briggs JM, Duan Y. Large-scale conformational dynamics of the HIV-1 integrase core domain and its catalytic loop mutants. *Biophys J* 2005;88(5):3133-46.
 226. Humphrey W, Dalke A, Schulten K. VMD: visual molecular dynamics. *J Mol Graph* 1996;14(1):33-8, 27-8.
 227. Files JC, Malpass TW, Yee EK, Ritchie JL, Harker LA. Studies of human platelet alpha-granule release in vivo. *Blood* 1981;58(3):607-18.
 228. Brandt E, Petersen F, Ludwig A, Ehlert JE, Bock L, Flad HD. The beta-thromboglobulins and platelet factor 4: blood platelet-derived CXC chemokines with divergent roles in early neutrophil regulation. *J Leukoc Biol* 2000;67(4):471-8.
 229. Brown AJ, Joseph PR, Sawant KV, Rajarathnam K. Chemokine CXCL7 Heterodimers: Structural Insights, CXCR2 Receptor Function, and Glycosaminoglycan Interactions. *Int J Mol Sci* 2017;18(4).

Vita

Aaron John Brown was born on November 28, 1987 in Portland, Oregon. He is the son of Carl H. Brown and Laura L. Brown and has a younger brother and sister. Aaron attended Baylor University from 2006-2010 and received the Achievement Baylor Scholarship and the President's Scholarship as well as the Outstanding Physics Student Award each of his four years there. He gained teaching experience through tutoring students in science and math while attending school. Aaron graduated with a Bachelor's of Science in Physics with a minor in Chemistry. After college, Aaron worked for a year as an Anesthesia Technician before starting graduate school at UTMB. While at UTMB, Aaron joined the laboratory of Dr. Krishna Rajarathnam, where he studied the structural basis of platelet chemokine CXCL7 monomer and dimer interactions with CXCR2 receptor and glycosaminoglycans. He received the Houston Area Molecular Biophysics Training Program Fellowship, as well as the McLaughlin Colloquium Poster and Travel Award and travel awards from UTMB. He has presented posters at numerous conferences including the Sealy Center Symposium (2013-2015), the Keck Conference (2013-2015), the Texas Protein Folders and Function meeting (2014-2016), and the Protein Society Symposium (2016). He currently has two publications, one to be submitted paper, and will be a co-author on a review in preparation.

Permanent address: 13768 SW Jenna Ct, Tigard, Oregon 97223

This dissertation was typed by Aaron John Brown.